

Aus dem Laser-Forschungslabor der Urologischen Klinik und Poliklinik

(Vorstand: Prof. Dr. med. Dr. h. c. mult. A. Hofstetter)

und

der Medizinischen Klinik-Innenstadt,

(Komm. Direktor Prof. Dr. D. Schlöndorff)

Pneumologie

(Leiter Prof. Dr. R. M. Huber)

der Ludwig-Maximilians-Universität München

**Pharmacokinetic studies on protoporphyrin IX induced by
5-aminolevulinic acid and its esters in a three-dimensional
lung tumor mini-organ culture model**

Dissertation

zum Erwerb des Doktorgrades der Humanbiologie

an der Medizinischen Fakultät der

Ludwig-Maximilians-Universität zu München

vorgelegt von

Mirna Castro

aus

Guayaquil – Ecuador

2005

Mit Genehmigung der Medizinischen Fakultät
der Universität München

Berichterstatter:

Prof. Dr. R. M. Huber

Mitberichterstatter:

Priv. Doz. Dr. M. Dellian

Prof. Dr. A. E. Goetz

Mitbetreuung durch den
Promovierten Mitarbeiter:

Dr. rer. nat. R. Baumgartner

Dekan:

Prof. Dr. med. D. Reinhardt

Tag der mündlichen Prüfung:

02.03.2005

CONTENTS

CONTENTS.....	i
1 INTRODUCTION.....	1
1.1 LUNG CANCER.....	1
1.1.1 Epidemiological facts.....	1
1.1.2 Etiology of bronchial carcinoma.....	2
1.1.3 Diagnostic approaches to lung cancer.....	3
1.1.4 Early detection, staging, and prognosis.....	5
1.1.5 Normal lung physiology and lung cancer biology.....	8
1.2 NEW TECHNIQUES FOR FLUORESCENCE DETECTION OF LUNG CANCER.....	12
1.2.1 5-Aminolevulinic acid induced protoporphyrin IX.....	12
1.2.2 5-ALA esters.....	17
1.2.3 Optical properties of porphyrins.....	19
1.2.4 Autofluorescence.....	20
1.3 OBJECTIVES OF THE STUDY.....	22
2 MATERIALS AND METHODS.....	23
2.1 BIOLOGICAL MATERIAL.....	23
2.2 LAB MATERIAL.....	23
2.2.1 Cell culture medium and supplements.....	24
2.2.2 Equipment, devices and instruments.....	25
2.3 METHODS.....	25
2.3.1 Preparation of media and agar plates.....	25
2.4 THE THREE-DIMENSIONAL MINI-ORGAN MODEL.....	27
2.4.1 Biopsy cultivation.....	27
2.4.2 The tumor cell line EPLC-32M1.....	27
2.4.3 Monolayer culture.....	28
2.4.4 Co-culture.....	29
2.5.1 Overview.....	30
2.5.2 Generation of the stable GFP-expressing EPLC-32M1 tumor cell line.....	31
2.6 INCUBATION WITH PHOTSENSITIZERS.....	33
2.6.1 Co-culture incubation with 5-ALA.....	33
2.6.2 Co-culture incubation with 5-ALA esters.....	36

3	RESULTS.....	37
3.1	THE THREE-DIMENSIONAL MINI-ORGAN MODEL	37
3.2	KINETICS OF 5-ALA INDUCED PPIX SYNTHESIS IN THE MINI-ORGAN MODEL.....	38
3.3	KINETICS OF ALA ESTERS IN THE MINI-ORGAN MODEL.....	43
3.4	KINETICS OF 5-ALA INDUCED PPIX FLUORESCENCE IN CO-CULTURES WITH GFP-EXPRESSING LUNG TUMOR CELLS.....	49
4	DISCUSSION	53
4.1	THE THREE-DIMENSIONAL MINI-ORGAN MODEL	53
4.2	PHARMACOKINETICS OF 5-ALA-INDUCED PPIX FORMATION IN THE MINI-ORGAN MODEL	54
4.3	5-ALA ESTERS IN THE MINI-ORGAN MODEL	56
4.4	GFP IN THE MINI-ORGAN MODEL.....	59
4.5	THE ROLE OF FLUORESCENCE DIAGNOSIS IN EARLY DETECTION OF BRONCHIAL CANCER	60
5	SUMMARY	61
6	SUMMARY (GERMAN TRANSLATION)	65
7	ABBREVIATIONS.....	69
8	REFERENCE LIST.....	71
9	CURRICULUM VITAE	81
10	ACKNOWLEDGEMENTS	85

1 INTRODUCTION

1.1 LUNG CANCER

1.1.1 Epidemiological facts

Lung cancer is one of the most common diseases worldwide and a leading cause of death in adults. Despite new techniques of detection and treatment, the 5-year survival rate for lung cancer patients continues to be $< 15\%$ (Fry *et al.*, 1996). The main reason for this low survival rate is that neoplastic lesions are usually detected at a late invasive stage. Early detection of lung cancer, preferably in stage I or carcinoma *in situ*, can increase the 5-year survival rate.

In many countries lung cancer is most frequently diagnosed between the sixth and the seventh decade of life. While lung cancer has been predominantly a disease of men, the increase in cigarette smoking by women has changed this situation dramatically. In most developed countries mortality rates range from 35 to 95 deaths per 100,000 in men and 10 to 20 deaths in women (Cancer Rates and Risks, 1997). Every year approximately 46,000 cases of bronchial carcinoma are diagnosed in Germany, and around 40,000 patients die from this disease (Statistisches Bundesamt, 1996).

Lung cancers are of epithelial origin. Epithelial bronchogenic carcinomas can be divided into three categories on a histological basis (Table 1): 1. benign, 2. dysplasia and carcinoma *in situ*, 3. malignant. The malignant tumors (class III) are further subdivided into small cell carcinoma (SCLC) and three other groups: squamous cell carcinoma, adenocarcinoma, and large cell carcinoma, which are termed non-small cell lung cancer (NSCLC) (WHO, 1997). The minor groups, adenosquamous carcinoma, carcinoid tumor, and others comprise only 5% of the total.

Non-small-cell lung cancer is the most common lung malignancy, accounting for 75% of all lung cancers. At the time of diagnosis, approximately 60% of non-small-cell lung cancer cases are locally advanced or metastatic, and more than 85% of patients diagnosed with this neoplasm die. The 5-year survival rate of patients presenting with locally advanced disease is about 10%, and for those with stage IV disease survival drops to 1% (Mountain, 1997). As this situation has not changed for the past two decades, new approaches for early diagnosis and more effective treatment are needed.

Table 1. World Health Organization histological classification of epithelial bronchogenic carcinoma (1997).

Class I	Benign
Class II	Dysplasia and carcinoma <i>in situ</i>
Class III	Malignant
A.	Squamous cell carcinoma (epidermoid) and spindle (squamous) carcinoma
B.	Small cell carcinoma
	1. Oat cell
	2. Intermediate cell
	3. Combined oat cell
C.	Adenocarcinoma
	1. Acinar
	2. Papillary
	3. Bronchoalveolar
	4. Mucus-secreting
D.	Large cell carcinoma
	1. Giant cell
	2. Clear cell

1.1.2 Etiology of bronchial carcinoma

Approximately 90% of lung cancers develop in individuals who have a history of tobacco consumption. In addition, a variety of occupational and environmental carcinogens increase the risk of lung cancer. Occupational exposure to asbestos, radon, and metals such as beryllium (known to be an animal carcinogen), copper, chromium, nickel, arsenic, and coal products carries an increased risk for lung cancer which is independent of that of smoking (Fraumeni, 1982). A dose-response effect has been established for occupational and probably non-occupational exposure to asbestos (Seidman *et al.*, 1996). This effect is synergistic with that of tobacco smoke (Kjuus *et al.*, 1986). While asbestos exposure increases the risk of lung cancer by fivefold among smokers (Hammond *et al.*, 1979), radon exposure increases it by about threefold (Samet, 1989). The evidence of risk from environmental exposure to radon has been considered equivocal, but a meta-analysis of the eight largest domestic studies showed a significantly increased trend for lung cancer risk from indoor radon exposure. There is no evidence that the risk lessens if the dose is reduced (Lubin and Boice, 1997).

Dietary habits seem to influence lung cancer risk as well. Several studies have demonstrated that a diet deficient in anti-oxidant micronutrients such as carotenoids and vitamins C and E, which act as free-radical scavengers, and selenium, a component of anti-oxidant enzymes,

may increase the risk of lung cancer (Kuale *et al.*, 1983; Ziegler, 1989). Although evidence for the involvement of these individual components is contradictory, the results of two studies suggested an inverse association between vegetable and fruit intake and lung cancer (Steinmetz *et al.*, 1993; Le Marchand *et al.*, 1993).

Molecular genetic analyses suggest that there may also be a genetic predisposition to certain types of cancer. An increased frequency of expression of certain oncogenes or tumor suppressor genes (e. g., ras and p53) or genes encoding enzymes involved in the metabolism of carcinogens may be associated with an increased risk of lung cancer (Heighway *et al.*, 1986; Shields, 1993). Chromosome abnormalities are present in lung cancer cells, but it is far from clear that these anomalies are the cause of the cancer rather than the result of the genetic instability observed in malignant transformation (Birrer and Minna, 1988). The causal chain of genetic changes has not yet been elucidated.

The definitively most effective way of decreasing death rates from lung cancer is prevention, i.e., to stop smoking. Squamous and small cell carcinomas as well as adenocarcinomas are associated with smoking. Their relative risk increases with the number of cigarettes smoked, the duration of smoking, the lower the age when starting to smoke, the extent of inhalation, the tar and nicotine content of the cigarettes smoked, and the use of unfiltered cigarettes (Loeb *et al.*, 1984). Unfortunately, there is a long latency between stopping smoking and risk normalization (Beckett, 1993). The risk of carcinoma correlates with the amount of smoked cigarettes. The so-called pack years factor is the product of the daily smoked cigarette packs and the years of consumption. This means that even in cases of abstinence for 20 or 30 years, the cancer risk for people who quit smoking remains higher than for people who have never smoked (Samet, 1991).

The tobacco business plays a very important financial role in the world economy. Alone in Germany tobacco consumption continues to rise annually by about 1.5%. The German Public Treasury reported in 1998 tax revenues from tobacco products amounting to 22 billion DM. This probably explains why the Government does not fight nicotine abuse more energetically.

1.1.3 Diagnostic approaches to lung cancer

Since early lung cancer lesions do not cause symptoms, less than 13% of lung cancer patients can be successfully treated with the help of surgery, chemotherapy, or radiotherapy. Chest

INTRODUCTION

symptoms usually appear when the cancer is advanced, and then only palliative treatment is possible. Experience with other organs containing epithelial cells such as the cervix, esophagus, and colon has shown that if the neoplastic lesions can be detected and treated during the intraepithelial stage, the cure rate can be improved (Lam *et al.*, 1993a).

Evidence of systemic symptoms may be detected only by taking a detailed history. A normal clinical examination does not exclude the possibility of lung cancer, particularly in the presence of finger clubbing. Therefore, patients with unexplained or persistent chest symptoms should have a chest X-ray (Thatcher, 1998). Chest X-ray used to be one of the most important tools in the diagnosis of lung cancer. It detects some tumors, but in case of hidden tumors an X-ray must be repeated after a couple of weeks. X-ray does not exclude the possibility of mediastinal tumors. Computed tomography (CT) provides a far better resolution of the lung lesions than X-ray film. Moreover, CT imaging can often detect lesions that cannot be resolved on X-ray film. It also allows the measurement of hilar and mediastinal lymph nodes and the investigation of the metastatic status of the liver and adrenal glands for use in staging. Magnetic resonance imaging (MRI) does not offer any advantage over CT scanning, and the clinical value of radionuclide scanning is limited by its lack of specificity (Kies *et al.*, 1978; Little *et al.*, 1986).

It is important to note that successful diagnosis and therapy of bronchial carcinoma depend on the histology of the neoplasias and their spread. Despite the advanced treatment modalities for small intraepithelial neoplastic lesions in the tracheo-bronchial tree, the identification and localization of such tumors remain problematic. Novel methods for detecting and localizing early lung cancer, therefore, deserve particular attention. One such method is a solid-state microscopy that is used for screening the cytology of sputum specimens. Sputum cytology is the only non-invasive method that can detect pre-malignant lesions or carcinoma *in situ* in the tracheo-bronchial tree. Unfortunately, the clinical benefit of sputum cytology is low (Lam *et al.*, 1993b). If three sputum samples are obtained, it is possible to diagnose up to 80% of central tumors, but the method's efficacy decreases for peripheral tumors, plummeting to 20% for those less than 3.0 cm in diameter (Ginsberg, 1997). It is, however, possible to improve the method's sensitivity by measuring the spatial variability of deoxyribonucleic acid (DNA) distribution in the nuclei of normal bronchial epithelial cells. Normal cells growing in the proximity of cancerous cells exhibit different DNA distribution patterns than normal cells of

individuals without cancer. This phenomenon is known as malignancy-associated changes (MAC; Burger *et al.*, 1981).

Sputum examination has one limitation: it does not provide information about the site of origin of the malignant cells. Currently, bronchoscopy is the only available diagnostic tool that can localize small, radiologically occult early cancers and provide specimens for cytological and histological investigations. Although it is an invasive technique, it can be safely performed under local anesthesia, with or without sedation. Nevertheless, the detection and localization of occult cancers by conventional fiber optic bronchoscopy still present difficulties. The use of conventional white light bronchoscopy prior to surgery is likely to miss significant dysplasia or carcinoma in situ in about 60 to 70 percent of cases. The main reason for this is the size of such carcinomas: they are only a few cell layers thick and have a surface diameter of a few millimeters (Woolner *et al.*, 1984). These small, thin lesions may not produce any abnormality that is visible to conventional white-light bronchoscopy. In some cases, subtle changes such as an increase in redness, granularity, or a slight thickening of the mucosa may be noted. While these changes are often observed with malignancies, they may also be associated with a variety of chronic irritative conditions (Lam *et al.*, 1993a).

1.1.4 Early detection, staging, and prognosis

Recent advances in imaging technology have not yet fulfilled their promise for screening lung cancer patients at risk. Strategies for dealing with early lung cancer fall into three categories: true screening programs for the evaluation of asymptomatic individuals; early detection programs for the evaluation of patients presenting with ambiguous symptoms; and early intervention programs aimed at stopping or reversing the processes involved in lung carcinogenesis before the development of invasive malignancy (Wagner and Ruckdeschel, 1995).

The value of screening for lung cancer in persons at increased risk remains controversial. Four randomized studies have been performed: Memorial-Sloan Kettering (Melamed *et al.*, 1984) and John Hopkins Lung Projects (Frost *et al.*, 1984) compared annual chest roentgenograms in a control group with roentgenograms and sputum cytology in an experimental group. The Mayo Lung Project and the Czechoslovak study compared regular and frequent rescreening roentgenograms in an experimental group with sporadic or infrequent re-screening in a control group. These trials came to the conclusion that screening

INTRODUCTION

for lung cancer is not beneficial. Improvements of certain aspects of screening were also taken into consideration, but only automated image cytometry in sputum analysis seems to yield better results than classic sputum cytology (Palcic *et al.*, 1991).

Restricting screening to smokers with impaired expiratory flow might enhance its efficacy, as smokers with chronic obstructive pulmonary disease (COPD) have more than threefold higher incidence of lung cancer than do smokers without COPD (Petty, 1995). The use of low-dose CT scanning might improve the early detection of small cancers by standard and lateral roentgenograms (Ryan, 2001). Furthermore, the search for potential tumor markers detectable in early bronchial neoplasia (Lang *et al.*, 2000) or in blood is still ongoing (Chen *et al.*, 1996). No screening strategy has yet been shown in a prospective trial to reduce lung cancer mortality. However, screening of a high-risk group of male smokers 45 years of age or older could provide a shift to diagnosis at an earlier stage and consequently make the findings of CT studies more reliable (Wagner, 1995).

It is important to estimate the stage of disease at diagnosis in order to determine the most suitable management for each individual patient. The method of staging now used worldwide is the TNM notation proposed by Denoix (1994). This system is based on the work of Mountain (Mountain *et al.*, 1974; Mountain, 1986, 1989, 1997). **T** stands for tumor (its size and how far it has spread within the lung and to nearby organs), **N** for spread to lymph nodes, and **M** for metastasis. The TNM classification provides a semi-quantitative description of the local and distant spread of tumor growth. Primary tumors are divided into four categories (T₁–T₄), depending on size and local infiltration. Lymph node spread is described according to site (N₁–N₃), and distant metastatic spread as absent (M₀) or present (M₁). Four stages: I, II, III (subdivided into IIIA and IIIB), and IV are defined. A new staging system has recently been approved by the UICC (International Union Against Cancer) and AJCC (American Joint Committee on Cancer) in which stages I and II have also been subdivided (Ginsberg, 1997; Table 2). Mediastinoscopy – a technique for determining the involvement of superior mediastinal lymph nodes - can facilitate accurate staging of tumors, which have not already been assessed as inoperable. Video-assisted thoracoscopy allows the identification of peripheral nodules that can then be biopsied or excised using minimally invasive techniques (Mack *et al.*, 1992). Thoracotomy allows the most refined staging, but may differ from assessments based on previous diagnostic procedures (Fernando and Goldstraw, 1990).

Table 2. Staging of non-small cell lung cancer (WHO, 1997)

Current staging*	
Stage 0	Carcinoma <i>in situ</i>
Stage IA	T ₁ N ₀ M ₀
Stage IB	T ₂ N ₀ M ₀
Stage IIA	T ₁ N ₁ M ₀
Stage IIB	T ₂ N ₁ M ₀
	T ₃ N ₀ M ₀
Stage IIIA	T ₃ N ₁ M ₀
	T ₁₋₃ N ₂ M ₀
Stage IIIB	T ₄ any N M ₀
	Any T N ₃ M ₀
Stage IV	Any T any N M ₁

* Staging is not relevant for occult carcinoma, designated TxNoMo.

The two most important functions of a staging system are to estimate the patient's prognosis and to guide suitable treatment. Unfortunately, staging systems are neither perfect nor can they provide absolute criteria with which every clinical scenario can be managed (Mountain, 1986). Even so, surgery remains the treatment of choice for all patients with clinical stage I or II disease (Naruke *et al.*, 1988). Surgical resection is, however, possible in only 20% to 30% of all patients with NSCLC, mainly because of locally advanced disease and a high incidence of distant metastases. For early-stage resectable NSCLC, the 5-year survival rate is 60% for stage I, 40% for stage II, and 20% for limited stage IIIA; in case of mediastinoscopy-positive N₂ disease, 5-year survival drops to 5% - 10%. The 5-year survival rate is even 0% in unresectable, locally advanced, bulky stage IIIA or IIIB diseases (Mountain, 1997; Nesbitt *et al.*, 1995).

In SCLC and many other malignancies, the serum lactate dehydrogenase levels appear to be an independent survival parameter (O'Connell *et al.*, 1986; Sørensen *et al.*, 1989). Other risk factors under investigation include ploidy, expression of epidermal growth factor receptors, neuroendocrine and genetic markers on the tumor cells (Ginsberg *et al.*, 1997) and a carbohydrate antigen related to the blood group antigen H (Miyake *et al.*, 1992). SCLC has a greater metastatic potential and is more sensitive to radiation treatment and chemotherapy than NSCLC. In the past, the most consistent prognostic variable in small-cell lung cancer was the spread of disease as determined by staging. The Veteran's Administration Lung Cancer Study Group developed a simple two-stage system for SCLC: **limited disease (LD)**

usually means that the cancer involves only one lung and the lymph nodes on the same side of the chest. **Extensive disease (ED)** signifies that the cancer has spread to the other lung, to lymph nodes on the other side of the chest, or to distant organs. The probability of survival for LD patients is significantly superior to that for patients with ED (Shepherd *et al.*, 1993).

1.1.5 Normal lung physiology and lung cancer biology

The lungs are two sponge-like organs located in the chest on the right and the left sides. Each is divided into several lobes. Together with the heart, great vessels, esophagus, thymus, and certain nerves, the lungs completely fill the thoracic cavity. They have a highly organized structure consisting of air-containing tubes, alveoli, blood vessels, and elastic connective tissue. Air is drawn in via the nose or mouth, through the trachea or windpipe, and then into the bronchi, tubes that enter into each lung. The bronchi divide further into bronchioles. The airways within the lungs are the continuation of those connecting the lungs to the nose and mouth. Termed the conducting portion of the respiratory system, these airways constitute a series of highly branched tubes that become smaller in diameter and more numerous at each branching, much like arteries and arterioles. The smallest of these tubes end in tiny blind sacs, the alveoli, which number approximately 300 million. All portions of these air pathways and alveoli receive a rich supply of blood via the blood vessels, which constitute a large portion of the total lung tissue (Fig. 1).

This conducting system of tubes serves several important functions:

- The epithelial linings contain hair-like projections, called cilia that constantly beat toward the pharynx. These cilia line the respiratory airways to the end of the bronchioles. In the same regions are epithelial glands, which secrete mucus.
- Particulate matter, such as dust contained in the inhaled air, adheres to the mucus, which is constantly moved by the cilia to the pharynx, and is then swallowed. Besides keeping the lungs clean, this mucus escalator is an important component of the body's defenses against bacterial infection, since many bacteria enter the body on dust particles. A major cause of lung infection is probably due to a reduction of ciliary activity by noxious agents; a single cigarette can cause the cilia to become non-motile for several hours. This coupled with the stimulation of mucus secretion induced by these same agents, may result in partial or complete airway obstruction due to the

stationary mucus. A second protective mechanism is provided by the phagocytic cells, which are present in large numbers in the respiratory tract lining. These cells, which engulf dust, bacteria, and debris, are also injured by cigarette smoke and other air pollutants.

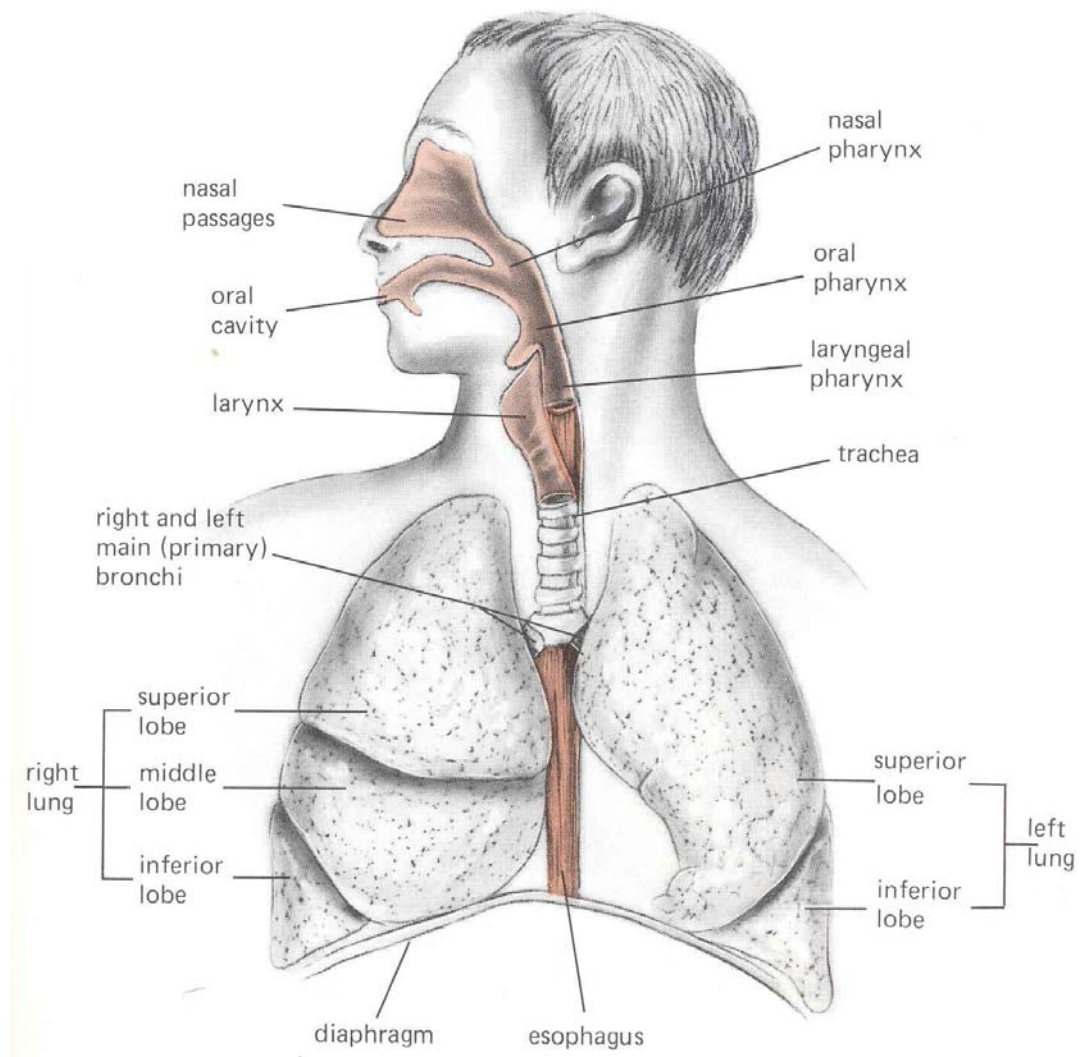


Figure 1: Schematic drawing of the human airway system. The airways and the esophagus are indicated in red. This picture was taken from Human Physiology, The Mechanisms of Body Function, Vander A. J, Sherman J. H. and Luciano D. S.; third edition 1980, McGraw-Hill Book Company.

- As air flows through the respiratory passages, it is warmed and moistened by contact with the epithelial lining.

INTRODUCTION

- The vocal cords, two strong bands of elastic tissue, lie stretched across the lumen of the larynx. The movement of air past them causes them to vibrate, providing the tones of phonation.
- The walls of the respiratory airways contain richly innervated smooth muscle sensitive to certain circulating hormones, e. g., epinephrine. Contraction or relaxation of this muscle alters the resistance to air flow.

Gas exchange in the lungs takes place at the alveoli. They are lined by a continuous single thin layer of epithelial cells resting on a thin basement membrane that in turn rests on a very loose mesh of connective tissue elements constituting the interstitial space of the alveolar walls. Most of the alveolar wall is occupied by capillaries, whose endothelial lining is separated from the alveolar epithelial lining by only the very thin interstitial space.

The alveolar epithelium also contains some thicker specialized cells (type II cells) that produce surfactant. The interstitial space contains phagocytic cell (macrophages) and other connective tissue cells, which function as part of the lung's defense mechanisms. Finally, pores in the alveolar membranes permit some flow of air between the alveoli. This collateral ventilation can prove very important when the duct leading to an alveolus is occluded by disease, since some air can still enter via pores between the alveolus and adjacent alveoli (Vander *et al.*, 1980; Fig. 2).

As mentioned above, the lung consists anatomically and physiologically of at least three separate parts. The trachea and main bronchi are normally lined by ciliated, pseudostratified, columnar epithelium and also contain neuroendocrine cells. The predominant types of tumors arising in large central airways are squamous cell and small cell carcinomas. The thickness of the epithelium lining gradually lessens as the airways become smaller.

The pseudostratified, ciliated columnar cells gradually give way to ciliated columnar and finally ciliated cuboidal cells in the terminal bronchioles. Epithelial mucous cells are found throughout the conducting airway. Interspersed among the cuboidal cells of the terminal and respiratory bronchioles are Clara cells, thought to produce the mucus covering for these small airways.

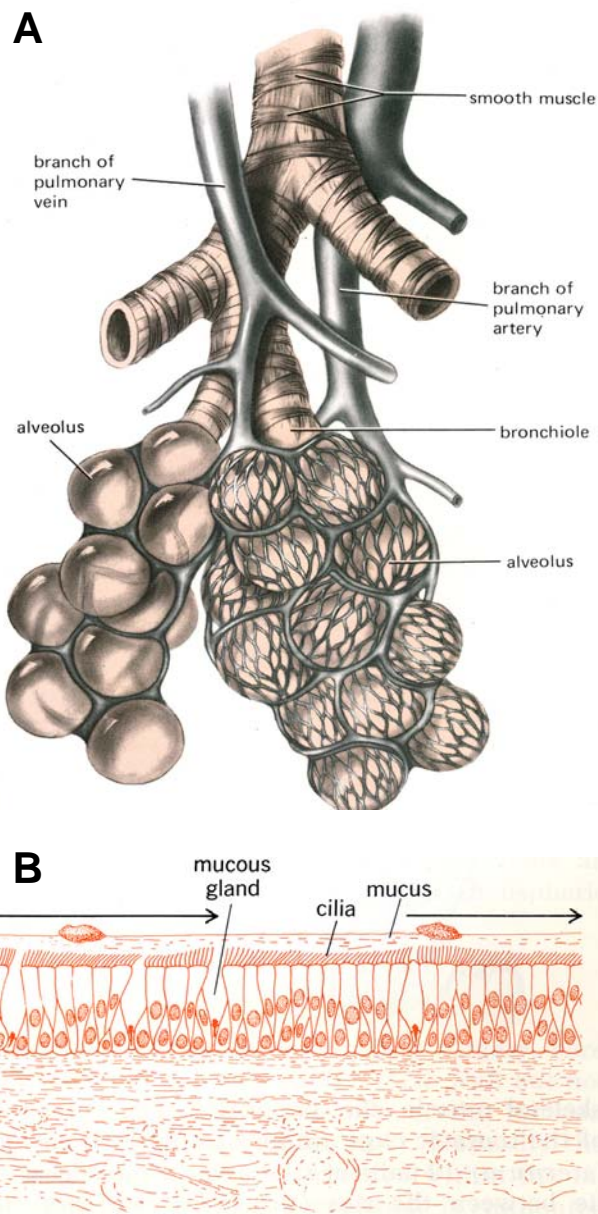


Figure 2: Macroscopic and microscopic components of the pulmonary system. (A) Bronchioles and alveoli represent the terminal structures of the lung where the gas exchange takes place. Note the mesh-like organization of the capillaries. (B) Schematic drawing of the ciliated pseudostratified epithelium of the alveoli. This picture was taken from Human Physiology, The Mechanisms of Body Function, Vander A. J, Sherman J. H. and Luciano D. S.; third edition 1980, McGraw-Hill Book Company.

and possibly also the differences in local metabolic transformation of procarcinogens and the effects of the extracellular matrix and paracrine growth factors on carcinogenesis (Mulshine *et al.*, 1992).

The predominant histology seen in peripherally arising lung cancers is adenocarcinoid. Lung adenocarcinomas can be divided morphologically into solid and bronchoalveolar types. At the cellular level, these tumors arise from type II pneumocytes that normally produce surfactant. The bronchoalveolar carcinomas are believed to arise from Clara cells that play a role in xenobiotic metabolism. Each of these cell types expresses characteristic differentiation markers that may form the basis for detection and therapeutic strategies (Table 3; Mulshine *et al.*, 1992).

Approximately one-fifth of lung carcinomas are undifferentiated large cell tumors that cannot be assigned to one of the above lineages. All histological types can be found admixed within a single tumor. This admixture is consistent with their development from a common stem cell of variable differentiation potential. The different tumor histologies and anatomic location of lung tumors may derive from the normal distribution of partially committed cell lineages, the variable penetration of different carcinogenic components of cigarette smoke into different regions of the lung,

Table 3. Markers of lung cancer differentiation

<i>Adenomatous</i>	<i>Neuroendocrine</i>	<i>Squamous</i>
Clara 10-kD protein	Chromogranin A	Cytokeratin
Surfactant-associated protein	Leu 7	Involucrin
Carcinoembryonic antigen	Neuron-specific enolase	Epidermal growth factor receptor
<i>ras</i> oncogene	Dopa decarboxylase	Transglutaminase

Normal cell and tumor types are characterized by a typical rather than absolute organ distribution. Lung cancers of all cell types may be found in any location within the tracheobronchial tree and lung. This finding implies that, while there may be some very early events common to the development of all types of lung cancer, further preneoplastic and neoplastic development can follow along several divergent lines. Screening strategies should be able to detect each of these. The shift observed in the proportion of lung cancers of the various histological types over the past several decades, with predominant cell type changing from squamous cell to adenocarcinoma, should be considered in a theory of lung cancer initiation and promotion (Devesa *et al.*, 1991).

1.2 NEW TECHNIQUES FOR FLUORESCENCE DETECTION OF LUNG CANCER

1.2.1 5-Aminolevulinic acid induced protoporphyrin IX

At the beginning of the twentieth century, many researchers started developing the concept of fluorescence detection of tumors. In 1933 Sutro and Burman observed that when surgically excised breast tissue was exposed to Wood's light, normal breast tissue fluoresced green, whereas breast cancer tissue fluoresced purple (Sutro and Burman, 1933). Since the color of tissue autofluorescence induced by ultraviolet light is variable and the intensity of the fluorescence is low, hence the difficulty to see the color, most of the research in fluorescence bronchoscopy since the 1960s has employed exogenous compounds such as hematoporphyrin derivatives or Photofrin to enhance the ability to detect early lung cancer (Lam and Profio, 1995). This kind of bronchoscopy is based on the fact that normal tissue fluoresces differently than abnormal tissue when exposed to a certain wavelength of light. According to this principle there are two methods for detecting early lung cancer: 1. the detection of the specific

changes in autofluorescence of tumor and normal tissue, and 2. the application of fluorochromes, which are preferentially accumulated in tumor tissues. In early investigations, patients were treated with photosensitizers such as hematoporphyrin derivative (HpD) or its partially purified form, dihematoporphyrin ether/ester (DHE), also known as Photofrin (Lipson *et al.*, 1961, 1964; Dougherty *et al.*, 1984).

The principles of fluorescence diagnosis of tumors are as follows: **a.** HpD or Photofrin emits a red fluorescence when excited by violet light, and this can be detected by sensitive imaging devices; and **b.** the concentration of HpD or Photofrin in malignant tumors is higher than in most nonmalignant tissue; thus tumors can be detected by their more intense fluorescence (Cortese *et al.*, 1979). However, the use of fluorescence detection with synthetic porphyrin mixtures still has certain limitations in diagnostic effectiveness mainly, due to side effects such as skin photosensitization and interference by tissue autofluorescence (Dougherty *et al.*, 1990). Therefore, new substances like protoporphyrin IX (PPIX) are being investigated.

It is well known that the concentration of endogenous protoporphyrin IX (PPIX), the immediate precursor in heme biosynthesis, can be enhanced by administration of 5-aminolevulinic acid (5-ALA). The biosynthetic pathway to heme consists of eight discrete enzyme-catalyzed steps, which are distributed between the mitochondrial and the cytosolic compartments of the cell (Batlle, 1993; Fig. 3).

The 5-aminolevulinic acid synthase (ALA synthase) reaction occurs in two steps in the mitochondria: 1. condensation of succinyl CoA and glycine to form enzyme-bound α -amino- β -ketoacid, and 2. decarboxylation of α -amino- β -ketoacid to form 5-aminolevulinate. This is the rate-limiting reaction of heme synthesis in the stroma, and it is, therefore, strictly regulated. There are two major means of regulating the activity of the enzyme. **The first** is by regulating the synthesis of the enzyme, which is important because its half-life is only about one hour. Enzyme synthesis is represented by heme and hematin. **The second** control is feedback inhibition by heme and hematin. Hence, heme plays a dual role in decreasing its own rate of synthesis. The product of the reaction, 5-ALA, diffuses into the cytoplasm, where the subsequent steps of heme synthesis take place.

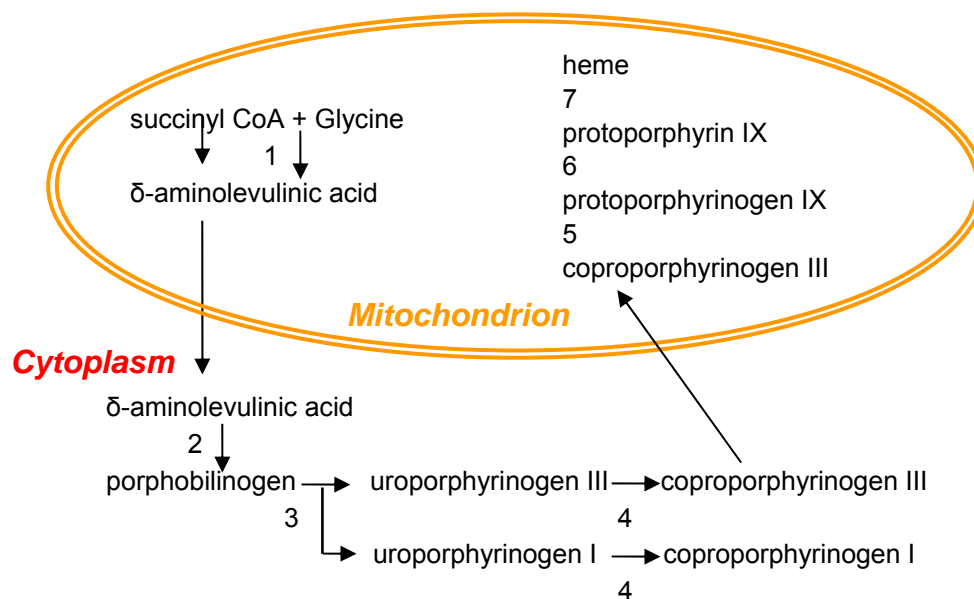


Figure 3: Heme biosynthesis – an overview. Note that heme biosynthesis takes place in both the mitochondrion and the cytoplasm of the cell. Therefore, the enzymatic machinery is located in both compartments and two of the intermediates, δ -aminolevulinic acid and coproporphyrinogen, have to be shuttled into the cytoplasm and the mitochondrion, respectively. Taken from NetBiochem; copyright: Baggott and Dennis, 1994, 1995.

The ALA dehydratase reaction is a condensation of two molecules of ALA to form porphobilinogen, the first pyrrole. The next step is the synthesis of uroporphyrinogen I and III. The production of uroporphyrin III requires two enzymes, and the substrates are four molecules of porphobilinogen. The first reaction is catalyzed by uroporphyrinogen I synthase. The second reaction is catalyzed by uroporphyrinogen III cosynthase. Uroporphyrinogen decarboxylase decarboxylates the acetic acid groups, converting them into methyl groups. The physiologically significant substrate is uroporphyrinogen III. The product is coproporphyrinogen III, which is transported back to the mitochondria, where the remainder of heme synthesis occurs. The mitochondrial enzyme, coproporphyrinogen III oxidase, catalyzes the next reaction, which produces protoporphyrinogen IX. Protoporphyrinogen IX oxidase converts the methylene bridges between the pyrrole rings to methenyl bridges. Resonance of double bonds around the entire great ring, with its resulting stabilization, is now possible. The product is protoporphyrin IX (PPIX). Finally, ferrochelatase adds iron (II) ions to PPIX, forming heme. The enzyme requires iron (II), and the reducing agents ascorbic acid and cysteine (Fig. 4).

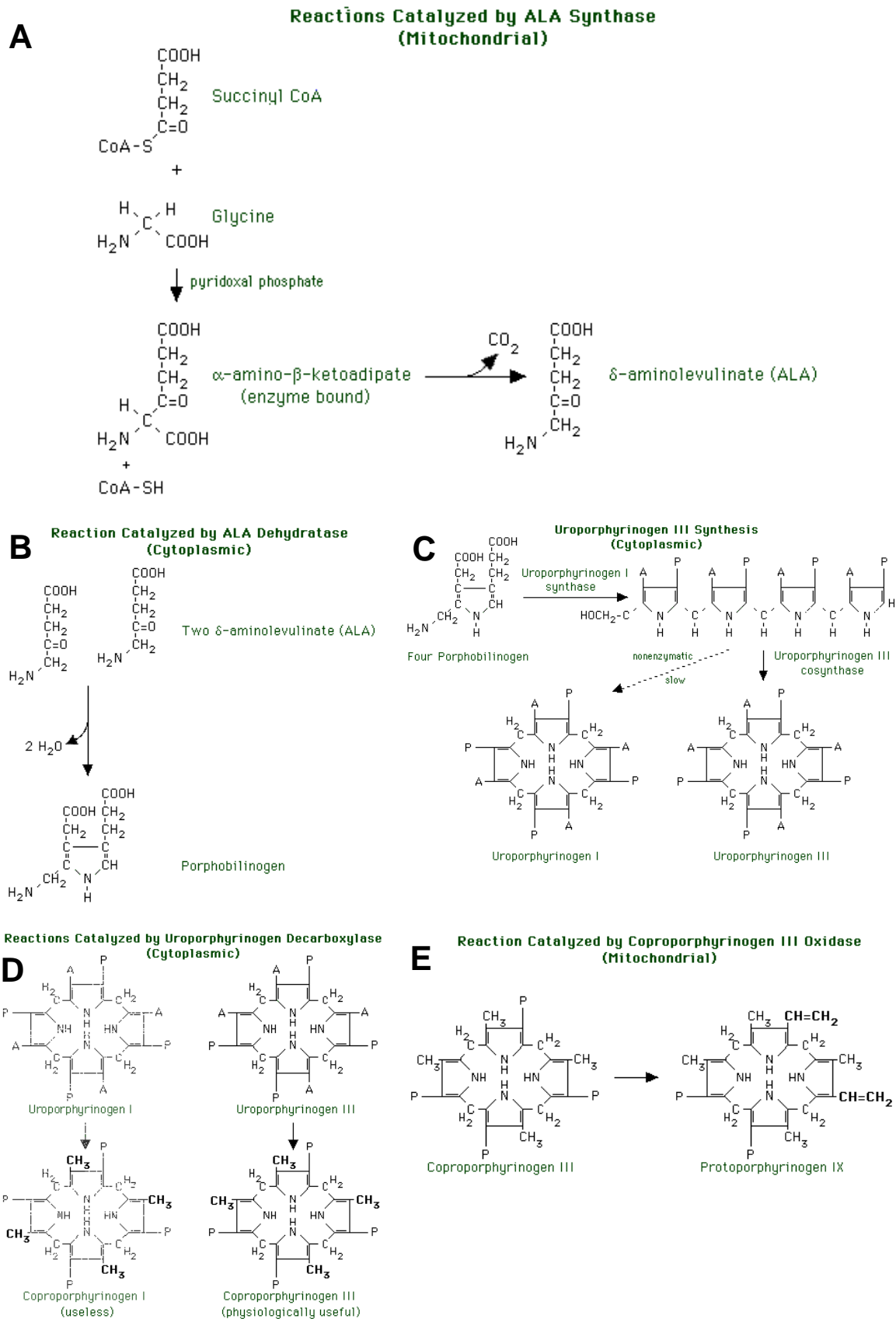


Figure 4A-E: Biosynthesis of Protoporphyrin IX from 5-aminolevulinic acid. Description see Legend to Figure 4G, F.

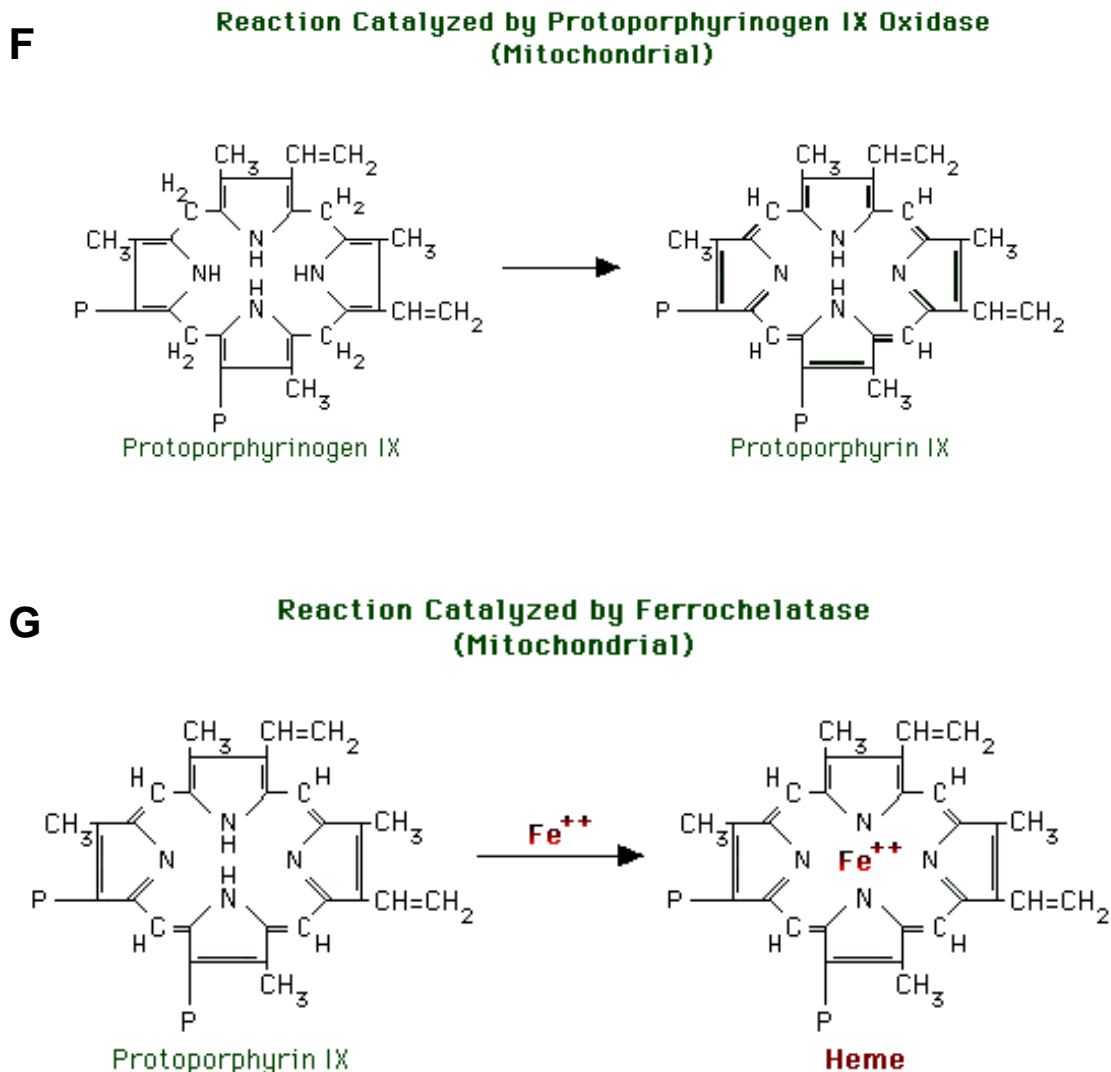


Figure 4F, G: Biosynthesis of Protoporphyrin IX from 5-aminolavulinic acid. Taken from NetBiochem; copyright: Baggott and Dennis, 1994, 1995.

It has been suggested that the deficiency in iron ions or ferrochelatase, the enzyme required for conversion of PPIX to heme, in tumors results in the accumulation of PPIX in contrast to normal host tissue (Batlle, 1993). According to Abels *et al.* (1997) and Fritsch *et al.* (1997), however, selective formation of PPIX in tumors is not primarily due to reduced ferrochelatase activity, but rather to active uptake of ALA.

PPIX is an efficient photosensitizer. Kennedy and colleagues initiated clinical applications of 5-ALA topically to treat skin cancer. Subsequently, 5-ALA was investigated for fluorescence detection and localization of dysplasias and early-stage malignant lesions in a variety of body sites (Kennedy *et al.*, 1990).

The clinical use of ALA is attractive for two reasons. First, PPIX preferentially accumulates in tumor tissue to a greater extent than other photosensitizing drugs, thus minimizing damage to normal surrounding tissues during treatment (Peng *et al.*, 1997; Webber *et al.*, 1997). Second, PPIX is rapidly cleared from the body, resulting in skin photosensitization lasting only 48 h (Regula *et al.*, 1995; Kennedy and Pottier, 1992).

As mentioned earlier, CIS and preneoplastic lesions (dysplasias) are difficult to detect and localize by standard white-light bronchoscopy. Novel fluorescence techniques were therefore developed to enhance the visual contrast between tumor and healthy tissue. Recently, fluorescence bronchoscopy has used 5-ALA administered as an aerosol (Baumgartner *et al.*, 1996). Preliminary clinical results showed that in more than 100 patients with an established or suspected lung cancer, the inhalation of 200 mg of 5-ALA diluted in 5 ml 0.9% NaCl solution by a conventional jet nebulizer or a volume-and-flow controlled inhalation device for a homogeneous deposition of a dose of 60 mg in 2.5 ml 0.9% NaCl solution is both feasible and safe. No side effects were registered apart from an occasional cough in patients who often have bronchitis. A relative disadvantage of exogenously applied 5-ALA is that the bronchoscopy can only be done (about 90–120 min) after the inhalation of 5-ALA, and it is also necessary to induce high levels of PPIX (Huber *et al.*, 1999).

1.2.2 5-ALA esters

Photodynamic diagnosis (PDD) and photodynamic therapy (PDT) are based on the selective accumulation of PPIX in tumorous tissue. Despite successful results after applying 5-ALA to detect or to treat several types of malignancies, there are significant limitations to the topical application of this compound because of its hydrophilic characteristics. Therefore, further improvements are needed.

Recently, results have shown that the chemical transformation of 5-ALA into its more lipophilic esters circumvents certain limitations of ALA-induced PPIX, such as shallow tissue penetration and inhomogeneous biodistribution, and enhances the total PPIX formation. In order to obtain maximal flux across biological barriers, balanced partition coefficients and good water and lipid solubilities are required. Excessively lipophilic substances may be accumulated in cell membranes, and the passive transport of hydrophilic molecules across these barriers may be hindered (Lange *et al.*, 1999).

INTRODUCTION

Kloek and colleagues (Kloek and Beijersbergen van Henegouwen, 1996, Kloek *et al.*, 1998) synthesized a range of ALA esters using alcohols of increasing carbon chain length, and demonstrated in cell lines and animal models that several ALA pro-drugs are capable of being absorbed, de-esterified, and converted into PPIX with higher efficiency than ALA itself. Gaullier *et al.* (1997) found that esterification of ALA with aliphatic alcohols reduces by 30-150-fold the amount of drug needed to reach the same level of PPIX accumulation as that obtained with non-esterified ALA in human cell lines. Furthermore, the maximum PPIX accumulation in cell lines was higher when long-chain 5-ALA esters were used rather than short-chained ALAs.

The mechanism and rate of ALA uptake in human cells are still not known (Peng *et al.*, 1997). ALA-methyl, -ethyl, and -propyl esters have been shown to induce more porphyrin fluorescence than ALA in normal mouse skin (Peng *et al.*, 1996). This is probably not due to enhanced uptake of these compounds into the cells of the skin but rather to enhanced penetration through the interstitial space of the tissue. The lower amounts of PPIX in cells treated with short-chained ALA esters may be caused by a low rate of uptake through a transport protein and slow passive diffusion, or to a slow rate of intracellular deesterification. The production of PPIX induced by ALA esters is related to the length of the aliphatic alcohol used for esterification (Gaullier *et al.*, 1997).

Studies performed by Davey *et al.* (1988) and Sawaki *et al.* (1990) showed that the use of esterified ALA for fluorescence labeling of cells is highly dependent on intracellular esterase activity. This might be a limitation for the use of ALA esters in PDT. Although in some cases the esterase content is higher in tumor cells than in their normal counterparts, the opposite has also been demonstrated (Markey *et al.*, 1993; Dube *et al.*, 1984).

Van den Bergh *et al.* (1999) have carried out experiments in an organ culture of pig bladder mucosa in order to screen the following 5-ALA esters: ALA-octyl, -butyl, -hexyl, methyl, and -ethyl. According to their study, ALA-hexyl ester and ALA-octyl ester gave the best results compared with ALA itself. 5-ALA showed less than half the maximum fluorescence intensity than the best esters, although two orders of magnitude more ALA was applied than ALA-hexyl ester or ALA-octyl ester. There was also a more homogeneous tissue distribution of ALA-hexyl ester than of ALA. Thus, these tests look promising for the application of 5-ALA esters in PDT.

1.2.3 Optical properties of porphyrins

The prerequisite for a dye to be a sensitizer is that its molecules must be able to undergo intersystem crossing from the initially excited singlet state to the triplet state. The sensitizer in the triplet state can then either transfer electrons to an acceptor or accept electrons itself from a suitable substrate in a so-called type I reaction, or transfer its energy to other molecules, e. g., ground-state oxygen (type II). In a type II pathway the reactive singlet oxygen is formed; it can oxidize most biological molecules.

A type I mechanism results in hydrogen atom or electron transfer reactions between the sensitizer and some substrate or either radicals or radical ions, which can react with oxygen to yield the superoxide radical anion $O_2^{\cdot-}$. At low pH the superoxide radical anion can be protonated to form the reactive HO_2^{\cdot} radical. Direct electron transfer from the excited state of the sensitizer to molecular oxygen to produce $O_2^{\cdot-}$ is also classified as a type I process. In the type II process the energy transfer from sensitizer to ground-state oxygen produces the excited singlet state of oxygen, 1O_2 (Fig. 5).

$S + h\nu$	\rightarrow	$^1S^*$	Absorption yields singlet
$^1S^*$	\rightarrow	$S + h\nu_F$	Fluorescence
$^1S^*$	\rightarrow	$^3S^*$	Crossing results in a long-lived triplet state
$^3S^* + O_2$	\rightarrow	$S + ^1O_2$	Energy transfer yields singlet oxygen
$^1O_2^* + \text{tissue}$	\rightarrow	Necrosis	

Figure 5: Activation mechanism of type II sensitizers. Stable state molecules can also undergo inter-system crossing to produce more stable triplet states. Then triplet state molecules transfer energy to ground-state oxygen to produce excited singlet oxygen.

Both singlet oxygen and superoxide cause oxidative destruction of tissue. They constitute the basis for photodynamic cancer therapy.

The porphyrins and related compounds such as the chlorines, the bacteriochlorins, and the phthalocyanines represent an important class of photosensitizers, because they are used in PDT of neoplasias. The photosensitizing ability of porphyrins is apparent in patients having some inborn error of metabolism. Perhaps the best example is erythropoietic protoporphyria which is characterized by a defect in the enzyme ferrochelatase. The altered enzyme is less stable than the normal enzyme. Consequently a higher protoporphyrin concentration occurs in

the patient's serum than normal, and the skin of these patients is photosensitive (Dubbelman and Shuitmaker, 1992).

When PPIX is exposed to light of wavelengths within its absorption spectrum, some of the energy of the absorbed photons is emitted as red fluorescence. PPIX fluorescence in tissue peaks around 635 nm, there is a lower secondary emission peak in the far red zone around 700 nm. When sufficiently intense, these wavelengths can be visualized by endoscopic devices that have been modified for exciting and detecting of fluorescence (Lam *et al.*, 1993a).

1.2.4 Autofluorescence

Detection of dysplasia and carcinoma *in situ* can also be achieved without using any exogenous drug. Autofluorescence of bronchial tissue was shown to differ between normal and transformed epithelium. Bronchial mucosa emits fluorescent light, with a major peak at 520 nm (green) and a minor peak around 630 nm (red) when it is illuminated with monochrome blue light (442 nm). A 10-fold decrease in fluorescence and a proportional change from green to red light can be observed in bronchial carcinoma *in situ* and dysplasia. The reason for this decrease in autofluorescence in premalignant tissues is not yet clear. Most of the fluorescence comes from the submucosa. Several factors may be involved in the decrease of fluorescence in malignant tissues, such as a decrease in the amount of fluorophors, a high concentration of absorbing but non-fluorescing species, changes in the macromolecular composition of the extracellular matrix and an increase in the number of cell layers (Hung *et al.*, 1991; Lam and Becker, 1996; Qu *et al.*, 1994).

On the basis of these differences, Palcic and colleagues (1991) developed an imaging system that clearly delineates the exact site and size of these lesions. The lung imaging fluorescence endoscope (LIFE) was developed by the British Columbia Cancer Agency research staff in collaboration with Xillix Technologies Corporation in Vancouver, Canada. LIFE consists of a helium-cadmium laser light source (442 nm), two image-intensified, charged coupled device (CCD) cameras with green and red filters, respectively, a computer with an imaging board, and a color video monitor. Two images at different wavelengths (red and green) are simultaneously captured and precisely registered by the imaging board. The images are then combined and processed by the imaging board using a specially developed algorithm that allows normal tissue to be distinguished clearly from malignant tissue when displayed as a pseudocolor image on the video monitor. Normal tissue appears green, and tumor tissue,

brown or brownish red. Biopsies for pathological confirmation can be performed on an abnormal area under direct vision. Fluorescence bronchoscopy using tissue autofluorescence is not a separate bronchoscopic procedure and does not require exogenous fluorescent drugs. Performed at the time of standard fiber optic bronchoscopy under local anesthesia, it provides added information to the diagnostic procedure.

The LIFE system has been tested in several studies. The results of one of these studies showed that the sensitivity of white light bronchoscopy in detecting moderate and severe dysplasia and carcinoma *in situ* was 48.4% with a specificity of 94%. With fluorescence imaging, the sensitivity was 72.5% with the same specificity, representing a 50% improvement in sensitivity.

The LIFE system has been able to improve the endoscopic detection of early lung cancer using autofluorescence bronchoscopy (AFB). However, the complexity of this system does not allow direct comparison with white-light and autofluorescence imaging. Similar systems without a laser source have been developed in Japan and Germany. Stepp *et al.* (1997) in collaboration with Karl Storz, Germany, developed a system consisting of two main components: a Xenon light source with an excitation by blue light and optical filters built into the bronchoscope. This system provides a better light intensity and readily allows change of mode between the white light and autofluorescence during a bronchoscopy. This system can further be used to detect drug-induced fluorescence by integrating various additional filters.

1.3 OBJECTIVES OF THE STUDY

Lung cancer continues to be one of the most common malignancies in the world. Better screening procedures could increase patient survival rate. However, strategies for the early detection of lung cancer are still under development, and there are no suitable in vitro models that could help improve current diagnostic techniques such as fluorescence bronchoscopy and photodynamic therapy (PDT) of the lung.

The aim of this investigation was to improve an organ culture of normal human bronchial mucosa co-cultivated with human lung tumor cells (EPLC-32M1) to study clinically relevant aspects directly under conditions that preserve the morphology of the original tissue in vivo. Prompted by the experience and preceding publications of our group on this topic, this study had the following aims:

- To study the kinetics of 5-aminolevulinic acid induced protoporphyrin IX (PPIX) fluorescence in normal epithelium and tumorous tissue.
- To analyze the kinetics of 5-ALA esters in comparison with 5-ALA in the mini-organ model.
- To improve the three-dimensional mini-organ model by using GFP-transfected bronchial tumor cells for better visual contrast between tumor and normal areas. This could greatly help when evaluating the different pharmacokinetics of the above-mentioned substances.
- To develop a model of normal respiratory mucosa, which remains viable for a prolonged period of time so that other parameters such as tumor cell proliferation or invasion could be measured in the future.

In summary, the point in developing or improving this three-dimensional mini-organ model was to allow direct biological studies on clinical biopsy material under viable conditions. Nevertheless, the model mimics only certain biological characteristics of tumors in vivo; for example, circulation and blood supply are not included.

2 MATERIALS AND METHODS

2.1 BIOLOGICAL MATERIAL

Biopsies with a diameter of 1-2 mm were taken from the bronchial wall (normal tissue) of 150 patients, undergoing routine fiber optic bronchoscopy at the Department of Pulmonology, Klinikum Innenstadt, Ludwig-Maximilians University (LMU), Munich. This study was approved by the LMU Committee on Medical Research Ethics, and all patients gave their written consent prior to bronchoscopy.

The tumor cell line EPLC-32M1 was derived from a human squamous cell carcinoma (Bepler *et al.*, 1988), which has been classified as a non-small-cell lung cancer (NSCLC). According to the histological classification of the original tumor, it was a epidermoid lung cancer. The tumor cell line was kindly provided by Dr. G. Jaques from the Philipps University Medical Center in Marburg in 1998.

2.2 LAB MATERIAL

- Culture flasks, 25 and 75 cm², NUNC, Denmark
- Multi-well dishes, 24 wells, #662160, Greiner Labortechnik, Solingen, Germany
- Petri dishes, Ø35 mm, #627 160, Greiner Labortechnik, Solingen, Germany
- Disposable scalpels, #22, Feather, Cologne, Germany
- Glass Pasteur pipettes, Brand GmbH + Co., Wertheim, Germany
- Disposable serological pipettes, 2, 5, 10, 25 ml, FALCON, Becton Dickinson Labware, France, S.A
- Centrifuge tubes, 14 ml, #188 261, Greiner Labortechnik, Solingen, Germany
- Cryotubes, Cryo Vials, #121 277, Greiner Labortechnik, Solingen, Germany
- Slides, normal and superfrost 76 x 26 mm, Menzel, #01/002 and 01/003, ResoLab, Bad Oeynhausen, Germany
- Cover glasses, 18 x 18 mm, Menzel, #01/13, ResoLab, Bad Oeynhausen, Germany
- Counting chamber, depth 0.100 mm; 0.0025 mm², Neubauer, Brand, Germany
- Electronic pipette controller, Hirschmann, Germany
- Tips, Eppendorf, Netheler-Hinz GmbH, Hamburg, Germany

2.2.1 Cell culture medium and supplements

- **RPMI 1640**, #F-1215, Biochrom, Berlin, Germany
- **BEGM**, Bronchial Epidermoid Growth Medium, #C-21260, ProCell, Heidelberg, Germany
- plus **Supplements**, #C-39160, ProCell, Heidelberg:
 - 2 ml Bovine Pituitary Extract
 - 0.5 µg/ml epidermal growth factor (EGF), human, recombinant
 - 5 mg/ml insulin, bovine
 - 500 µg/ml hydrocortison
 - 500 mg/ml epinephrine
 - 6.5 ng/ml tri-iodo-L-thyronine
 - 10 mg/ml transferrin
 - 100 ng/ml retinoic acid
 - 100 mg/ml gentamicin, 2000x
 - 0.05 mg/ml amphotericin B, 2000x
- **DMEM** Dulbecco's Modified Eagle's Medium, powder, #52100-021, Life Technologies, Karlsruhe, Germany
- **HEPES**; N-2-hydroxyethylpiperacine-N'-2-ethansulfonic acid, powder, #11344-025, Life Technologies, Karlsruhe, Germany
- **NCS**, Newborn calf serum, thermal inactivated, #26010-041, Life Technologies, Karlsruhe, Germany
- **Fungizone**, amphotericin B, 250 µg/ml, #15290-026, Life Technologies, Karlsruhe
- **Penstrep**, penicillin (10,000 IU/ml), streptomycin (10,000 µg/ml), #15140114, Life Technologies, Karlsruhe, Germany
- **L-glutamine**, 220 MM, #25030-024, Life Technologies, Karlsruhe, Germany
- **Trypsin**, solution 0.25%, #25050-014, Life Technologies, Karlsruhe, Germany
- **EDTA**, ethylenediaminetetraacetic acid, 0,02%, #E-8008, Sigma, Deisenhofen, Germany
- **Agar Noble**, powder, #A-5431, Sigma, Deisenhofen, Germany
- **PBS**, Phosphate Buffered Saline, #14040-091, Life Technologies, Karlsruhe, Germany
- **Ethanol**, pure, Pharmacy, Klinikum Großhadern, Munich, Germany
- **DMSO**, Dimethyl sulfoxide, #802912, Merck-Schuchardt, Hohenbrunn, Germany
- **SUPERFECT Reagent**, Transfection, 1.2 ml; #301305, Qiagen GmbH, Hilden, Germany

- **Geneticin (G 418)**, selective sulfate antibiotic 5 g, #11811-031, Life Technologies/Gibco BRL, Paisley, Scotland
- **Hank's solution**, (without phenol red), 500 ml, Pharmacy, Klinikum Grosshadern, Munich, Germany
- **5-Aminolaevulinic acid**, Medac GmbH, Hamburg, Germany
- **5-ALA esters**, Photocure, Oslo, Norway

2.2.2 Equipment, devices and instruments

- **Laminar Airflow**, Heraeus, Munich, Germany
- **Incubator**, Heraeus, Munich, Germany
- **Water bath**, Julabo 19, Julabo Labortechnik GmbH, 77960 Seelbach, Germany
- **Centrifuge**, Megafuge 2.0, Sepatech, Osterode, Germany
- **Microscope**, LEICA DM IRBE, Type 307-072.056, GmbH Wetzlar, Germany
- **Camera**; STORZ, Tricam SL pal 202220 20, Karl Storz-Endoscopy, Germany
- **Eppendorf pipettes**, 0,5-10 μ l ; 10-1000 μ l, Eppendorf, Hamburg, Germany
- **Water bath with pump**, Roth, Germany

2.3 METHODS

2.3.1 Preparation of media and agar plates

Preparation of Bronchial Epidermoid Growth Medium (BEGM)

- 500 ml BEGM
- Supplements

The ingredients of the supplements were thawed and then mixed with BEGM medium. This solution could be stored for 2 weeks at 4°C.

Preparation of RPMI medium

- 500 ml RPMI Medium
- 5 ml L-glutamine
- 50 ml NCS
- 400 μ l amphotericin B

MATERIALS AND METHODS

- 400 μ l penicillin-streptomycin

The complete medium could be stored for at least 2 weeks at 4°C.

Preparation of DMEM medium (wash medium)

- 200 ml DMEM with 25 mM HEPES
- 22,4 ml NCS
- 320 μ l non-essential amino acids
- 800 μ l amphotericin B
- 440 μ l penicillin-streptomycin

This solution was stored at 4°C.

Co-culture medium

- 80 ml BEGM + supplements
- 20 ml RPMI medium

Both media were mixed, freshly prepared for each experiment, and stored at 4°C.

Preparation of agar plates

- 2.25 g Agar Noble, powder
- 150 ml distilled water
- 30 ml DMEM (double concentrated)
- 6 ml NCS
- 75 μ l non-essential amino acids
- 240 μ l amphotericin B
- 120 μ l penicillin-streptomycin

Agar powder was dissolved with a magnetic stirrer in distilled water at 50°C. The thus obtained agar solution was sterilized by autoclaving. To prepare the tissue culture plates, the agar solution was heated in a microwave oven and then DMEM was added. By means of an automatic pipettor the agar gel was uniformly distributed in 20-well plates. The ready agar plates were wrapped and stored at 4°C.

2.4 THE THREE-DIMENSIONAL MINI-ORGAN MODEL

2.4.1 Biopsy cultivation

Biopsies were usually taken from visually normal mucosa at the tracheal carina or from one of the main bronchi. One to four biopsies, 1-2 mm in size, were obtained from each patient. Immediately after removal, the tissue specimens were aseptically transferred to a test tube containing Dulbecco's modified Eagle's medium (DMEM) supplemented with 10% heat-inactivated newborn calf serum (Bals *et al.*, 1998). Afterward the biopsies were washed several times with DMEM medium in Petri dishes in order to remove all remaining mucus or blood. The washed biopsies were transferred to 16-mm multi-well dishes coated with 0.5 ml of Agar Noble. One biopsy was cultured in each well in the presence of 200 μ l BEGM. Each culture was numbered and evaluated under a light microscope according to the following criteria:

- size (number of visual fields)
- percentage of the epithelialized borders of the biopsy
- percentage of the surface having ciliated epithelium

The medium was changed the first time after 2 or 3 days of culture and thereafter twice a week. Every week tissue cultures were transferred to a new well. The cultures were maintained at 37°C in 5% CO₂. In case of contamination with fungus or bacteria, the whole plate was discarded. Within 10 to 14 days the tissue cultures were mostly covered by epithelia and could be used for the three-dimensional model.

2.4.2 The tumor cell line EPLC-32M1

The tumor cell line EPLC-32M1 established in Marburg was obtained from a lymph-node metastasis of a patient with moderately differentiated squamous cell carcinoma of the lung. In order to establish a stable tumor cell line, tumor specimens were transplanted into nude mice and then the resulting tumors were cultivated (Bepler *et al.*, 1988; Heidtmann *et al.*, 1992). Generally, nude mouse xenografts histologically resembled the patients' tumors. These tumor cells show epitheloid, slightly elongated features in culture with highly refractory cell borders and perinuclear granulation. They contain a single, central, round nucleus with even chromatin pattern, and two or more nucleoli. At confluence, a cobblestone-like monolayer with an occasional piling-up of cells could be observed. The periodic acid-Schiff (PAS)

MATERIALS AND METHODS

reaction indicative of mucus production was negative. EPLC-32M1 cells grow adherently with population doubling times (PDT) of 16 hours and form colonies on the average size of 512 per 10,000 cells (cloning efficiency: 5.1%). The saturation density corresponds to 500,000 cells per cm² (Bepler *et al.*, 1988; Ulbricht *et al.*, 1995).

EPLC-32M1 cells produce human chorionic gonadotropin (HCG) as determined by radio immunoassay and display high-affinity binding sites for epidermal growth factor (EGF) identified by radio-receptor assay. Over-expression of the c-myc proto oncogene was observed (Bepler *et al.*, 1988) (Table 4).

Table 4. Expression of marker proteins in the tumor cell line EPLC-32M1 (according to Bepler *et al.*, 1988).

Biochemical characteristics:	
DDC (U/mg)	<0.1
NSE (ng/mg)	97.4
α -HCG (ng/mg)	115.6
β - HCG (ng/mg)	<0.2
EGF max binding (fmol/mg)	490
<hr/>	
Oncogene expression	
c-myc	+++
N-myc	-
L-myc	-
c-myb	-

Abbreviations: DDC = L-Dopa decarboxylase, NSE = Neuron-specific enolase, HCG = Human chorionic gonadotropin, EGF = Epidermal growth factor

2.4.3 Monolayer culture

EPLC-32M1 cells were cultivated in 25-cm² culture flasks containing RPMI 1640 medium supplemented with 10% NCS. Cells were incubated at 37°C in 5% CO₂. The growth medium was changed every 2 or 3 days, and when the mono-layer culture was confluent, cells were split. Generally, the tumor cells were seeded at such a density that confluence was reached by the end of the week. Therefore, it was necessary to split them only once a week to maintain the same growth rate. The EPLC-32M1 cell line was kept as a constantly growing culture, and every six passages cells were frozen in liquid nitrogen for future experiments.

2.4.4 Co-culture

To prepare the three-dimensional model, biopsies from normal tissue of patients were required as well as the EPLC-32M1 tumor cell line. After 10 days of culture biopsies became completely epithelialized. Parts of the organ culture's surface consisted of a denuded basement membrane or an exposed fibrillar stroma of connective tissue with vascular elements covered with a continuous layer of epithelium. Cilia were not present in all biopsies. Considerable variation in the amount of motile cilia among the different biopsies was observed after the cultivation period (Al-Batran *et al.*, 1997; 1998).

Organ cultures were pre-cultivated for 2 weeks and then cut into two pieces with a scalpel. The obtained tissue fragments were carefully placed into the 16-mm multi-well dishes coated with Agar Noble with the help of a 2-ml pipette. The medium was immediately removed. It was important not to injure the surface of the fragments. The samples were observed under a light microscope in order to define the wound site. Then the tissue fragments were inoculated with 1.2 μl of an EPLC-32M1 tumor cell suspension after the fifth or seventh passage. Tumor cells were seeded at the wound surface using an Eppendorf pipette (0.5-10 μl). The resulting co-cultures were incubated for about an hour, and then 50 μl co-culture medium was pipetted into the co-cultures. The three-dimensional models were kept at 37°C in 5% CO₂. After 24 hours of incubation the co-cultures were washed several times and transferred into fresh agar-coated wells with 200 μl co-culture medium. Every two to three days the co-cultures were transferred to fresh wells, and the whole agar-coated plate was changed every week to avoid contamination. The co-cultures chosen for the experiments were 14 or 20 days old (Fig. 6).

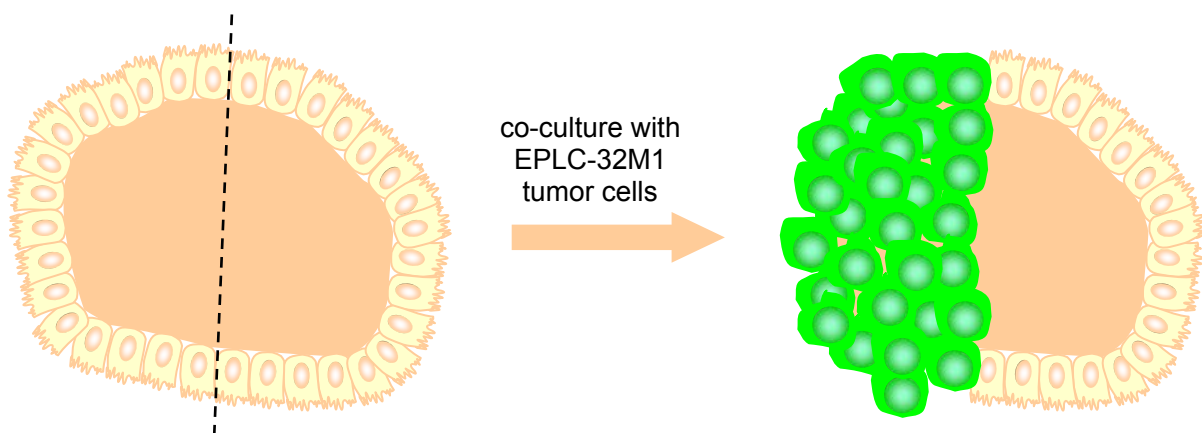


Figure 6: Schematic representation of co-culture of normal bronchial epithelium with EPLC-32M1 tumor cells. Epithelial biopsies were cut with a scalpel and the “wound” was seeded with tumor cells.

2.5 THE GREEN FLUORESCENT PROTEIN (GFP)

2.5.1 Overview

The natural phenomenon of bioluminescence, in which visible light is generated by an organism as a result of a chemical reaction, has fascinated scientists for many years. Nowadays bioluminescence has revolutionized in vivo studies of dynamic processes. Green bioluminescence was known to be a feature of marine coelenterates, but only in 1971 with the discovery by Morin and Hastings did the knowledge that the green color derives from an intrinsically green fluorescent protein become widespread. Most of the work on characterizing this protein was done in the laboratories of Frank Johnson and Osamu Shimomura (Shimomura and Johnson, 1975) and of John Blinks. Blinks studied the bioluminescence of the jellyfish *Aequorea victoria* and characterized the tandem of proteins responsible for the light emission, namely aequorin and the green fluorescent protein (Blinks *et al.*, 1978).

A. victoria is a hydromedusan jellyfish found mainly at Friday Harbor, WA, U.S.A. Its bioluminescence arises from a photoprotein found in specialized photocytes in the umbrella of the organism (Fig. 7). The photoprotein aequorin contains luciferin which is (coelenterazine) bound to the protein with oxygen. Binding of calcium ions (Ca^{2+}) to the protein triggers the oxidation of coelenterazine to coelenteramide and the consequent emission of blue light; for this reason, the complex is often called the blue fluorescent protein (BFP). However, light emitted by *A. victoria* is blue-green, because the excited state BFP undergoes radiationless energy transfer to GFP to produce an excited state of GFP, which emits green light as it

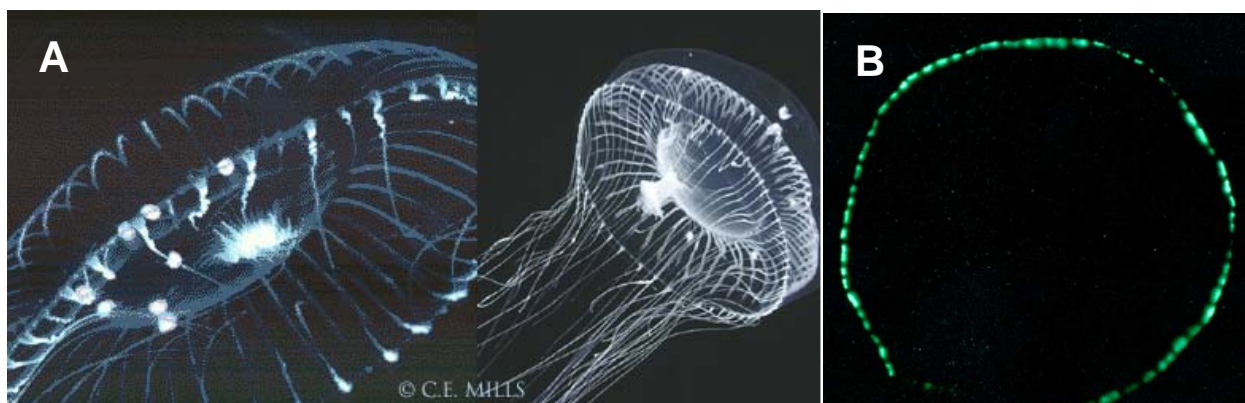


Figure 7: The hydromedusan jellyfish *Aequorea victoria*. (A) Picture obtained with an overhead flash in an aquarium. (B) Green bioluminescence emitted from the rim of the jellyfish. Taken from: Mills, C.E. 1999-present. Bioluminescence of *Aequorea*, a hydromedusa. Electronic internet document available at <http://faculty.washington.edu/cemills/Aequorea.html>. Published by the author, web page established June 1999, last updated (19 June 2003).

relaxes to its ground state.

Green fluorescent protein is comprised of 238 amino acids. It is extremely stable in neutral buffers up to 65°C, displaying a broad range of pH stability from 5.5 to 12 (Prasher *et al.*, 1992). GFP has a major excitation peak at 395 nm (with a minor peak at 475 nm) and an emission maximum at 509 nm (Morise *et al.*, 1974). The main advantage of GFP is that it exhibits strong visible fluorescence without requiring cofactors or other enzymes. Its enormous flexibility as a non-invasive marker in living cells allows for numerous other applications such as a cell lineage tracer, reporter of gene expression, and as a potential measure of protein-protein interaction and sub-cellular protein localization.

2.5.2 Generation of the stable GFP-expressing EPLC-32M1 tumor cell line

To enhance resolution of the visualized tumor cell infiltration in the three-dimensional mini-organ model, the EPLC-32M1 tumor cell line was transfected with a GFP expression vector. The mammalian expression vector pEGFP-N1 (Fig. 8) was purchased from CLONTECH Laboratories, Palo Alto, CA, USA). The vector was transformed into a dam-host, and fresh DNA was made. EPLC-32M1 cells were maintained in RPMI medium supplemented with 10% NCS. Cells were seeded the day before transfection in a 60-mm dish with 5 ml of growth medium containing serum and antibiotics (Fungizone/Penstrep). The optimal confluence for transfection was 60% - 80%. EPLC-32M1 cells were incubated with the transfection mixture containing 5 µg of plasmid DNA and Superfect reagent. Transfection was made according to QIAGEN's protocol for stable transfection. Cells were harvested by Trypsin/EDTA 48 hours after transfection, and subcultured at a ratio of 1:10 in the appropriate selective medium containing Geneticin G418. Stable fluorescent clones were selected and isolated. The clones were amplified and transferred by conventional cell culture methods. One EPLCGFP clone (No. 37) was chosen because of its high-intensity GFP fluorescence and stability. The three-dimensional model was prepared with the GFP-transfected cells according to the procedure mentioned in 4.4. The crucial step in transfecting cells is choosing the adequate transfection method. After attempts with electroporation and $\text{Ca}_3(\text{PO}_4)_2$ transfections, the liposome-mediated method was chosen, since it resulted in a very high transfection efficiency in the EPLC-32M1 cell line.

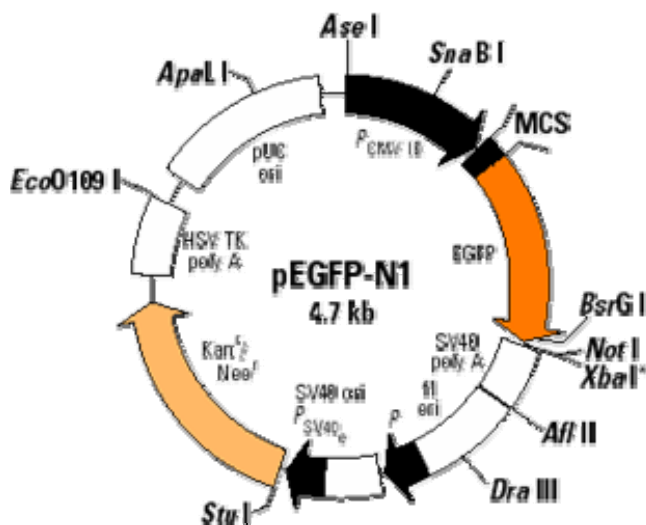


Figure 8: Vector for establishment of stable transfectants expressing enhanced green fluorescent protein (EGFP). The expression of EGFP is driven by the human cytomegalovirus (CMV) promoter. The expression of the bacterial neomycin gene is controlled by the simian virus 40 (SV40) early promoter and allows for selection of Geneticin (G418)-resistant transfectants.

Source: www.clontech.com.

The transfected tumor cells were continuously kept under observation to detect any changes in the growth phase. No changes were observed. Tumor cells proliferated at the same rate as the non-transfected cells. This was an important prerequisite for the next experiments. Also the 5-ALA uptake was observed in cell culture. As shown in Fig. 9, most of the transfected cells developed a striking PPIX-fluorescence after 5-ALA incubation. Using 405 nm excitation (Hg-lamp), both PPIX and GFP fluorescence could be viewed simultaneously.

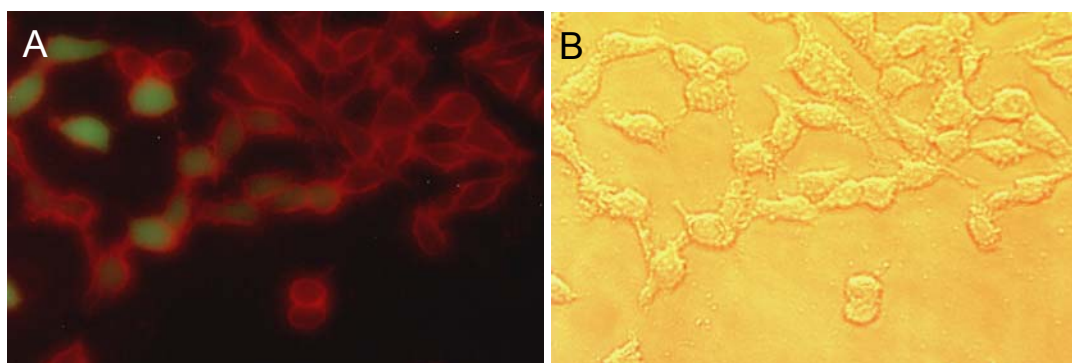


Figure 9: 5-ALA mediated fluorescence in EGFP-expressing EPLC-32M1 lung tumor cells. Cell were cultivated in chamber slides, incubated with 0.6 mM 5-ALA for 15 min and fluorescence of PPIX and GFP was simultaneously recorded under Hg lamp illumination using 405 nm excitation (A). A transmitted light picture of the same area is shown in (B).

2.6 INCUBATION WITH PHOTSENSITIZERS

2.6.1 Co-culture incubation with 5-ALA

To study the pharmacokinetics of 5-ALA-induced PPIX fluorescence in the mini-organ model, a solution of 3 mg 5-ALA was incubated in 10 ml Hank's medium containing non-essential amino acids for 15 min at 37°C. Afterward the co-culture was washed twice avoiding direct sunlight and then placed into a tempered chamber (Effenberg, Munich, Germany) containing only Hank's medium mounted on a confocal microscope (DMIRBE, LEICA, Munich, Germany; Fig. 10). Images of the co-cultures were obtained with a 2.5x lens. To visualize PPIX-fluorescence, the co-culture was illuminated for about 2 seconds with an Hg lamp ($\lambda = 405 \text{ nm}$). Fluorescence intensities were registered at about 635 nm (maximum peak of PPIX fluorescence) and at 509 nm (GFP fluorescence emission). The experimental set-up is shown in Fig. 11.

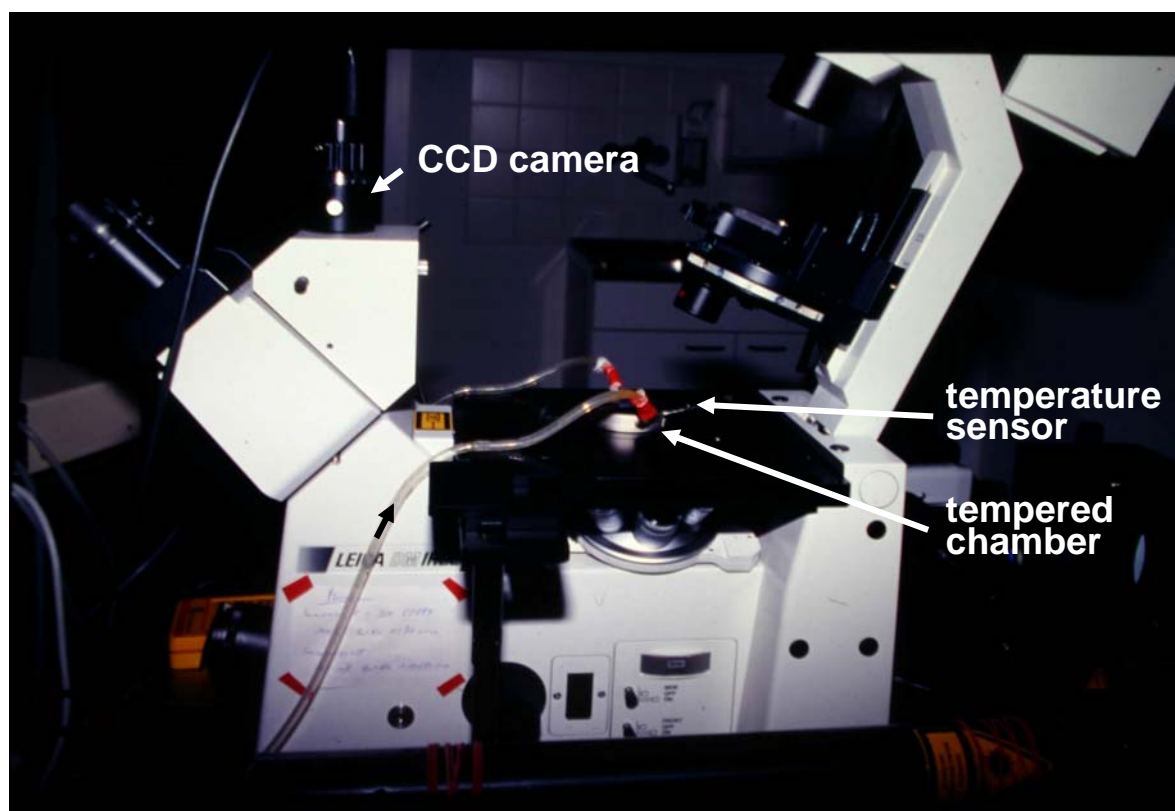


Figure 10: Fluorescence microscope with mounted tempered chamber for recording of the fluorescence of co-cultures. The chamber was tempered by continuously pumping water from a 37°C water bath through the metal casing of the co-culture.

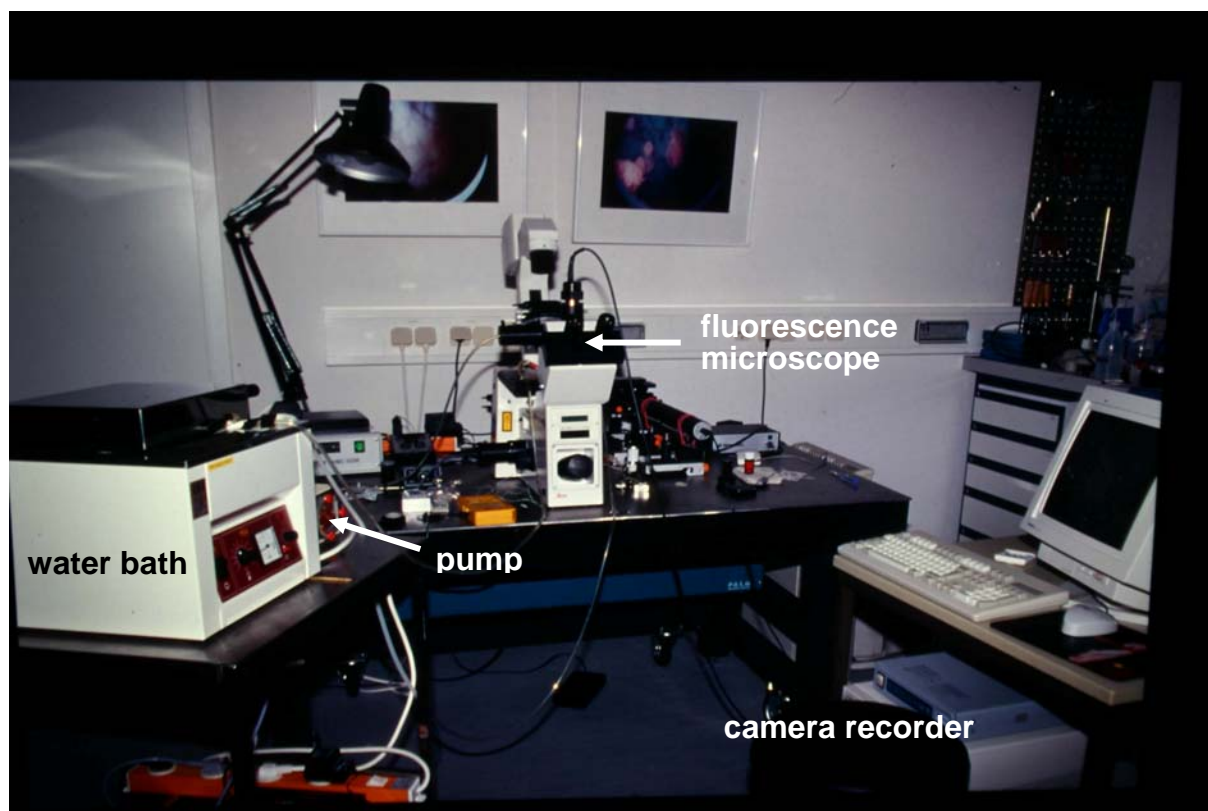


Figure 11: Experimental set-up for recording of fluorescence of co-cultures. The temperature in the co-culture was controlled by pumping water from the 37°C bath (left, foreground) through the incubation chamber mounted on the confocal microscope. The recorded fluorescence was directly processed and displayed on the computer screen.

Fluorescence images of the co-culture were recorded by a three-chip color CCD camera (Stemmer Imaging, GmbH, Puchheim, Germany) with the help of OPTIMAS Software (OPTIMAS Corporation, Seattle, Washington 98124-0467). Images were taken 30, 45, 60, 75, 90, 105, 120, 140, 160, 190, 220, 250, 280, 310 min after beginning incubation with 5-ALA. PPIX fluorescence intensities in tissue (excitation 375 – 440 nm) were quantified by using the OPTIMAS image analysis system macro in pre-determined areas of interest (AOI). Three AOIs were defined at the borders of the normal tissue in the organ culture comprising normal epithelium and three at the borders of the tumor. With another OPTIMAS macro based on densitometry, fluorescence intensities of these AOIs were evaluated. Nonlinear system response was corrected by a corresponding gamma-correction. (Fluorescence intensity values thus determined increased linearly with increasing intensity). Values were calculated automatically in EXCEL. To correct for illumination inhomogeneities during measurements, a shade correction was applied by dividing the obtained values by a standard reference, which consisted of a homogeneous fluorescent silicon slice (ELASTOSIL, pigment paste FL RAL

9010, LR RTV-2, Wacker-Chemie GmbH, Munich, Germany). Finally, values from EXCEL were exported into SIGMA PLOT 2001, a statistical software (Jandel Scientific, California, U.S.A.) for further evaluation. Intensity in the red channel of the image (peak of PPIX fluorescence) was evaluated as a parameter of the amount of PPIX in tissue. The autofluorescence was part of this fluorescence intensity in tissue, which was considered constant throughout the measurement. Autofluorescence intensities (measured in the green channel) were subtracted from the measured intensities in order to dissociate PPIX fluorescence from unspecific background fluorescence. The resulting PPIX fluorescence intensities in tumor and in normal epithelium of the co-culture model were graphed as a function of the time after beginning of incubation. A three compartment model was used in the present study to evaluate the take-up of 5-ALA and the transformation of 5-ALA into PPIX (Heil, 1996). This mathematical model is fitted numerically to each single measured fluorescence kinetic: The first compartment is represented by the volume of rinsing solution applied to the co-culture, the second compartment is allocated to a theoretical volume of storage of 5-ALA or 5-ALA esters (intra- and extra-cellular), and the third compartment is equivalent to the volume of storage for the synthesized PPIX. The formula for the numerical fit is as follows,

whereby $c(t)$ represents the concentration of PPIX at time t , k_1 - k_3 are different variables and

$$c(t) = \frac{c(0) * k_1 * k_2}{k_2 - k_x} * \left(\frac{(e^{-k_x * t} - e^{-k_3 * t})}{k_3 - k_x} + \frac{(e^{-k_3 * t} - e^{-k_2 * t})}{k_3 - k_2} \right) + i$$

i denotes a constant offset. $k_1 - k_3$ and i were the fit variables.

From the fit-curves for $c(t)$ to the experimental data, the maximal intensities (I_{max}) and the times after incubation, where I_{max} was obtained were determined.

The Mann-Whitney-test was used for nonparametric one-way test analysis for variance and comparison of independent samples. The PPIX fluorescence intensities of tumor and normal epithelium in co-cultures were compared using the SIGMA Statistical software package (Jandel Scientific, U.S.A.).

Data show the median, the mean \pm the standard error of the mean as well as several percentiles from the bottom to the top: 5%, 10%, 25%, 75%, 90% and 95%.

2.6.2 Co-culture incubation with 5-ALA esters

5-ALA, 5-ALA methyl, butyl, and hexyl esters were dissolved in Hank's medium containing non-essential amino acids; co-cultures were incubated for 15 min at 37°C. After incubation, the same procedure as in **6.1** was followed. In this set of experiments co-cultures were kept after measurements and were transferred into fresh agar-coated wells with co-culture medium. Cultivation of the samples continued under the same conditions for about 3 weeks. During this period of time, it was possible to perform new measurements with the same co-cultures, but with different concentrations of a certain ALA-ester, beginning with the lowest: 0.12 mM, 0.24 mM, 1.2 mM, and 2.4 mM.

3 RESULTS

3.1 THE THREE-DIMENSIONAL MINI-ORGAN MODEL

From previous studies it is well documented that human bronchial tissue can be kept in viable conditions *in vitro* (Cailleau *et al.*, 1959; Barrett *et al.*, 1976, Al-Batran, 1997; Bals *et al.*, 1998). The present study has also shown that human bronchial mucosa can be maintained for a prolonged period of time as a non-adhesive organ culture using the agar overlay technique. The organ cultures could be preserved for at least 2 months under the conditions described in the Material and Methods section (2.4.4). At the start of the culture period, only parts of the tissue fragments were covered with epithelium. In some biopsies, a fraction of the epithelial cells were ciliated. After about 7 or 10 days of culture, the tissue fragments became more or less spherical and a few of them were completely covered by epithelium. The epithelial cells at the border of the cut surface migrated to cover the rest of the fragment. The new epithelium was thin compared to the intact epithelium. Sometimes shorter cilia were seen forming clusters of various sizes spread all over the surface of the organ culture. This finding suggests an ongoing formation of cilia during the first 2 weeks of culture. An increasing number of cilia during the second week of culture also support the notion that cell differentiation processes take place in this mini-organ model. However, throughout the first 2 months the morphology of the epithelium is variable and presents some changes such as the loss of goblet cells, loss of ciliated cells, appearance of shorter surface cells. These changes suggested that the culture conditions, although maintaining viability after that time, are not able to maintain normal differentiation. The mechanism of these morphological changes is not completely understood.

Another important feature of the mini-organ model is that the tumor cells (EPLC-32M1) invaded mostly into the wounded area of the co-culture and did not attach to or destroy the epithelial structure. However, in older co-cultures (over 21 days old) the tumor cells caused partial damage to the epithelia and in some cases, a massive invasion into the stroma was observed.

3.2 KINETICS OF 5-ALA INDUCED PPIX SYNTHESIS IN THE MINI-ORGAN MODEL

The mini-organ model consisting of normal human bronchial mucosa co-cultivated with human lung tumor cells (EPLC-32M1) was used to study the kinetics of 5-ALA-induced PPIX fluorescence in normal epithelium and in tumorous tissue. Fluorescence intensity was taken as parameter for the amount of PPIX in the tissue. As early as 15 min after having finished the 15 min incubation period, PPIX fluorescence was obvious in normal epithelium as well as in the tumor in 4 of 24 co-cultures (Fig. 12A, B), whereas in the remaining 20 co-cultures PPIX fluorescence was first detected in tumorous areas (Fig. 13A, B).

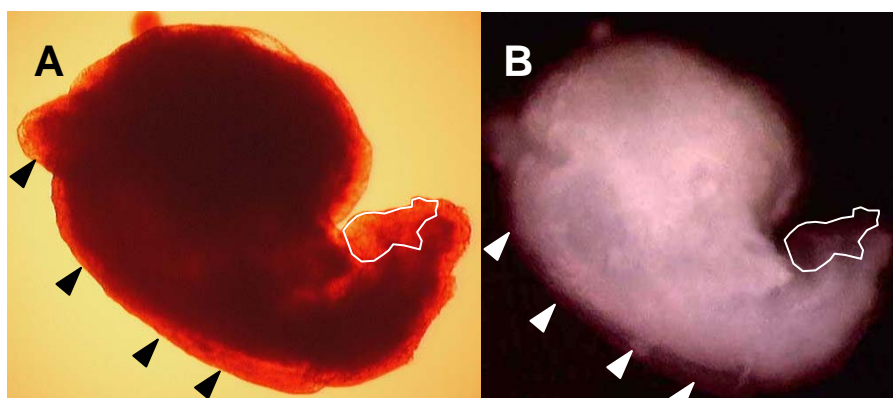


Figure 12: Simultaneous accumulation of 5-ALA-induced PPIX in normal epithelium and tumor. The co-culture was incubated with 1.2 mM 5-ALA for 15 min, washed and 15 min later photographed with transmitted light (A) or under UV illumination (B) (see Materials and Methods section for details). The fluorescence image shows PPIX accumulation in normal bronchial epithelium (white arrowheads) and in tumor (marked area). Note the intensive autofluorescence of the connective tissue (B). In (A) the normal bronchial epithelium is marked with black arrowheads.

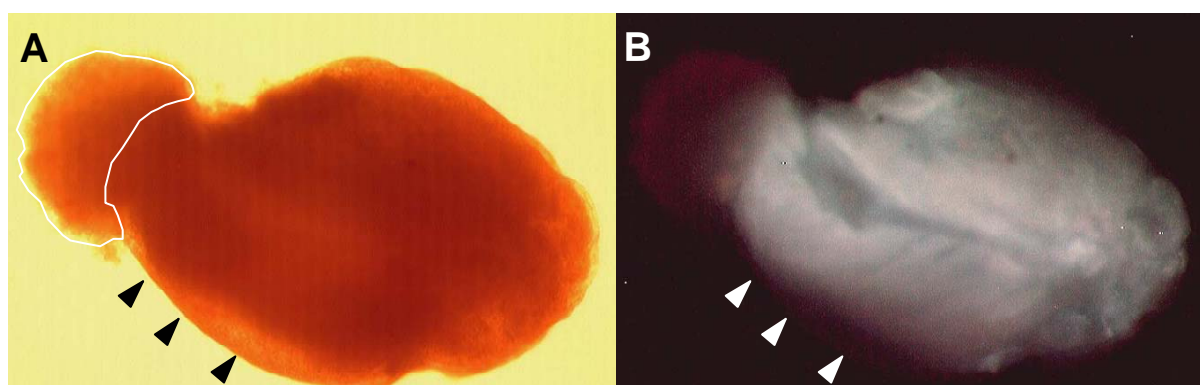


Figure 13: Differential accumulation of 5-ALA-induced PPIX in normal epithelium and tumor. The co-culture was incubated with 5-ALA as described in Fig. 12. (A) Transmitted light, UV illumination (B). Note the preferential PPIX fluorescence in the tumor (marked area) of a co-culture 15 min after a 15 min incubation with 5-ALA.

During the first measurements (30–60 min) after incubation with 5-ALA a preferential PPIX accumulation in tumor was detected. Also a steady increase of PPIX fluorescence intensity in tumor was observed from 60-180 min after application of 5-ALA, nevertheless, in normal tissue the PPIX fluorescence intensity increased within 100 and 200 min after the end of the incubation period, reaching a maximum before fluorescence began to fall. A maximum of PPIX fluorescence intensity in tumor was observed between 130 and 180 min after the beginning of incubation (Fig. 14A, B).

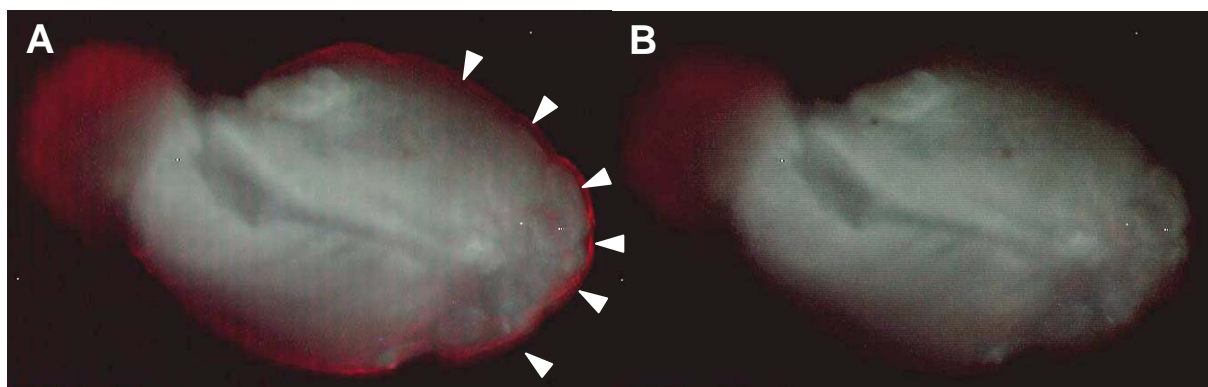


Figure 14: Kinetics of accumulation of 5-ALA-induced PPIX in normal epithelium and tumor. The co-culture was incubated with 5-ALA as described in Fig. 12. Pictures were taken under UV illumination after 160 min where maximum fluorescence was observed (A) or 340 min (B). Note the strong PPIX fluorescence in the tumor (marked area) and clear fluorescence in the normal epithelium (white arrowheads) of the co-culture (A). Only a faint fluorescence can be visualized in both tumor and normal epithelium after 340 min (B).

In figures: 13B, 14A, B it is possible to see the strong autofluorescence of connective tissue in the center of the mini-organ model. And also, it is possible to observe that the surface epithelium represents a barrier for the invading tumor cells.

The pharmacokinetics of 5-ALA-mediated PPIX fluorescence in tumor and normal tissue of a representative young co-culture are depicted in Fig. 15.

On the other hand, the AOIs placed in tumor showed different PPIX fluorescence intensities after 50 or 60 min probably due to an inhomogeneous synthesis of PPIX. A highly significant difference ($p < 0.001$) between the maximum of PPIX fluorescence intensity in tumor and normal epithelium was found (Fig. 16).

RESULTS

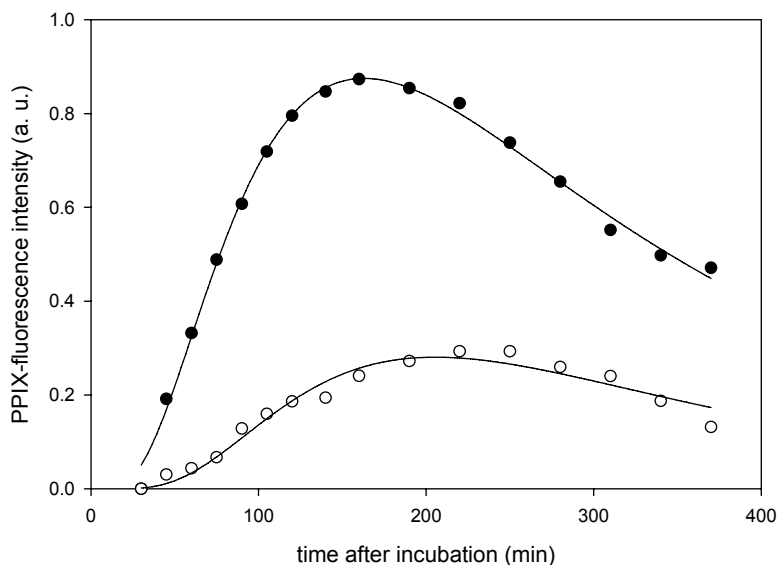


Figure 15: Pharmacokinetics of 5-ALA-induced PPIX fluorescence. A representative young co-culture was cultivated for 16 days and then incubated for 15 min with 1.2 mM 5-ALA, washed and the PPIX fluorescence intensities were recorded in tumor (●) and normal epithelium (○). Solid line: three-compartment fit.

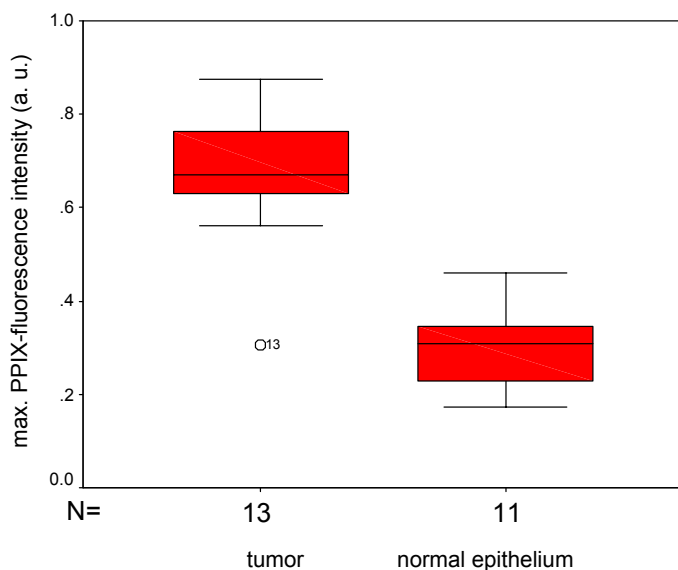


Figure 16: Differential accumulation of 5-ALA-induced PPIX in tumor and normal bronchial epithelium. The co-cultures were cultivated for 16 days, and then incubated with 1.2 mM 5-ALA for 15 min. After washing, PPIX fluorescence intensities were measured over 6 hrs every 15-30 min. The median and the 5/25/75/95 percentiles of maximal PPIX fluorescence intensities as derived from the fit for tumorous and normal areas are indicated. The number of experiments is given below the x-axis. The difference between maximum PPIX fluorescence intensities in tumor and in normal tissue was highly significant ($p < 0.001$).

PPIX fluorescence intensities at the borders of the tumor were higher than at the borders of the normal epithelium as well as in the whole normal tissue. The tumor borders tended to reach PPIX fluorescence maxima earlier than the borders of the normal epithelium. The maximum of PPIX fluorescence intensity in tumor and normal epithelium was reached nearly at the same time (Fig. 17).

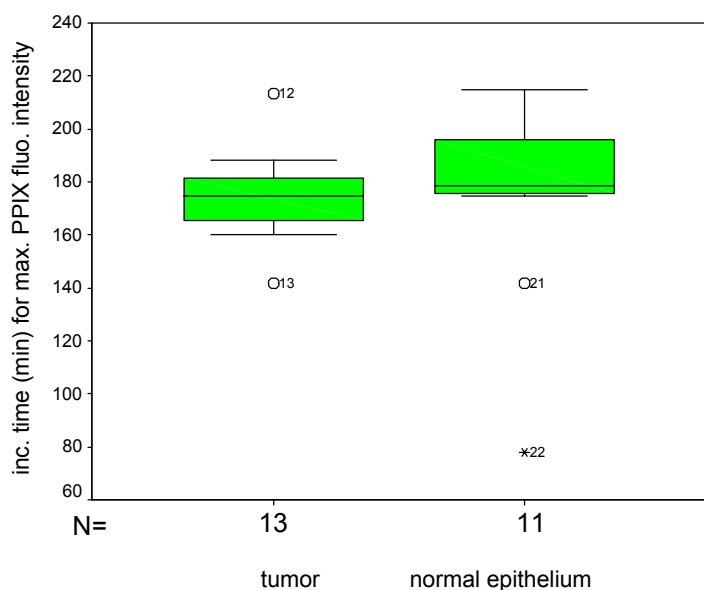


Figure 17: Time needed to reach maximal accumulation of 5-ALA-induced PPIX in tumor and normal bronchial epithelium. The co-cultures were incubated with 1.2 mM 5-ALA for 15 min, then washed and PPIX fluorescence intensities were measured over 6 hrs every 15-30 min. The median and the 5/25/75/95 percentiles of the times needed to reach maximal PPIX fluorescence intensities as derived from the fit for tumorous and normal areas are indicated. The number of experiments is given below the x-axis. The time difference between maximum PPIX fluorescence intensities in tumor and in normal tissue was not significant.

In the present work, young and old co-cultures were analyzed separately due to the marked differences in the surface between the mini-organ models after 16 days or 21-30 days of

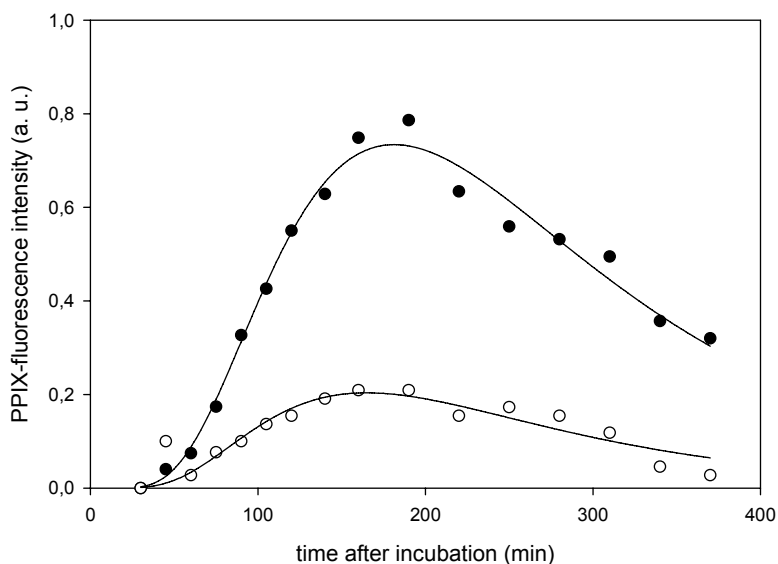


Figure 18: Pharmacokinetics of 5-ALA-induced PPIX fluorescence. A representative older co-culture was cultivated for 28 days and then incubated for 15 min with 1.2 mM 5-ALA, washed and the PPIX fluorescence intensities were recorded in tumor (●) and normal epithelium (○).

RESULTS

cultivation. A massive invasion of tumor cells into the stroma of older mini-organ models was seen (21–30 days), also a rapid rise of PPIX fluorescence in tumor and in normal epithelium was observed (Fig. 18). The maximum of PPIX fluorescence intensity in tumors was significantly different ($p < 0.05$) from the maximum of PPIX fluorescence intensity in normal epithelium (Fig. 19).

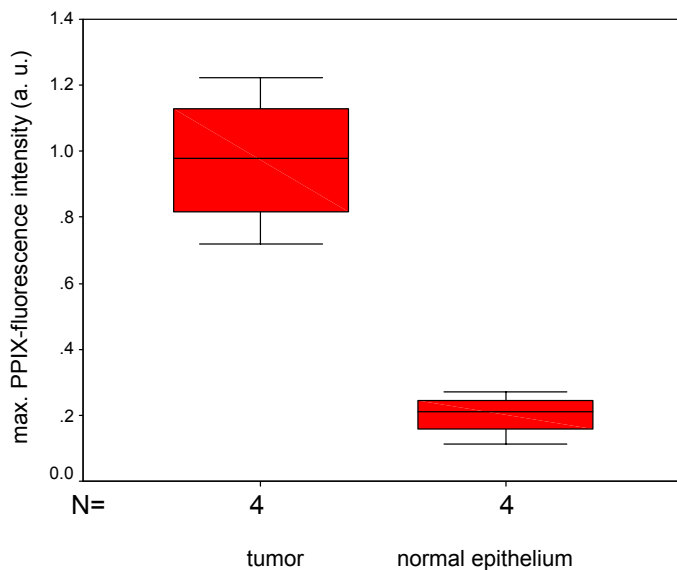
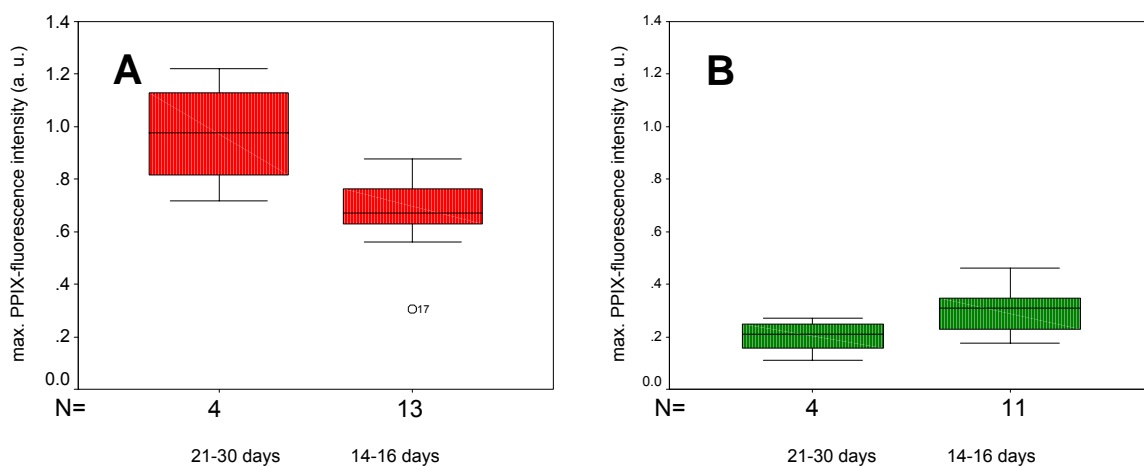


Figure 19: Differential accumulation of 5-ALA-induced PPIX in tumor and normal bronchial epithelium. The co-cultures were cultivated for 28 days and then incubated with 1.2 mM 5-ALA for 15 min. After washing, PPIX fluorescence intensities were measured over 6 hrs every 15-30 min. The median and the 5/25/75/95 percentiles of maximal PPIX fluorescence intensities as derived from the fit for tumorous and normal areas are indicated. The number of experiments is given below the x-axis. The difference between maximum PPIX fluorescence intensities in tumor and in normal tissue was significant ($p < 0.05$).

Comparing both groups of co-cultures: (14-16 days) and (21-30 days), the PPIX fluorescence intensity level in tumors of older organ cultures was significantly higher ($p < 0.05$; Fig. 20A). In normal epithelium, PPIX-fluorescence intensities levels were about the same (Fig. 20B).



Figures 20: Maximal PPIX accumulation in tumor (A) and in normal epithelium (B) of standard (14-16 d) or extended co-cultures (21-30 d). The co-cultures were incubated for 15 min with 1.2 mM 5-ALA and then washed. The median and the 5/25/75/95 percentiles of maximal PPIX fluorescence intensities for tumorous and normal areas are indicated. The number of experiments is given below the x-axis. The difference between maximum PPIX fluorescence intensities in tumor tissue in standard and extended co-cultures was significant ($p < 0.05$). Similar PPIX levels were reached in normal epithelium of both groups of co-cultures (B).

3.3 KINETICS OF ALA ESTERS IN THE MINI-ORGAN MODEL

The co-cultures were incubated in solutions containing different concentrations of various 5-ALA esters. According to published data (Peng *et al.*, 1996; Uehlinger *et al.*, 2000), a “wider window” of concentrations is observed among the ALA esters at which optimal PPIX accumulation can be measured. Several concentrations were tested in the mini-organ model in order to determine the concentration of each of the 5-ALA derivatives for optimal differential labeling of tumor and normal areas in the co-culture while keeping the viability of the tissue. Four concentrations were chosen for this study: 0.12 mM, 0.24 mM, 1.2 mM and 2.4 mM, except for 5-ALA butyl ester. Due to a low signal, an extra concentration (0.48 mM) was tested (Fig. 21).

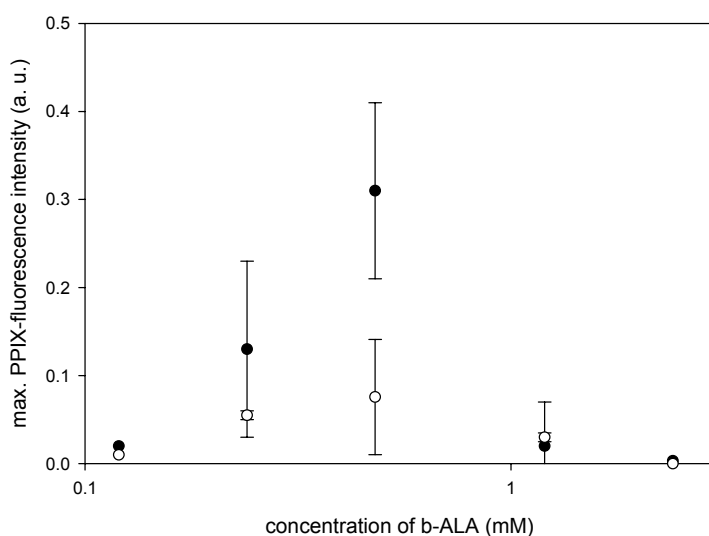


Figure 21: Semi-logarithmical representation of the PPIX fluorescence intensity in tumor and in normal epithelium as a function of 5-ALA butyl ester (b-ALA) concentrations. The mini-organ model was incubated for 15 min with 5-ALA butyl ester (0.12 mM, 0.24 mM, 0.48 mM, 1.2 mM and 2.4 mM) and then washed before starting fluorescence measurements. An extra concentration (0.48 mM) was chosen and tested due to the low signal of PPIX fluorescence obtained in tumor (●) as well as in normal epithelium (○) with the standard concentrations.

The dependency of maximal PPIX fluorescence intensity in tumor and in normal tissue from the four above mentioned concentrations after application of h-ALA and m-ALA is depicted in Figure 22. Then the most suitable ALA esters concentrations for further experiments were chosen according to the present data: 0.48 mM for b-ALA; 2.4 mM for m-ALA and 0.24 mM for h-ALA.

The mini-organ models were incubated during the same period of time (15 min) as with 5-ALA with the above mentioned optimal concentrations for every 5-ALA ester. The same procedure was used for this set of experiments as already described in Material and Methods.

RESULTS

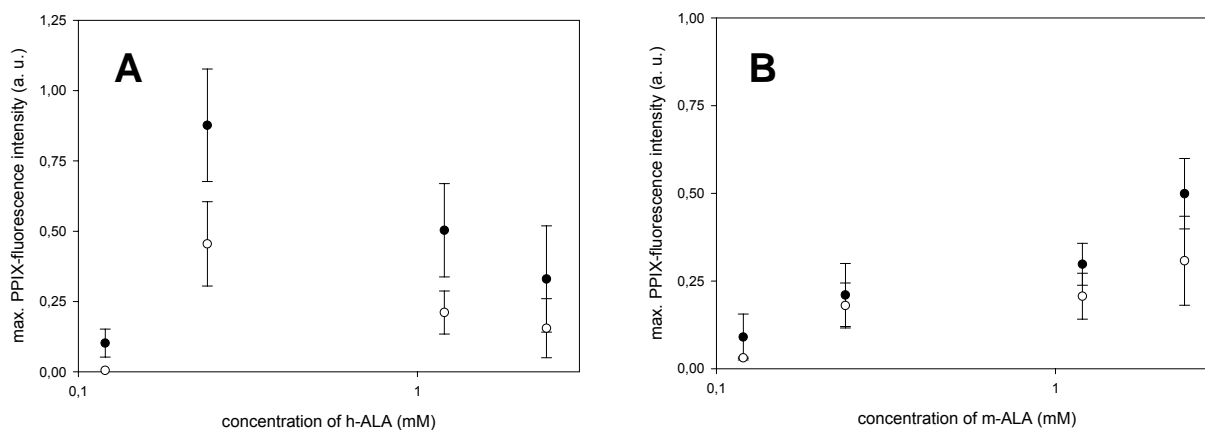


Figure 22: Semi-logarithmical representation of the PPIX fluorescence intensity in tumor and in normal epithelium as a function of 5-ALA hexyl ester (A) and 5-ALA methyl ester concentrations (B). The mini-organ model was incubated for 15 min with 0.12 mM, 0.24 mM, 1.2 mM and 2.4 mM 5-ALA hexyl ester (A) and 5-ALA methyl ester (B), respectively and then washed before recording maximal PPIX fluorescence intensity in tumor (●) as well as in normal epithelium (○). The most suitable 5-ALA esters concentrations for further experiments were chosen according to the present data: 0.24 mM for h-ALA and 2.4 mM for m-ALA.

In the following fluorescence micrographs of co-cultures in white light and blue light at the beginning and at the end of the measurements it is possible to observe the marked differences of PPIX accumulation in tumor and normal epithelium of several co-cultures incubated with b-ALA, m-ALA and h-ALA respectively (Fig. 23A-I). Co-cultures incubated with b-ALA presented a lower signal of PPIX fluorescence than co-cultures treated with m-ALA or h-ALA. Moreover, a strong PPIX fluorescence intensity and a homogeneous PPIX accumulation in tumor was observed in the co-cultures incubated either with m-ALA or with h-ALA.

The pharmacokinetics of PPIX fluorescence accumulation in a representative co-culture after application of b-ALA, m-ALA and h-ALA at their optimal concentrations are depicted in Figure 24A to C. Comparison of the kinetics of 5-ALA esters revealed that b-ALA shows lower PPIX levels than h-ALA and m-ALA. B-ALA did not return to pre-incubation intensity levels after reaching its maximal level of PPIX in tumor as well as in normal epithelium (Fig. 24B). Maximal PPIX accumulation was observed in co-cultures incubated with m-ALA and h-ALA respectively. H-ALA induced the highest PPIX fluorescence intensity at a significantly lower concentration (0.24 mM) in contrast to 5-ALA (1.2 mM), m-ALA (2.4 mM) and b-ALA (0.48mM). In the co-culture with h-ALA, PPIX reached a maximum in tumorous and normal areas at about the same time (Fig. 24C).

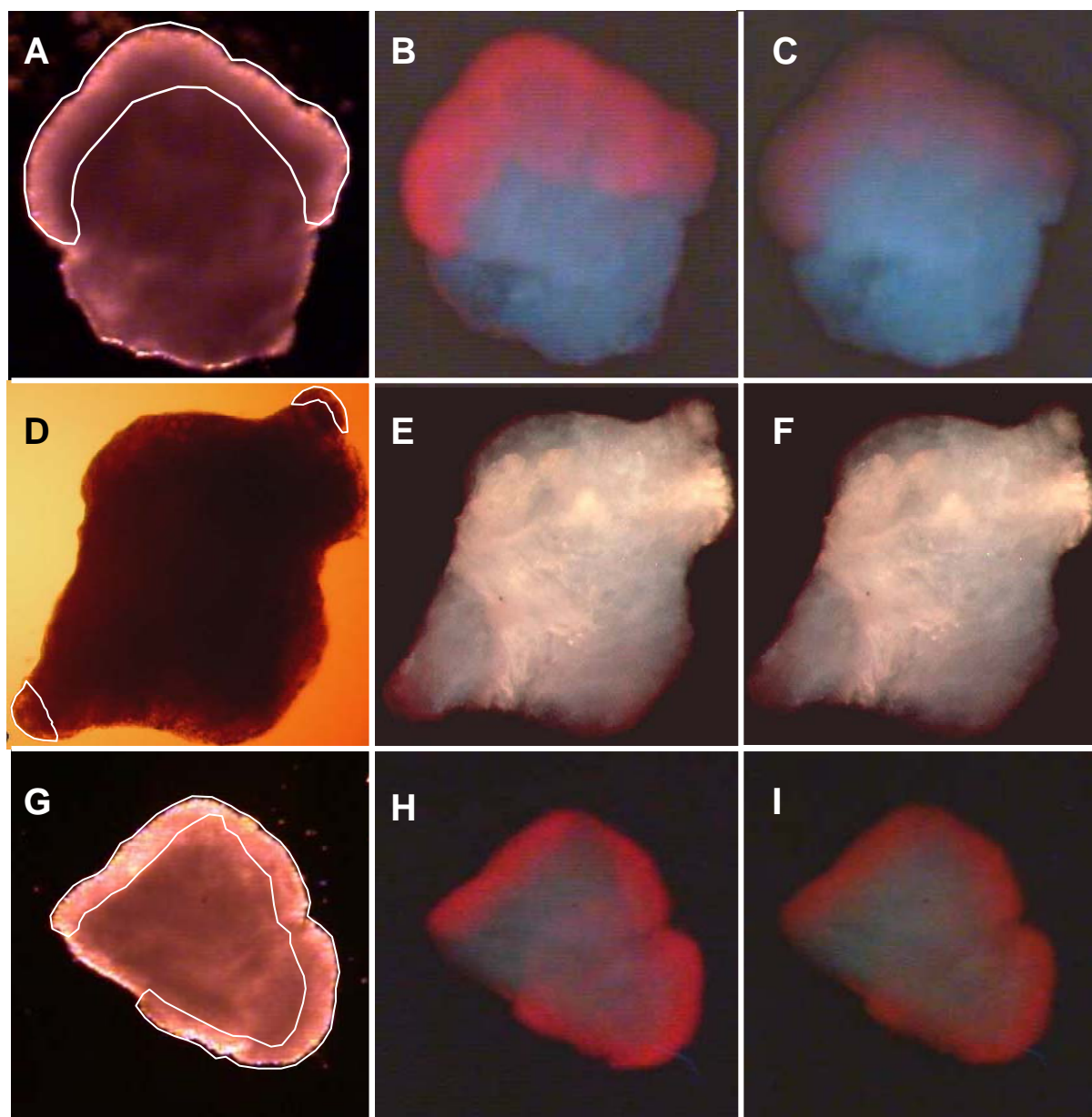
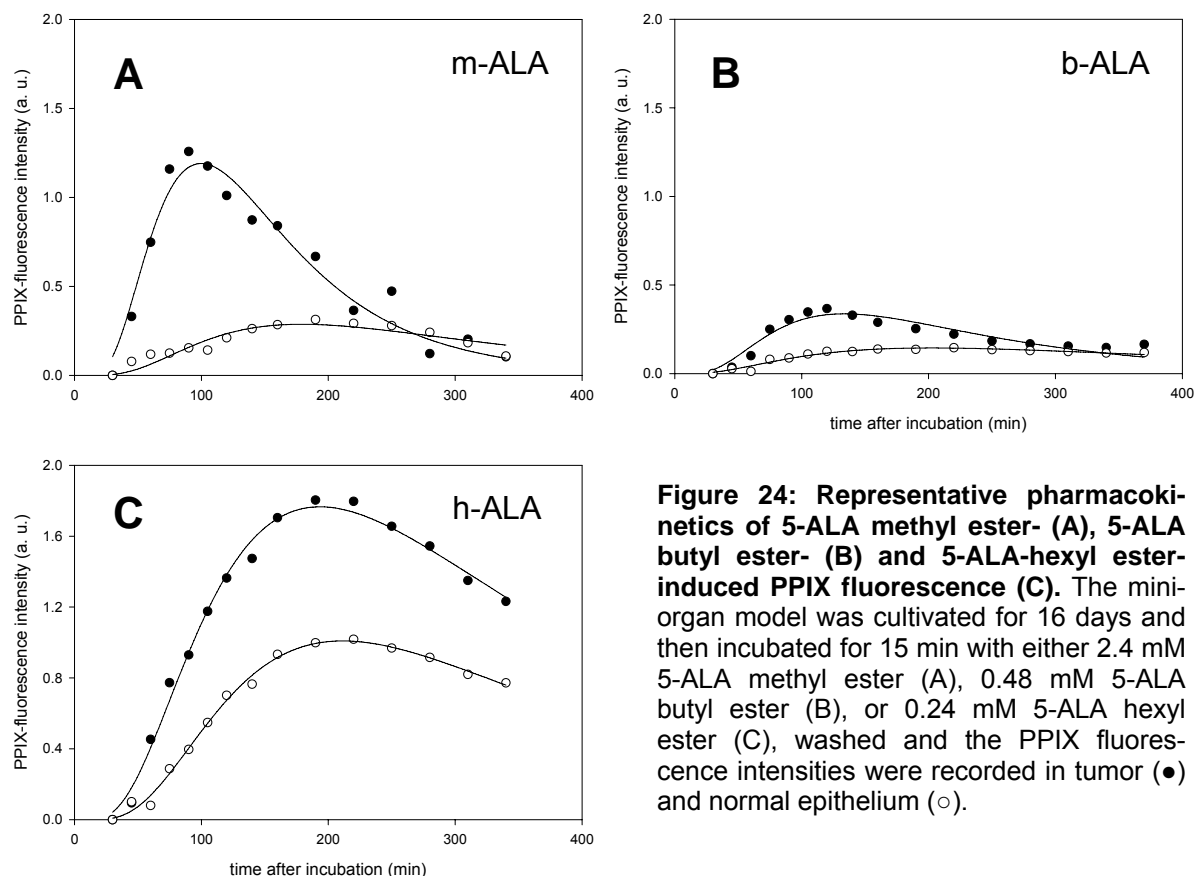


Figure 23: Kinetics of accumulation of 5-ALA methyl ester- (A-C), 5-ALA butyl ester- (D-F) and 5-ALA hexyl ester-induced PPIX fluorescence in normal epithelium and tumor (G-I). The co-cultures were incubated with optimal concentrations of 5-ALA esters (2.4 mM m-ALA, 0.48 mM b-ALA and 0.24 mM h-ALA) for 15 min and washed. Pictures were taken under white light (A, D, G) or UV illumination either after maximal accumulation of PPIX fluorescence in tumorous areas of the co-cultures was observed (B, E, H) (see Figure 24). Only a low level residual PPIX fluorescence can be seen after 340 min (C, F, I). Note the strong PPIX fluorescence in the tumors at the fluorescence maximum (see regions corresponding to the area circumscribed with a white line).

A sharp peak of PPIX fluorescence intensity in tumor was observed in the kinetics of the co-cultures incubated with m-ALA dropping fast to almost ground levels (Fig. 24B). Summarizing the results of the in vitro measurements of PPIX accumulation in several co-cultures treated with the 5-ALA esters, it was found that co-cultures incubated in 0.48 mM b-

RESULTS

ALA yield very low fluorescence signals, although PPIX fluorescence intensity was significantly ($p < 0.01$) elevated in tumorous areas compared to normal tissue (Fig. 25A).



Summarizing the results of the in vitro measurements of PPIX accumulation in co-cultures treated with the 5-ALA esters and 5-ALA (Fig. 25A, B), it was found that the maximal PPIX fluorescence intensity in co-cultures incubated in 2.4 mM of m-ALA did significantly differ between tumor and normal epithelium, but the PPIX intensity maximum was reached earlier in tumor than in normal tissue ($p < 0.05$). Maximal PPIX fluorescence intensities in tumorous and in normal areas were not statistically significantly different neither in co-cultures treated with 5-ALA nor with m-ALA, although the optimal m-ALA concentration was twice higher (2.4 mM) than the concentration of 5-ALA.

The co-cultures incubated in 0.48 mM of b-ALA yield very low fluorescence signals, although PPIX fluorescence intensity was significantly ($p < 0.01$) elevated in tumorous areas compared to normal tissue. However, times to reach maximal PPIX fluorescence intensity in both areas was not significantly different. The difference between maximum PPIX

fluorescence intensities induced by 5-ALA and b-ALA was significant in tumor tissue ($p < 0.01$) as well as in normal epithelium ($p < 0.01$).

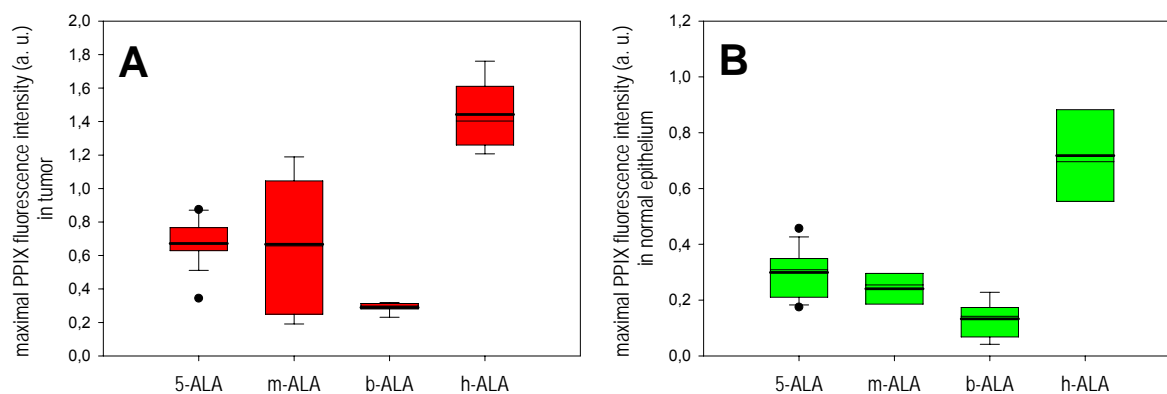


Figure 25: Differential accumulation of 5-ALA and m-, b-, h-ALA-induced PPIX fluorescence in tumor (A) and normal bronchial epithelium (B) of co-cultures. Co-cultures were incubated with 1.2, 2.4, 0.48 and 0.24 mM of 5-, m-, b-, h-ALA respectively for 15 min, then washed and PPIX fluorescence intensities as derived from the fit were measured over 6 hrs every 15-30 min. The median and the 5/25/75/95 percentiles of maximal PPIX fluorescence intensities for tumorous and normal areas are indicated. PPIX fluorescence intensity was significantly higher in tumors compared to normal epithelium ($p < 0.01$), except for b-ALA and h-ALA.

The values plotted in Figure 25 A and B indicate a significantly higher PPIX accumulation in tumor compared to normal epithelium ($p < 0.05$) in co-cultures incubated with 0.24 mM of h-ALA. Times needed to reach PPIX fluorescence intensity maxima did not differ significantly

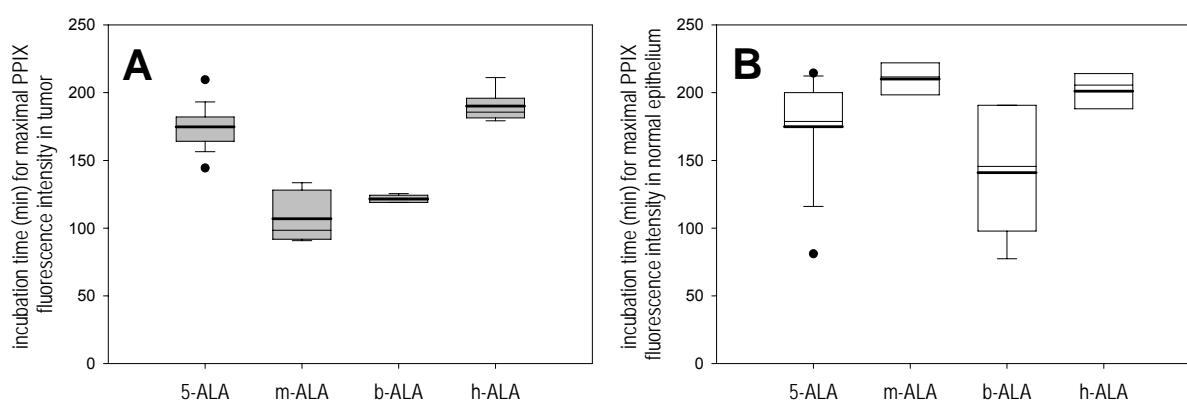


Figure 26: Time needed for maximal accumulation of 5-ALA and m-, b-, h-ALA-induced PPIX fluorescence in tumor (A) and normal bronchial epithelium (B) of co-cultures Co-cultures were incubated with 1.2, 2.4, 0.48 and 0.24 mM of 5-, m-, b-, h-ALA respectively for 15 min, then washed and PPIX fluorescence intensities as derived from the fit were measured over 6 hrs every 15-30 min. The median and the 5/25/75/95 percentiles of maximal PPIX fluorescence intensities for tumorous and normal areas are indicated. Times needed to reach PPIX fluorescence maxima in tumor and normal epithelium were significantly different only for m-ALA ($p < 0.05$).

RESULTS

between tumors and normal epithelia except for m-ALA (Fig. 26A, B). As compared with 5-ALA, the optimal concentration for h-ALA was 5 times lower (0.24 mM), but it showed a 2-fold higher PPIX fluorescence intensity in tumor as well as in normal epithelium.

Analyzing the distribution of PPIX fluorescence intensity ratios between tumor and normal epithelium (T/NE) at 635 nm (representing PPIX accumulation in both areas of the mini-organ model) the values of fluorescence intensities were first assorted according to the substances and then averaged. The results are depicted in the Figure 27 containing box-plots with a bold black line as the mean value as well as the median and several percentiles from the bottom to the top: 5%, 10%, 25%, 75%, 90%, 95%.

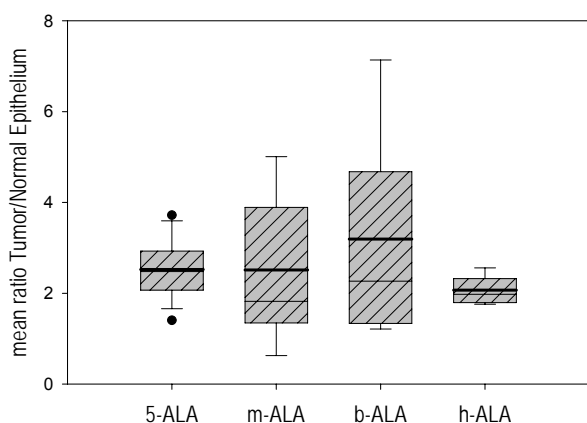


Fig. 27: Tumor/Normal Epithelium ratios of 5-ALA and m-, b-, h-ALA in the mini-organ model. The bold black line shows the mean value, the other black line the median and several percentiles from the bottom to the top: 5%, 10%, 25%, 75%, 90% and 95%. 5-ALA and h-ALA show a better distribution of PPIX in the co-cultures. M-ALA and b-ALA present a PPIX distribution with a positive skew, so far the highest ratio was observed by b-ALA, but also not a consistency in the PPIX distribution in tumorous and normal areas.

The mean ratio referred as “T/NE ratio” of co-cultures incubated with 5-ALA did not show an increased value with respect to the T/NE ratio of co-cultures treated with m-ALA. On the other hand, all percentiles from the box-plot representing m-ALA ratios are higher than in the box-plot representing 5-ALA ratios. 5-ALA shows a higher overall consistency in its distribution in tumorous and normal areas. A comparison of T/NE ratios between 5-ALA and b-ALA presented a mean contrast from 2.52 (5-ALA) to 3.19 (b-ALA), and also all percentiles $\geq 50\%$ from the box-plot representing b-ALA ratios show a PPIX distribution with a positive skew in comparison to the box-plots showing the 5-ALA and m-ALA ratios. This could be one of the explanations for an inhomogeneous distribution of b-ALA-induced PPIX in tumor and normal epithelium. The T/NE ratios distribution of PPIX fluorescence intensities between 5-ALA and h-ALA show a mean contrast from 2.52 to 2.06 respectively, and also a homogeneous distribution of PPIX in tumorous and in normal areas. Indeed, according to the present results, the mean T/NE ratio of 5-ALA is higher than the h-ALA mean ratio, but the

difference is not statistically significant. The m-, and b-ALA T/NE ratios compared with the 5-ALA T/NE ratio also proved to be non-significantly different in the Mann-Whitney-Test.

3.4 KINETICS OF 5-ALA INDUCED PPIX FLUORESCENCE IN CO-CULTURES WITH GFP-EXPRESSING LUNG TUMOR CELLS

In order to improve the present mini-organ model, the EPLC-32M1 tumor cell line was transfected with a GFP expression vector. Using GFP-transfected tumor cells in the organ co-culture system, the visualization of tumor areas and the evaluation of the pharmacokinetics of 5-ALA-induced PPIX fluorescence in vitro were greatly enhanced (Fig. 31A-C). After the 15 min of incubation with 5-ALA, the first fluorescence measurements were performed in the co-culture. As shown in Fig. 31B, PPIX accumulated first of all at the borders of the mini-organ model, exclusively in the bronchial epithelium, and the tumorous areas showed a strong GFP fluorescence, thereby demonstrating a stable high-level GFP expression in vitro during the culture period.

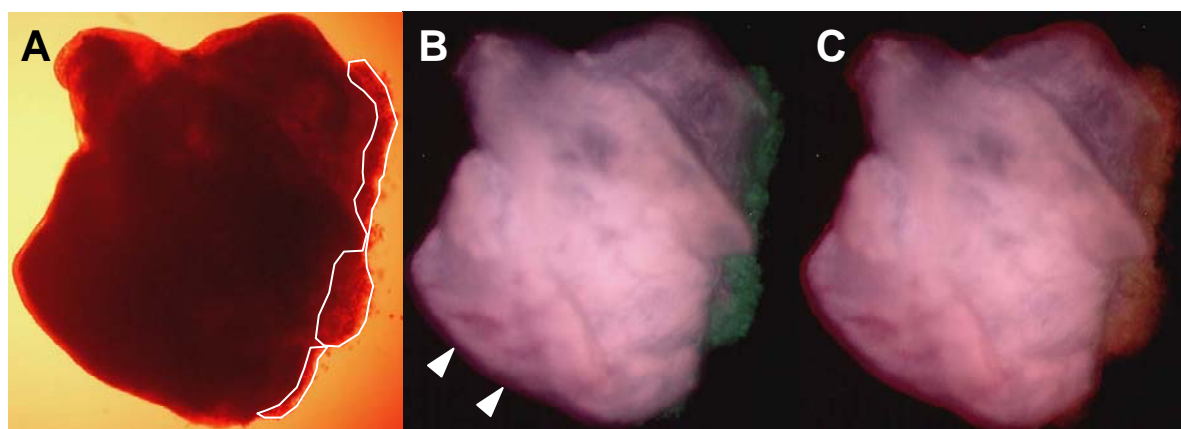


Figure 31: Kinetics of accumulation of 5-ALA-induced PPIX fluorescence in co-cultures consisting of normal epithelium and GFP-expressing lung tumor cells. The co-cultures were cultivated for 15 days and then incubated with 1.2 mM 5-ALA for 15 min and washed. Pictures were taken under white light (A) or UV illumination either 30 min (B) or 160 min later (C). Note preferential accumulation of PPIX in the bronchial epithelium of the co-culture after 30 min of 5-ALA removal (white arrowheads in B) and maximal PPIX fluorescence in the tumor area (see regions corresponding to the area circumscribed with a white line) of the co-culture (C).

A rapid rise of PPIX fluorescence in tumor was achieved 60 min after the end of incubation with 1.2 mM of 5-ALA as shown in the pharmacokinetics in Fig. 32. According to the present results, the highly significant difference ($p < 0.001$) of PPIX accumulation between tumor and normal tissue in several co-cultures was obvious (Fig. 33A). In addition, a significant

RESULTS

difference in the time profiles of maximal PPIX accumulation ($p < 0.001$) was found in tumor as well as in normal areas of the co-cultures (Fig. 33B).

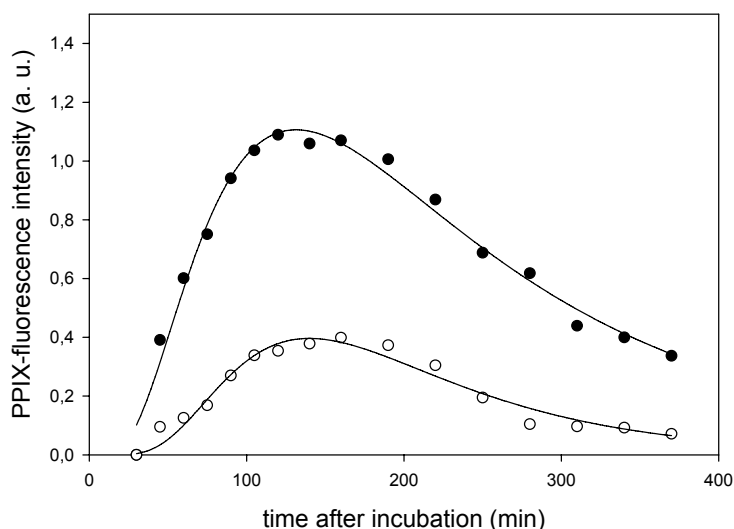


Figure 32: Pharmacokinetics of 5-ALA-induced PPIX fluorescence in a co-culture cultivated with GFP-expressing lung tumor cells. The mini-organ model was cultivated for 16 days and then incubated for 15 min with 1.2 mM of 5-ALA, washed and the PPIX fluorescence intensities were recorded in tumor (●) and in normal epithelium (○).

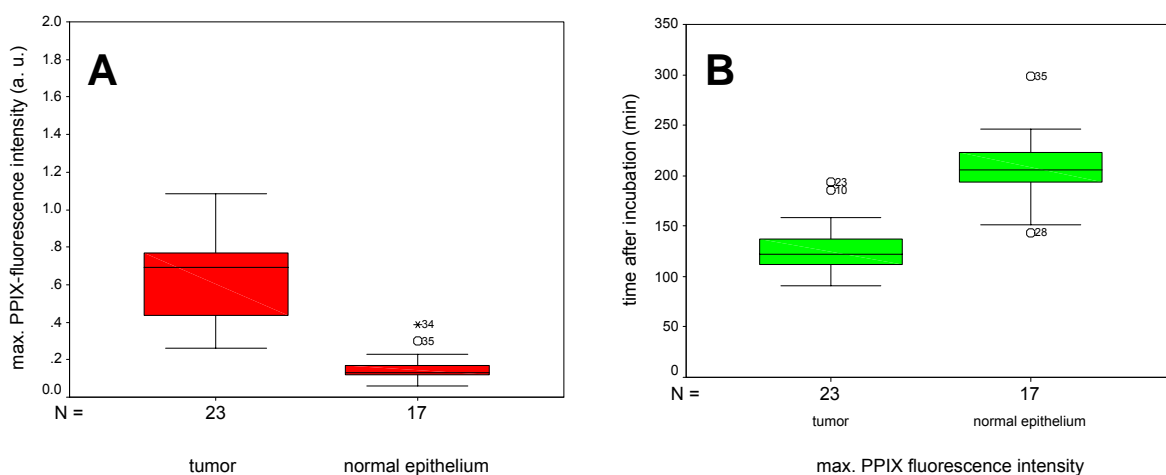


Figure 33: Differential accumulation (A) and time needed for maximal accumulation (B) of 5-ALA-induced PPIX fluorescence in co-cultures consisting of normal epithelium and GFP-expressing lung tumor cells. Co-cultures were cultivated for 14-16 days, then incubated with 1.2 mM 5-ALA for 15 min and washed. For experimental details see Legend to Figure 25. The difference of maximal PPIX fluorescence intensity in tumors and normal epithelium was highly significant ($p < 0.001$). Times needed to reach PPIX fluorescence maxima differed significantly between tumors and normal epithelia ($p = 0.001$).

No significant increase of PPIX levels in tumor was detected between the co-cultures made with GFP-expressing lung tumor cells and without (Fig. 34A, B).

However, a significant difference in the time profiles of maximal PPIX accumulation ($p < 0.01$) was found in normal epithelium. PPIX fluorescence kinetics in normal epithelium and tumorous portions after incubation with 5-ALA are well differentiated.

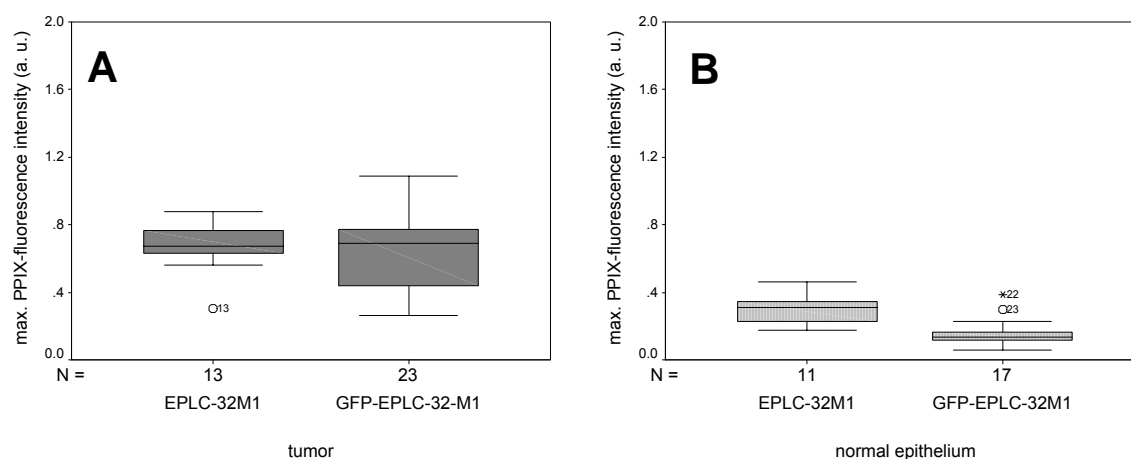


Figure 34: Maximal PPIX accumulation in tumor (A) and in normal epithelium (B) of co-cultures cultivated with the lung tumor cell line EPLC-32M1 or the GFP-transfected lung tumor cell line (GFP-EPLC-32M1). The co-cultures were incubated for 15 min with 1.2 mM 5-ALA and then washed. No significant difference ($p=0.987$) of PPIX levels in tumor in both groups of co-cultures was detected (A). Similar PPIX levels were reached in normal epithelium of both groups of co-cultures (B).

4 DISCUSSION

4.1 THE THREE-DIMENSIONAL MINI-ORGAN MODEL

The great advantage of the three-dimensional mini-organ model is that it mimics *in vivo* conditions a lot better than cell culture experiments or two-dimensional cultures. In the present study, the fact of having a confrontation between normal tissue and tumor cells and notwithstanding the more complex culture system, the three-dimensional mini-organ model provides a different sensitivity to chemical and physical anti-tumoral treatments.

There are major differences between both culture methods, three-dimensional and two-dimensional cultures *in vitro*: In an organ culture the intercellular matrix and the intercellular relationship are preserved, this is not the case in a tissue culture, where the intercellular relationship is altered and the intercellular matrix is removed. Besides that, the two-dimensional cultures require an interaction with a solid artificial substrate (Schleich *et al.*, 1976).

A spheroid culture is also a three-dimensional model, however it mimics only certain aspects of the tumor such as proliferation status, oxygen concentration and part of the metabolic activity. This type of model lacks the interaction between tumor and normal tissue. Frequently mentioned drawbacks by using 3D spheroid cultures are the time- and labor-consuming culturing techniques. Furthermore, effects on the spheroids due to mechanical manipulation (agitation, transportation, pipetting, suspension culture) or chemicals (coating substrates) cannot be excluded (Santini *et al.*, 1999). Another crucial point for effective experiments regarding the pharmacokinetics of drugs is the homogeneity in size distribution, reproducibility, and a short formation time for the spheroids. Kelm *et al.*, (2002) suggested that spheroid growth after 10 days may be hampered by a decay in conditions, such as spontaneous degradation of glutamine, photo-degradation of some vitamins and amino acids, and increased osmolarity due to evaporation.

Another advantage of the three-dimensional mini-organ model is a remarkable stability during the culture time (a month). Also it is a good alternative to animal experiments, by avoiding expensive animal tumor models and corresponding ethical problems.

Nevertheless the three-dimensional mini-organ model presents certain disadvantages: 1. The size variability among co-cultures, which depends on the size of the biopsies. This might have

contributed to the high variance of fluorescence intensities observed with co-cultures used in the experiments of the present study. Therefore one can also expect such variances in the pharmacokinetics in clinical trials. 2. The quality of the tissue which depends on health conditions of the donors. It is well known from the work of Auerbach (Auerbach *et al.*, 1961) that the bronchial epithelium of human patients with bronchitis or smoking histories, especially those with bronchogenic squamous cell carcinomas, show variable numbers of abnormal areas including metaplasia, dysplasia, and other changes. All these factors might affect the nature of the human bronchial epithelium in culture. Although, in this work, fluorescence measurements were performed only at the borders of the co-culture, marked differences from co-culture to co-culture were observed, probably due to the differences in the morphological structure of the epithelium. As mentioned in the Methods section, biopsies were usually obtained from the upper lobe carina and selected according to their size and the presence of cilia in order to minimize fluctuations in the fluorescence measurements.

4.2 PHARMACOKINETICS OF 5-ALA-INDUCED PPIX FORMATION IN THE MINI-ORGAN MODEL

One of the aims of this work was to assess the pharmacokinetics of 5-ALA-induced PPIX fluorescence in normal human bronchial epithelium as well as in tumor. PPIX appears to localize exclusively in the mucosa rather than the connective tissue and muscle of hollow organs (Bedwell *et al.*, 1992; Loh *et al.*, 1993). This was also the case in the mini-organ model, as a representative model of the human bronchial mucosa co-cultivated with tumor cells. PPIX accumulation was always registered in the normal epithelium of the co-culture, and with a higher intensity in tumorous areas. It is well known that after 5-ALA application a marked enrichment of porphyrins is usually observed in tumors as compared to normal tissues. This may be due to the low activity of ferrochelatase (El-Sharabay *et al.*, 1992) and probably also to the high activity of the rate-limiting enzyme PBGD in cancerous cells (Gibson *et al.*, 1998). The synthesis and cellular accumulation of PPIX is presumably a function of local ALA uptake, porphyrin synthesis, iron depletion and lymphatic or vascular clearance of PPIX (Tope *et al.*, 1998).

A higher PPIX fluorescence intensity was mostly achieved in the tumor areas compared to the normal epithelium. This might be explained by an increased metabolic activity of 5-ALA processing enzymes or a higher stability of PPIX within tumor cells. In the case of the old co-

cultures, a high PPIX fluorescence intensity was detected in tumor as well as in the normal epithelium. Moreover, a similarity was found among the shapes of the PPIX fluorescence kinetics in tumor from various co-cultures, but the PPIX fluorescence kinetics in normal tissue presented differences in the shape from one co-culture to another, which means PPIX accumulation is quite heterogeneous in normal areas. The present study is not dealing with questions like the way of 5-ALA application, nevertheless, this is an issue to consider at patients treatment as PPIX kinetics in normal and tumorous tissue might depend on the route of administration. Oral and intravenous administration of 5-ALA in humans has been described leading to accumulation of PPIX in several organs including the skin (Peng *et al.*, 1995; Loh *et al.*, 1993). Other investigators have demonstrated the suitability of applying 5-ALA by intravenous injection, leading to a faster accumulation of PPIX within tumor than topical administration for superficial bladder carcinomas (de Blois *et al.*, 2001; Kriegmair *et al.*, 1994).

In a Phase-I-study in lung tumor patients the best interval between inhalation and PDD (about 90 – 120 min after inhalation) has already been evaluated (Huber, 1999). There are no side effects apart from the occasional cough in these patients mostly affected by bronchitis. In the three-dimensional mini-organ model the maximal PPIX fluorescence intensity was also achieved in tumor approximately 2 hours after the incubation with 5-ALA, on the other hand, PPIX fluorescence was still present in the normal epithelium of the co-culture after 7 or 8 hours. The time at which maximal PPIX fluorescence intensity in patients was detected correlates with the time kinetics in the proposed model, showing in this way its suitability for pharmacokinetics studies of different photosensitizers.

The present study shows good selective accumulation of PPIX in tumor and in normal epithelial areas of the co-culture model versus connective tissue after application of 5-ALA. The difference between maximum PPIX fluorescence intensities in tumor and in normal epithelium was highly significant ($p < 0.001$). However, an unresolved issue is still the desirable differential distribution between tumor and normal tissue, since PPIX levels in the normal epithelium remain variably.

4.3 5-ALA ESTERS IN THE MINI-ORGAN MODEL

To compare the pharmacokinetics of the 5-ALA methyl, butyl, hexyl ester with that of 5-ALA induced PPIX fluorescence in the three-dimensional mini-organ model, the PPIX fluorescence intensity dependence from different ALA-ester concentrations was considered. The reason for using a more lipophilic compound than 5-ALA is because 5-ALA shows a poor ability to diffuse through biological membranes, and as a consequence, a high dose of 5-ALA must be administered in order to increase PPIX in the tumorous tissue at a level required for PDD and/or PDT. Also, one pursues a deeper penetration in tissue and a more homogeneous interstitial availability.

According to the results obtained in the present work, h-ALA induced the highest PPIX fluorescence intensity at a significantly lower concentration (0.24 mM) in contrast to 5-ALA (1.2 mM), m-ALA (2.4 mM) and b-ALA (0.48 mM). One may expect h-ALA to be a suitable drug for PDD and PDT. The PPIX fluorescence intensity observed with h-ALA was two-fold higher compared to the 5-ALA induced PPIX fluorescence intensity, which could improve photodetection of bronchial carcinoma. The amount of the applied h-ALA in the co-culture model was 5 times lower than that of 5-ALA reaching in general a higher signal. The optimal concentration of 5-ALA esters is crucial in order to guarantee PPIX formation without exceeding the concentration threshold, at which PPIX level decreases. Studies performed in cultured cells from the lung and bladder by Uehlinger *et al.* (2000) have also shown the influence of the concentration on PPIX formation induced by 5-ALA and its esters. It was observed that a reduction of PPIX formation at higher concentrations than the optimal concentration is correlated to a reduction in cell viability as determined by measuring the mitochondrial activity. In the present work, a decay of the PPIX fluorescence intensity in co-cultures incubated with high concentrations of h-ALA was observed. This indicates a certain grade of cytotoxicity of h-ALA in the mini-organ model. After the measurements, a few of these co-cultures were kept under normal culture conditions, and within 2 days they were observed under a light microscope. The epithelium appeared to be damaged and even cellular lysis was detected.

In addition, PPIX distribution in tumorous areas of the three-dimensional mini-organ model appeared to be more homogeneous after incubation with h-ALA or m-ALA as shown in the box plots (Fig. 25A-B). This probably implies a better drug penetration, which could lead to improved therapeutic results *in vivo*. However, Bigelow *et al.* (2001) performed studies with

spheroids incubated with h-ALA and showed that the membrane esterase activity in the outermost cells limits the PPIX production rather than the saturation of the hem biosynthetic pathway. Saturation of esterase activity seems to play a role in establishing the more uniform spatial distribution of porphyrin fluorescence observed in spheroids models incubated with h-ALA.

High tumor selectivity after topical application of m-ALA has been reported by Peng *et al.* (2001). In their study PPIX fluorescence was selectively and homogeneously distributed in thick basal cell carcinoma (BCC) lesions with little fluorescence seen in the dermis. These facts are of clinical relevance since m-ALA exhibits less photo-toxicity in local normal tissue during PDT. In agreement with this report, PPIX pharmacokinetics in the mini-organ model after application of m-ALA showed a substantial differential distribution of PPIX between tumor and normal epithelium. Furthermore, PPIX induced by m-ALA was rapidly eliminated from normal and tumorous areas in comparison to PPIX induced by h-ALA or 5-ALA.

A prodrug suitable for PDT should ideally have lipophilic as well as hydrophilic properties. Increased lipophilicity of an ALA derivate contributes to higher bioavailability by enhancing the penetration rate through membranes. However, when an ALA derivate is too lipophilic, it may accumulate in membranes without being liberated in order to exert its biological action (Guy and Hadgraft, 1992; Bonina *et al.*, 1995). The fact that butyl-ALA and methyl-ALA failed to induce high levels of PPIX in the co-culture model at lower concentrations than 5-ALA, does not necessarily imply that these compounds will be useless in any situation. Reports from other authors (Casas *et al.*, 2001; Bigelow *et al.*, 2001) indicate that these esters might have a better performance when administered systematically. One must also bear in mind that the prodrug stability is of importance, as 5-ALA esters require esterases to be converted into the active drug. If the suitable esterases are not present, one cannot expect effects at all from the prodrug, even if it has good diffusion properties. Therefore, it might be necessary to use enhancers in order to optimize 5-ALA and its derivates penetration.

Incubating the three-dimensional mini-organ model with high doses of 5-ALA esters did not present any advantage in detecting PPIX fluorescence, on the contrary, cell lysis in the normal epithelium was observed. Therefore, it makes sense to investigate the efficacy of 5-ALA esters applied in lower doses. H-ALA meets this demand at a concentration of 0.24 mM, also

DISCUSSION

m-ALA could be a good candidate applied in low doses as PPIX could still be detected adequately without cytotoxicity effects for the normal tissue.

The pharmacokinetics of b-ALA-induced PPIX in the co-cultures presented a distribution with positive skew of PPIX in the normal epithelium. This might be due to the fact that after reaching the maximum PPIX intensity in normal tissue, PPIX residuals remained for hours until they were eliminated (see Fig. 25B). In the pharmacokinetics of co-cultures incubated with h-ALA, PPIX fluorescence intensities drop until a low level, which last for a couple of hours after finishing the experiment. In reports from other authors (Chang *et al.*, 1996; Bachor *et al.*, 1996; Iinuma *et al.*, 1995) a plateau has also been observed in the pharmacokinetics of 5-ALA esters after reaching the maximal PPIX fluorescence intensity in cell cultures derived from bladder tumors and in rat urothelium *in vivo*. Probably this plateau is caused by both the balance between PPIX synthesis and PPIX utilization, which should happen with all precursors, and the penetration of precursors into deeper lying cells, which should increase with liposolubility of the 5-ALA esters (Marti *et al.*, 1999).

5-ALA esters such as h-ALA and m-ALA may diffuse passively across the plasma membrane, and thereby bypass totally or in part the receptor-mediated transport mechanism of 5-ALA, or use another active or facilitated transport mechanism than 5-ALA. The production of PPIX induced by 5-ALA esters is influenced by the aliphatic chain length of the alcohol used for esterification (Gauillier *et al.*, 1997). Also this phenomenon might be attributed to the membrane esterase activity, which is apparently involved in limiting PPIX synthesis in the interior of the tumor cells.

In regards to the ratios T/NE, it was possible to observe not a very strong PPIX range of dispersion in co-cultures treated with 5-ALA and h-ALA, but co-cultures incubated with m-ALA or b-ALA presented a skewed distribution of PPIX (Fig. 27). However, if to compare these 4 T/NE ratios, 5-ALA and m-ALA showed the best ratios. On the other hand, a stronger PPIX fluorescence intensity was reached only with a lower concentration of h-ALA. And the highest T/NE ratio was obtained with b-ALA, although it showed a very weak PPIX fluorescence signal in tumor as well as in normal epithelium.

4.4 GFP IN THE MINI-ORGAN MODEL

Optical imaging of tumorous areas in the mini-organ model has been challenging, because tumor cells usually do not have a specific optical quality that clearly distinguishes them from normal tissue. Tumor cell imaging aided by endogenous GFP fluorescence presents powerful features. Tumor cells transfected with a GFP expression plasmid provide a selective image with a very high intrinsic contrast to the other tissues. GFP expression in the tumor cells is stable over indefinite time periods allowing a better visualization of tumor growth and metastasis.

The GFP-expressing lung tumor cell line EPLC-32M1 has become an invaluable new tool to improve the three-dimensional mini-organ model. According to the present data, the cell growth rate was not altered after transfection, and the GFP-transfected tumor cells invaded the wounded surface of the organ model as before. With this step it was possible to show a replication and an enhanced resolution of selective organ colonization *in vitro*. The main reason to have used GFP-transfected tumor cells in the co-culture model was the fact that during the evaluation of the PPIX accumulation in tumor and normal tissue, it was not always possible to identify the demarcation of tumor areas, accurately. GFP clearly facilitated this task. In this work it has been demonstrated that this GFP-enhanced organ model facilitates the study and evaluation of the pharmacokinetics of 5-ALA induced PPIX, specially in co-cultures that didn't have a flawless epithelium. As the tumor cells always attached to the wounded side, but in the case of a lack of epithelium in the co-culture, it was observed that tumor cells also invaded the underlying stroma. Then before transfecting tumor cells it was hard to judge if those areas were tumor free or not.

In the present work it was also shown that the GFP-transfection of the lung tumor cells did not change their invasive behaviour. The use of *E. coli* derived reporter gene *lacZ* as a marker for identifying disseminated cells in animal models, has been utilized and recommended by several investigators (Rømer *et al.*, 1995; Fjellbirkeland *et al.*, 1998), however, they have observed that the *lacZ* transfection may modify some phenotypic characteristics of lung tumor cell lines.

The three-dimensional mini-organ model with GFP-transfected tumor cells could be used to optimize the formulation of 5-ALA esters in regards to their retention in the tissue of interest.

4.5 THE ROLE OF FLUORESCENCE DIAGNOSIS IN EARLY DETECTION OF BRONCHIAL CANCER

More effective methods for early detection of lung cancer are needed. Fluorescence detection using differences in tissue autofluorescence among pre-malignant, malignant and normal bronchial tissues has opened up a new possibility of detecting and localizing early lung cancer lesions (Lam *et al.*, 1993b; Lam and Profio,1995). On the other hand, the method of autofluorescence bronchoscopy has limitations regarding sensitivity and specially specificity.

Fluorescence bronchoscopy is potentially useful in the preoperative assessment of patients with lung cancer to determine the extent of the endobronchial spread and to detect dysplastic lesions or *in situ* carcinomas that are invisible on conventional white light examination (Lam and Becker, 1996). 5-ALA has been investigated for fluorescence detection and localization of dysplasia and early stage malignant lesions in different body sites. An advantage of 5-ALA is that the spectral properties of PPIX are known, however, the administered ALA dose and the time interval between administration and the fluorescence measurements for a given route of delivery must still be optimized, because the tissue contrast depends strongly on these factors (van der Veen *et al.*, 1994; Heyerdahl *et al.*, 1997; Loh *et al.*, 1993). On account of this, there is a need of a tumor model *in vitro* suitable for pharmacokinetics studies. In the present work it has been shown the advantage of the three-dimensional mini-organ model to elucidate the pharmaco-kinetic properties of 5-ALA and 5-ALA esters in order to optimize the drug delivery. The differences in the kinetics and PPIX fluorescence intensities in tumor and in normal epithelium have a clinical relevance, as these characteristics are needed to be studied before drug application.

Moreover, in the co-culture model it was possible to observe that the fluorescence intensity induced by 5-ALA or 5-ALA esters can be much stronger than autofluorescence. This might facilitate the scanning of large tissue areas and also reduce costs in the clinical application.

5 SUMMARY

Lung cancer is one of the most common malignancies in the world and remains the leading cause of cancer death among men and women in developed countries, accounting for more deaths than breast, prostate and colorectal cancers combined. The cure for lung cancer is low (<15%) due to the lack of screening methods, the propensity for early spread, and the inability to cure metastatic disease. However, when people are diagnosed with early stage lung cancer, their chances of 5-year survival can be as high as 90%, hence the importance of methods for early diagnosis and minimally invasive treatment modalities. During the past few years, fluorescence bronchoscopy and endobronchial photodynamic therapy (PDT) have evolved as promising technologies. The purpose of this thesis was to establish an *in vitro* model for lung cancer and to investigate clinically relevant pharmacokinetic parameters for the optimization of 5-aminolevulinic acid (5-ALA) application.

The present study suggests that the *in vitro* three-dimensional mini-organ model consisting of normal human bronchial mucosa co-cultivated with human lung tumor cells (EPLC-32M1) is a good alternative to mono-layer or even spheroid cell culture due to a much closer similarity to the *in vivo* situation. It largely obviates the necessity for animal experiments to investigate various clinically relevant questions, e.g. drug pharmacokinetics.

The three-dimensional mini-organ model has been applied to elucidate the accumulation of the fluorescing photosensitizer protoporphyrin IX (PPIX) after delivery of 5-aminolevulinic acid (5-ALA) or some of its esters:

- The optimal concentration for maximal accumulation of PPIX in tumor without causing damage to the normal tissue was determined for 5-ALA methyl, butyl and hexyl ester. Fluorescence intensity was taken as parameter for the amount of PPIX in the tissue.
- The co-culture model was used to study the pharmacokinetics of 5-ALA-induced PPIX fluorescence and its esters in normal epithelium and in tumorous areas.
- The time needed to reach maximal accumulation of 5-ALA-induced PPIX in tumor and in normal epithelium was analyzed.
- Improvement of the three-dimensional mini-organ model by using GFP-transfected EPLC-32M1 lung tumor cells in the organ co-culture system was studied.

SUMMARY

5-ALA-induced PPIX fluorescence showed marked differences in the kinetics in tumor and normal epithelium as the concentration of PPIX within tumorous areas was higher than in normal tissue. PPIX fluorescence in tumor increased faster in most of the cases than in normal tissue, but also tended to decay earlier. The results of this study show that the relative fluorescence intensities of PPIX in tumor and normal epithelium are a function of the incubation time, concentration, distribution, and kinetics in tumorous and normal tissue.

A number of 5-ALA derivatives are being used in order to modify and improve the tissue distribution of the PPIX. The tumor/normal epithelium ratios (T/NE ratio) of PPIX fluorescence induced by 5-ALA and its esters were comparable and showed in general a good contrast in the three-dimensional mini-organ model. However, comparing 5-ALA with 5-ALA hexyl ester, 5-ALA hexyl ester induced a 2-fold higher PPIX fluorescence intensity in tumor as well as in normal epithelium at a 5 times lower concentration (0.24 mM). A slight tendency to a rapid PPIX accumulation in tumor and in normal epithelium was observed in co-cultures incubated with 5-ALA methyl ester. In addition, maximal PPIX fluorescence intensities in these co-cultures show individual variations in tumor as well as in normal epithelium. The highest T/NE ratio was observed with 5-ALA butyl ester, but also an inhomogeneous distribution of PPIX in tumorous and normal areas. In general, it was possible to use the same mini-organ model for further experiments, which indicates that 5-ALA esters at their optimal concentrations are not toxic.

Amongst the 5-ALA esters, 5-ALA hexyl ester is clearly to be favored as it combines homogeneous distribution, high T/NE ratio, high fluorescence intensities, and the lowest drug concentration needed. Due to its lipophilic nature, an enhanced tissue penetration has been assumed compared to the other esters as well as 5-ALA. In clinical studies 5-ALA hexyl ester has been used successfully to detect early carcinoma in the urinary bladder by fluorescence imaging.

In an attempt to further enhance the co-culture model, green fluorescent protein (GFP) expression plasmid-transfected lung tumor cells were used in the mini-organ model. Comparable results were obtained in the pharmacokinetics of 5-ALA between co-cultures made with GFP transfected and untransfected lung tumor cells. But GFP expression highly improved the experiment conditions, whereby a higher contrast was reached at the tumor/normal epithelium boundaries.

One of the main targets of the present work was to establish a model which allows the optimization of application parameters for 5-ALA-based fluorescence diagnosis for the early detection of lung cancer. The maximum of PPIX fluorescence intensity in the co-culture model was detected between 130 and 180 min after the beginning of incubation with 5-ALA. Clinical results obtained by Huber *et al.* indicate that a photodynamic diagnosis should be performed approximately 2 hours after topical administration of 5-ALA to patients. Thus the co-culture model corroborates the clinical observation and yields a quantitative confirmation both for the time delay between drug application and fluorescence bronchoscopy (or endobronchial PDT) and for the T/NE contrast that can be expected. The results also suggest that inhalation of 5-ALA hexyl ester at a lower concentration and slightly shorter time interval could enhance the procedures.

Since the transport of 5-ALA by blood are not taken into consideration in the present mini-organ model, the results of this study could primarily be applied to topical application of 5-ALA and its derivatives, in the case of lung cancer per inhalation of these compounds.

In order to obtain a significant improvement of patient survival, the number of tumors identified in early stages has to be increased. This could be achieved by enhanced sputum cytology screening. Then, optimized fluorescence bronchoscopy can be applied to localize early lesions with high sensitivity and endoluminal PDT can treat these lesions minimally invasive.

6 SUMMARY (GERMAN TRANSLATION)

Lungenkrebs ist weltweit die häufigste maligne Erkrankung. Sie stellt die Haupttodesursache bei krebserkrankten Männern und Frauen in den westlichen Industrienationen dar und fordert mehr Tode als Krebserkrankungen der Brust, der Prostata, des Kolons und Rektums zusammengefasst. Mangels geeigneter diagnostischer Methoden zur Früherkennung, aufgrund der frühen Metastasierung und dem Fehlen von Heilungsmöglichkeiten bei Metastasierung, ist die Heilungrate für Lungenkrebs sehr niedrig (<15%). Bei Erkennung des Lungenkrebses im Frühstadium kann die 5-Jahres-Überlebensrate allerdings bis zu 90% betragen. Daraus ergibt sich die Notwendigkeit zur Entwicklung von Methoden für die Frühdiagnose und minimal invasiven Behandlungsmodalitäten. In dieser Hinsicht viel versprechend erscheinen die in den letzten Jahren entwickelten Technologien der Fluoreszenzbronchoskopie und endobronchialen photodynamischen Therapie (PDT). Das Ziel dieser Arbeit war die Etablierung eines *in vitro*-Modells für Lungenkrebs und die Untersuchung klinisch relevanter pharmakokinetischer Parameter für die Optimierung der 5-Aminolevulinsäure (5-ALA)-Anwendung.

Die hier vorgestellte Arbeit legt nahe, dass das dreidimensionale Miniorganmodell aus normaler menschlicher Bronchialschleimhaut und kokultivierten menschlichen Lungentumorzellen (EPLC-32M1) eine Alternative zu einschichtigen Zellkulturen oder sogar zu Sphäroidzellkulturen aufgrund seiner größeren Nähe zur *in vivo*-Situation darstellt. Tierexperimente zur Lösung verschiedener klinisch relevanter Fragen, wie z.B. die Untersuchung der Pharmakokinetik eines Medikaments, werden dadurch weitgehend überflüssig.

Das dreidimensionale Miniorganmodell wurde zur Analyse der Anreicherung des fluoreszierenden „Photosensitizer“ (lichtempfindliche Wirksubstanz) Protoporphyrin IX (PPIX) nach Gabe von 5-ALA und verschiedenen 5-ALA-Estern verwendet. Im Einzelnen wurden folgende Untersuchungen durchgeführt:

- Es wurde die optimale 5-ALA-Methyl-, 5-ALA-Butyl- und 5-ALA-Hexylester-Konzentration für die maximale Anreicherung von PPIX im Tumor bestimmt, bei der es zu keiner Schädigung des Normalgewebes kommt.

SUMMARY (GERMAN TRANSLATION)

- Das Kokulturmodell wurde zur Analyse der Pharmakokinetik von 5-ALA- und 5-ALA-Ester-induzierter PPIX-Fluoreszenz in normalem Epithel und Tumorbereichen verwendet.
- Die Zeit zum Erreichen maximaler Anreicherung von 5-ALA-induziertem PPIX in Tumor und normalem Epithel wurde analysiert.
- Das dreidimensionale Miniorganmodell wurde durch die Verwendung von „*green fluorescent protein*“ (GFP)-transfizierten EPLC32M1-Lungentumorzellen im Organkokultursystem verbessert.

Eine stark erhöhte PPIX-Konzentration in Tumorarealen im Vergleich zum Normalgewebe ließ auf eine deutlich unterschiedliche Kinetik der 5-ALA-induzierte PPIX-Fluoreszenz in Tumor und normalem Epithel schließen. In den meisten Fällen nahm die PPIX-Fluoreszenz rascher im Normalgewebe zu, neigte aber dazu, früher wieder abzufallen. Zusammengefasst zeigte diese Studie, dass die relativen PPIX-Fluoreszenzintensitäten, die in Tumor- und Normalepithel gefunden werden, abhängig von der Inkubationszeit, Konzentration, Verteilung und Kinetik der 5-ALA-Derivate in Tumor- und Normalgewebe sind.

Eine Reihe von 5-ALA-Derivaten findet zur Verbesserung der Gewebeverteilung von PPIX Verwendung. Das Verhältnis der 5-ALA- bzw. 5-ALA-Ester-induzierten PPIX-Fluoreszenz in Tumor- und Normalepithel (T/NE-Verhältnis) war vergleichbar und führte gewöhnlich zu einem guten Kontrast im Miniorganmodell. Allerdings zeigt sich beim Vergleich von 5-ALA mit 5-ALA-Hexylester, dass mit 5-ALA-Hexylester eine zweifach höhere PPIX-Fluoreszenzintensität in Tumor und Normalepithel bei einer fünffach niedrigeren Konzentration (0,24 mM) erzielt werden konnte. Tendenziell akkumulierte PPIX rascher im Tumor und Normalepithel nach Inkubation der Kokulturen mit 5-ALA-Methylester. Es zeigten sich individuelle Schwankungen bei den maximalen PPIX-Fluoreszenzintensitäten, die in diesen Kokulturen in Tumor und in normalem Epithel erreicht wurden. Das höchste Fluoreszenzintensitätsverhältnis zwischen Tumor und Normalepithel wurde mit dem 5-ALA-Butylester beobachtet. Dies war jedoch mit einer inhomogenen Verteilung von PPIX in Tumor- und Normalgewebe verbunden. Meist war es möglich, die Miniorganmodelle für weitere Experimente zu verwenden, was nahe legt, dass 5-ALA-Ester bei ihren optimalen Konzentrationen nicht toxisch sind.

Unter den getesteten 5-ALA-Estern ist eindeutig dem 5-ALA-Hexylester der Vorzug zu geben, da er Eigenschaften, wie homogene Verteilung, ein hohes T/NE-Verhältnis sowie hohe Fluoreszenzintensitäten bei niedriger Konzentration in sich vereinigt. Man nimmt an, dass der Grund für die im Vergleich zu 5-ALA und den anderen untersuchten 5-ALA-Estern beobachtete erhöhte Gewebepenetration in seiner lipophilen Natur zu suchen ist. In klinischen Studien wurde 5-ALA-Hexylester erfolgreich zum Nachweis von Harnblasenkarzinomen im Frühstadium durch Fluoreszenzbildgebung eingesetzt.

Zur weiteren Verbesserung des Kokulturmodells wurden GFP-Expressionsplasmid-transfizierte Lungentumorzellen im Miniorganmodell verwendet. Vergleichbare Resultate wurden in Bezug auf die 5-ALA-Pharmakokinetik in Kokulturen mit GFP-transfizierten oder untransfizierten Tumorzellen erzielt. Durch die GFP-Expression wurde jedoch ein höherer Kontrast im Tumor/Normalepithel-Übergangsbereich erzielt, was die Durchführung der Experimente sehr erleichterte.

Eines der Hauptziele dieser Arbeit war die Etablierung eines Modells zur Optimierung der Applikationsparameter für die 5-ALA-basierte Fluoreszenzdiagnose zur Früherkennung von Lungenkrebs. Maximale PPIX-Fluoreszenzintensitäten waren im Kokulturmodell 130 bis 180 Minuten nach Gabe von 5-ALA beobachtbar. Ergebnisse klinischer Untersuchungen von Huber und Mitarbeiter zeigten, dass bei Patienten eine photodynamische Diagnose ungefähr zwei Stunden nach topischer 5-ALA-Gabe durchgeführt werden soll. Das Kokulturmodell bestätigt also diese klinischen Befunde qualitativ und quantitativ, insbesondere die zeitliche Verzögerung zwischen der Medikamentengabe und nachfolgender Bronchoskopie (oder endobronchialer PDT) und den zu erwartenden T/NE-Kontrast. Des Weiteren legen die Ergebnisse nahe, dass Inhalation von 5-ALA-Hexylester bei einer vergleichsweise niedrigeren Konzentration und etwas kürzerer Einwirkdauer das Verfahren verbessern sollte.

Da der Transport von 5-ALA im Blut im hier vorgestellten Miniorganmodell nicht mit einbezogen werden kann, sollten die Ergebnisse dieser Studie hauptsächlich bei der topischen Applikation von 5-ALA und seinen Derivaten, im Falle von Lungenkrebs durch Inhalation dieser Verbindungen, Anwendung finden.

Um eine deutliche Verbesserung beim Überleben von Patienten zu erzielen, muss der Anteil der Patienten erhöht werden, bei denen Tumore früh diagnostiziert werden. Sputumzytologische Reihenuntersuchungen mit erhöhter Empfindlichkeit wäre eine der Möglichkeiten dieses

SUMMARY (GERMAN TRANSLATION)

Ziel zu erreichen. Idealerweise könnten sich optimierte Fluoreszenzbronchoskopie zur Lokalisierung von frühen Läsionen mit hoher Sensitivität und endoluminale PDT zur minimal invasiven Behandlung dieser Läsionen anschließen.

7 ABBREVIATIONS

AFB	autofluorescence bronchoscopy
ATCC	American Joint Committee on Cancer
B-ALA	5-ALA butyl ester
BCC	basal cell carcinoma
CCD	charged coupled device (camera)
CIS	carcinoma in situ
COPD	chronic obstructive pulmonary disease
CT	computed tomography
DHE	dihematoporphyrin ether / ester
ED	extensive disease
5-ALA	5-aminolevulinic acid
GFP	green fluorescent protein
h-ALA	5-ALA hexyl ester
HpD	hematoporphyrin derivative
LD	limited disease
LIFE	lung imaging fluorescence endoscope
MAC	malignancy-associated changes
m-ALA	5-ALA methyl ester
MRI	magnetic resonance imaging
NaCl	sodium chloride
NE	normal epithelium
NSCLC	non-small cell lung cancer
PDD	photodynamic therapy
PDT	photodynamic diagnosis
PPIX	protoporphyrin IX
SCLC	small cell carcinoma
T	tumor
TNM	tumor / lymph nodes / metastasis
UICC	International Union Against Cancer
WHO	World Health Organization

8 REFERENCE LIST

- Abels C., Fritsch C., Bolsen K, Szeimies R.-M., Ruzicka T., Goerz G., Goetz A. E. (1997). Photodynamic therapy with 5-aminolevulinic acid-induced porphyrins of an amelanotic melanoma in vivo. *J. Photochem. Photobiol. B.* 40: 76-83
- Al-Batran S., Astner S., Huber R. M. (1997). Drei-Dimensionale Kokultur aus humanem Bronchialepithel und Tumorzellen: Ein Modell für das Bronchialkarzinom in vitro. *Pneumologie* 51: 242
- Al-Batran S., Gamarra F., Huber R. M. (1998). Invasionscharakteristika von Tumorzellen in drei-dimensionalen Kokulturen aus humanem Bronchialepithel und der Tumorzelllinie EPLC-32M1. *Atemwegs- und Lungenerkrankungen*; 24: 327-328
- Auerbach O., Stout A. P., Hammond E. C. (1961). Changes in bronchial epithelium in relation to cigarette smoking and in relation to lung cancer. *New Engl. J. Med.*; 265: 253-267
- Bachor R., Reich E., Ruck A., Hautmann R. (1996). Aminolevulinic acid for photo-dynamic therapy of bladder carcinoma. *Urol. Res.*; 24: 285-289
- Bals R. Gamarra F., Kaps A., Grundler S., Huber R. M., Welsch U. (1998). Secretory cell types and cell proliferation of human bronchial epithelial cells in an organ-culture system. *Cell Tissue Res.*; 293: 573-577
- Barrett L. A., McDowell M., Frank A. L., Harris C.C., Trump B. F. (1976). Long-term organ culture of human bronchial epithelium. *Cancer Res.*; 36: 1003-1010
- Battle A. M. (1993). Porphyrins, porphyrias, cancer and photodynamic therapy – a model for carcinogenesis. *J. Photochem. Photobiol. B.*; 20: 5-22
- Baumgartner R., Huber R. M., Schultz H., Stepp H., Rick K., Gamarra F., Leberig A. and Roth C. (1996). Inhalation of 5-aminolevulinic acid: a new technique for fluorescence detection of early lung cancer. *J. Photochem. Photobiol. B.*; 36: 169-174
- Beckett W. S. (1993). Epidemiology and etiology of lung cancer. *Clin. Chest Med.*; 14: 1-15
- Bedwell J., MacRobert A. J., Phillips D., Bown S. G. (1992). Fluorescence distribution and photodynamic effect of ALA-induced PPIX in the DMH rat colonic tumor model. *Br. J. Cancer*; 65: 818-824
- Bepler G., Köhler A., Kiefer P., Havemann K., Beisenherz K., Jaques G., Gropp C., Haeder M. (1988). Characterization of the state of differentiation of six newly established human non-small-cell lung cancer cell lines. *Differentiation*; 37: 158-171
- Bigelow C. E., Mitra S., Knuechel R., Foster T. H. (2001). ALA- and ALA-hexyl ester-induced protoporphyrin IX fluorescence and distribution in multicell tumor spheroids. *Br. J. Cancer*; 85: 727-734
- Birrer M. J., Minna J. D. (1988). Molecular genetics of lung cancer. *Semin. Oncol.*; 15: 226-235

REFERENCE LIST

Blinks J. R., Prendergast F. G., Allen D. G. (1978). Photoproteins as biological calcium indicators. *Pharmacol. Rev.*; 28: 1-93

de Blois A. W., Thissen M., Bruijn H. S., Grouls R. J., Dutrieux R. P., Robinson D. J., Neumann H. A. (2001). In vivo pharmacokinetics of protoporphyrin IX accumulation following intracutaneous injection of 5-aminolevulinic acid. *J. Photochem. Photobiol. B.*; 61: 21-29

Bonina F. P., Montenegro L., Trapani G., Franco M., Liso G. (1995). In vitro evaluation of N-acyllactam esters of indo-methacin as dermal prodrugs. *Int. J. Pharm.*; 124: 45-51

Burger G., Jetting U., Rodenacker K. (1981). Changes in benign cell populations in cases of cervical cancer and its precursors. *Anal. Quant. Cytol. Histol.*; 3: 261-271

Cailleau R., Crocker T., Wood D. A. (1959). Attempted long-term culture of human bronchial mucosa and bronchial neoplasms. *J. Natl. Cancer Inst.*; 22: 1027-1037

Cancer Rates and Risks. National Institutes of Health, National Cancer Institute. Available at <http://rex.nci.nih.gov/NCIPubInterface/raterisk/rates38.html>

Casas A., Fukuda H., Di Venosa G., Balle A. (2001). Photosensitization and mechanism of cytotoxicity induced by the use of ALA derivatives in photodynamic therapy. *British Journal of Cancer*; 85(2): 279-284

Chang S. C., MacRobert A. J., Bown S. G. (1996). Biodistribution of protoporphyrin IX in rat urinary bladder after intravesical instillation of 5-aminolevulinic acid. *J. Urol.*; 155: 1744-1748

Chen X. Q., Stroun M., Magnenat J. L., Nicod L. P., Kurt A. M., Lyautey J., Leddery C., Anker P. (1996). Microsatellite alterations in plasma DNA of small cell lung cancer patients. *Nat. Med.*; 2: 1033-1035

Cortese D.A., Kinsey J. H., Woolner L. B., Payne W. S., Sanderson D. R., Fontana R. S. (1979). Clinical application of a new endoscopic technique for detection of in situ bronchial carcinoma. *Mayo Clin. Proc.*; 54: 635-641

Denoix P.F. (1994). TNM classification. *Bull. Inst. Nat. Hyg. Paris*; 1: 1-69

Devesa S. S., Shaw G. L., Blot W. J. (1991). Changing patterns of lung cancer incidence by histological type. *Cancer Epidemiol. Biomarkers Prev.*, 1: 29-34

Dougherty T. J., Potter W. R., Weishaupt K. R. (1984). The structure of the active component in hematoporphyrin derivative. In: Doiron D. R., Gomer C. J., eds. *Porphyrin localization and treatment of tumors*. Alan R. Liss, New York, pp. 301-314

Dougherty T. J., Cooper M., Mang T. S. (1990). Cutaneous phototoxic occurrences in patients receiving photofrin. *Lasers Surg. Med.*; 10: 485-488

Dubbelman T. M. A. R., Shuitemaker J. J. (1992). Photosensitizers. *Selected Topics in Photobiology*, Jain V. and Goel H., eds. Indian Photobiology Society, New Delhi, pp. 95-107

- El-Sharabay M. M. H., El-Wassel A. M., Hafez M. M., Salim S. A. (1992). Porphyrin metabolism in some malignant diseases. *Br. J. Cancer*; 65: 409-412
- Fernando H. C., Goldstraw P. (1990). The accuracy of clinical evaluation intrathoracic staging in lung cancer as assessed by post-surgical pathological staging. *Cancer*; 65: 2503-2506
- Fjellbirkeland L., Bjerkvig R, Laerum O. D. (1998). Non-small-cell lung carcinoma cells invade human bronchial mucosa in vitro. *In Vitro Cell. Dev. Biol. Anim.*; 33: 333-340
- Fraumeni J. F. Jr., Blott W. J. (1982). Lung and Pleura. In: *Cancer epidemiology and prevention*. Schottenfeld D., Fraumeni J. F. Jr., eds. W. B. Saunders, Philadelphia, pp. 564-582
- Fritsch C., Abels C., Goetz A. E., Stahl W., Bolsen K., Ruzicka T., Goerz G., Sies H. (1997). Porphyrins preferentially accumulate in a melanoma following intravenous injection of 5-aminolevulinic acid. *Biol. Chem.*; 378: 51-57
- Frost J. K., Ball W. C., Levin M. L., Tockman M. S., Baker R. R., Carter D., Eggleston J. C., Erosan Y. S., Gupta P. K., Khouri N. F., Marsch B. R., Stitik F. P. (1984). Early lung cancer detection: Results of the initial (Prevalence) Radiologic and Cytologic Screening in The John Hopkins Study. *Am. Rev. Respir. Dis.*; 130: 549-554
- Fry W., Menck H. R., Winchester D. P. (1996). The National Cancer Data Base report on lung cancer. *Cancer*, 77: 1947-55
- Gaullier J., Berg C., Peng Q., Anholt H., Selbo P., Ma L., Moan J. (1997). Use of 5-aminolevulinic acid esters to improve photodynamic therapy on cells in culture. *Cancer Res.*; 57: 1481-1486
- Gibson S. L., Cupriks D. J., Havens J. J., Nguyen M. L., Hilf R. (1998). A regulatory role for porphobilinogen deaminase (PBGD) in δ -aminolaevulinic acid (δ -ALA)-induced photosensitization. *Br. J. Cancer*; 77: 235-243
- Ginsberg R. J., Vokes E. E., Raben A. (1997). Non-small cell lung cancer. In: *Cancer Principles and Practice of Oncology*. De Vita J. R., Hellman, S., Rosenberg S. A., eds. J. B. Lippincott Company, Philadelphia, pp. 858-911
- Ginsberg R. J. (1997). Controversies in staging non-small cell lung cancer. *Lung Cancer*; 18 (Suppl. 2): 142
- Guy R. H., Hadgraft J. (1992). Percutaneous penetration enhancement: physio-chemical considerations and implications for prodrug design. In: *Prodrugs - Topical and Ocular Drug Delivery*. Sloan K. B., ed. Decker, New York, pp. 1-6
- Hammond E. C., Selikoff I. J., Seidman H. (1979). Asbestos exposure, cigarette smoking and death rates. *Ann. N. Y. Acad. Sci.*; 330: 473-490
- Heidtmann H. H., Elsässer H. P., Salge U., Hejmanns J., Erbil C., Schwartz-Albiez R, Havemann K. (1992). Plasminogen activator system and xenograft growth patterns in human non-small-cell lung cancer cell lines. *Fibrinolysis*; 6 (Suppl. 4): 77-82

REFERENCE LIST

Heighway J., Thatcher N., Cerny T., Hasleton P. S. (1986). Genetic predisposition to human lung cancer. *Brit. J. Cancer*; 53: 453-457

Heil P. (1996). Fluoreszenzspektroskopische In-vivo-Untersuchungen der Pharmakokinetik und des Ausbleichens von 5-Aminolävulinsäure-induzierten Porphyrinen. Dissertation an der Medizinischen Fakultät der LMU München

Heyerdahl H., Wang I., Liu D. L., Berg R., Andersson-Engels S., Peng Q., Moan J., Svanberg S., Svanberg K. (1997). Pharmacokinetic studies on 5-aminolevulinic acid-induced protoporphyrin-IX accumulation in tumors and normal tissues. *Cancer Lett.*; 112: 225-231

Huber R. M., Gamarra F., Hautmann H., Häußinger K., Wagner S., Castro M., Baumgartner R. (1999). 5-Aminolevulinic Acid (ALA) for the fluorescence detection of bronchial tumors. *Diagnostic and Therapeutic Endoscopy*; 5: 113-118

Hung J., Lam S., LeRiche J. C., Palcic B. (1991). Autofluorescence of normal and malignant bronchial tissue. *Lasers Surg. Med.*; 11: 99-105

Iinuma S., Bachor R., Flotte T., Hasan T. (1995). Biodistribution and phototoxicity of 5-aminolevulinic acid-induced PPIX in an orthotopic rat bladder tumor model. *J. Urol.*; 153: 802-806

Kelm J. M., Timmins N. E., Brown C. J., Fussenegger M., Nielsen L. K. (2003). Method for generation of homogeneous multicellular tumor spheroids applicable to a wide variety of cell types. *Biotechnol. Bioeng.*; 6(20); 83(2): 173-180

Kennedy J. C., Pottier R. H., Pross D. C. (1990). Photodynamic therapy with endogenous protoporphyrin IX: basic principles and present clinical experience. *J. Photochem. Photobiol. B.*; 6: 143-148

Kennedy J. C., Pottier R. H. (1992). Endogenous protoporphyrin IX, a clinically useful photosensitizer for photodynamic therapy. *J. Photochem. Photobiol. B.*; 14: 275-292

Kies M. S., Baker A. W., Kennedy P. S. (1978). Radionuclide scans in staging of carcinoma of lung. *Surg. Gynecol. Obstet.*; 147: 175-176

Kjuus H., Skjaerven R., Langard S., Lien J. T., Aamodt T. (1986). A case-reference study of lung cancer, occupational exposure and smoking II: Role of asbestos exposure. *Scand. J. Work Environ. Health*; 12: 203-209

Kloek J., Beijersbergen van Henegouwen G. M. (1996). Prodrugs for 5-aminolevulinic acid for photodynamic therapy. *Photochem. Photobiol.*; 64: 994-1000

Kloek J., Akkermans W., Beijersbergen van Henegouwen G. M. (1998). Derivatives of 5-aminolevulinic acid for Photodynamic therapy: enzymatic conversion into protoporphyrin. *Photochem. Photobiol.*; 67: 150-154

Kriegmair M., Baumgartner R., Knuechel R., Steinbach P., Emsam A., Lumper W., Hofstadter F., Hofstetter A. (1994). Fluorescence photodetection of neoplastic lesions following intravesical instillation of 5-aminolevulinic acid. *Urology*; 44: 6736-6741

- Kuale G., Bjelke E., Gatt J. J. (1983). Dietary habits and lung cancer risk. *Int. J. Cancer*; 31: 397-405
- Lam S., MacAulay C., Hung J., LeRiche J., Profio A. E., Palcic B. (1993a). Detection of dysplasia and carcinoma in situ with a lung imaging fluorescence endoscope device. *J. Thorac. Cardiovasc. Surg.*; 105: 1035-1040
- Lam S., MacAulay C., Palcic B. (1993b). Detection and localization of early lung cancer. *Chest*; 103/1 (Suppl.): 12s-14s
- Lam S., Profio A. E. (1995). Fluorescence tumor detection. In *Minimally Invasive Techniques in Thoracic Medicine and Surgery*. Hetzel M. R., ed. Chapman & Hall, London, p. 179
- Lam S., Becker H. D. (1996). Future diagnostic procedures. *Chest Surg. Clin. N. Am.*; 6: 363-380
- Lang S. M., Stratakis D. F., Freudling A., Ebelt K., Oduncu F., Hautmann H., Huber R. M. (2000). Detection of K-ras and p53 mutations in bronchoscopically obtained malignant and non-malignant tissue from patients with non-small cell lung cancer. *Eur. J. Med. Res.*; 5: 341-346
- Lange N., Jichlinski P., Zellweger M., Forrer M., Marti A., Guillou L., Kucera P., Wagnieres G., van den Bergh H. (1999). Photodetection of early human bladder cancer based on the fluorescence of 5-aminolaevulinic acid hexyl ester-induced proto-porphyrin IX: a pilot study. *Br. J. Cancer*; 80: 185-193
- Le Marchand L., Hankin J. H., Kolonel N. L., Beecher G. R., Wilkens L. R., Zhao L. P. (1993). Intake of specific carotenoids and lung cancer risk. *Cancer Epidemiol. Biomarkers Prev.*; 2: 183-187
- Lipson R. L., Baldes E. J., Olsen A. M. (1961). The use of a derivative of hematoporphyrin in tumor detection. *J. Natl. Cancer Inst.*; 26: 1-12
- Lipson R. L., Baldes E. J., Olsen A. M. (1964). Further evaluation of the use of hematoporphyrin derivative as an aid for endoscopic detection of malignant disease. *Dis. Chest*; 46: 676-679
- Little A. G., DeMeester T. R., Ryan J. W. (1986). The use of radionuclide scans in lung Gallium-67 scanning for preoperative staging. In: *Current Concepts in Thoracic Surgery*. Kittle C. F., ed. W. B. Saunders, Philadelphia, pp. 122-126
- Loeb L. A., Ernster V. L., Warner K. E., Abbotts J., Laszlo J. (1984). Smoking and lung cancer: An overview. *Cancer Res.*; 44: 5940-5958
- Loh C. S., MacRobert A. J., Bedwell J., Regula J., Krasner N., Bown S. G. (1993). Oral versus intravenous administration of 5-aminolaevulinic acid for photodynamic therapy. *Br. J. Cancer*; 68: 41
- Lubin J. H., Boice J. D. (1997). Lung cancer risk from residential radon: meta-analysis of eight epidemiological studies. *J. Natl. Cancer Inst.*; 89: 49-57

REFERENCE LIST

- Mack M. J., Aronoff R. J., Acuff T. E., Douthit M. B., Bowman R. T., Ryan W. H. (1992). Present role of thorascopy in the diagnosis and treatment of diseases of the chest. *Ann. Thorac. Surg.*; 54: 403-409
- Marti A., Lange N., van den Bergh H., Sedmera D., Jichlinski P., Kucera P. (1999). Optimisation of the formation and distribution of photoporphyrin IX in the urothelium: an in vitro approach. *J. Urol.*; 162: 546-552
- Melamed M. R., Flehinger B. J., Zaman M. B., Heelan R. T., Perchick W. A., Martini N. (1984). Screening for early lung cancer: results of the Memorial Sloan-Kettering study in New York. *Chest*; 86: 44-53
- Miyake M., Taki T., Hitomi S., Hakomori S. (1992). Correlation of expression of H/Le y/Le b antigens with survival in patients with carcinoma of the lung. *N. Engl. J. Med.*; 327: 14-18
- Morise H., Shimomura O., Johnson F. H., Winant J. (1974). Intermolecular energy transfer in the bioluminescent system of *Aequorea*. *Biochemistry*; 13: 2656-2662
- Mountain C. F., Carr D. T., Anderson W. A. (1974). A system for the clinical staging of lung cancer. *Am. J. Roentgenol. Radium Ther. Nucl. Med.*; 120: 130-138
- Mountain C. F. (1986). A new international staging system for lung cancer. *Chest*; 89 (Suppl.): 225-233
- Mountain C. F. (1989). Value of the new TNM staging system for lung cancer. *Chest*; 96 (Suppl.): 47-49
- Mountain C.F.(1997): Revisions in the International System for Staging Lung Cancer. *Chest*, 111: 1710-1717
- Mulshine J., Linnoila R. I., Treston A. M., Scott F. M., Quinn K., Avis I., Shaw G. L., Jensen S. M., Brown P., Birrer M. J. (1992). Candidate biomarkers for application as intermediate end points of lung carcinogenesis. *J. Cell Biochem. (Suppl.)* 16G: 183-186
- Naruke T., Goya T., Tsuchiya R., Suemasu K. (1988). Prognosis and survival in resected lung carcinoma based on the new international staging system. *J. Thorac. Cardiovasc. Surg.*; 96: 440-447
- Nesbitt J. C., Putnam J. B. Jr., Walsh G. L., Roth J. A., Mountain C. F. (1995). Survival in early-stage lung cancer. *Ann. Thorac. Surg.*; 60: 466-472
- O'Connell J. P., Kris M. G., Gralla R. J., Groshen S., Trust A., Fiore J. J., Kelsen D. P., Heelan R. T., Golbey R. B. (1986). Frequency and prognostic importance of pretreatment clinical characteristics in patients with advanced non-small cell lung cancer treated with combination chemotherapy. *J. Clin. Oncol.*; 4: 1604-1614
- Palcic B., Lam S., Hung J., MacAulay C. (1991). Detection and localization of early cancer by imaging techniques. *Chest*; 99: 742-743

- Peng Q., Moan J., Warloe T., Iani V., Steen H. B., Bjørseth A., Nesland J. M. (1996). Build-up of esterified aminolevulinic-acid-derivative-induced porphyrin fluorescence in normal mouse skin. *J. Photochem. Photobiol. B.*; 34: 95-96
- Peng Q., Berg K., Moan J., Kongshaug M., Nesland J. M. (1997). 5-Aminolevulinic acid-based photodynamic therapy: principles and experimental research. *Photochem. Photobiol.*; 65: 235-251
- Peng Q., Soler A. M., Warloe T., Nesland J. M., Giercksky K. E. (2001). Selective distribution of porphyrins in skin thick basal cell carcinoma after topical application of methyl 5-aminolevulinate. *J. Photochem. Photobiol. B.*; 62: 140-145
- Petty L. (1995). Lung Cancer Screening. *Compr. Ther.*; 21; 432-437
- Prasher D. C., Eckenrode V. K., Ward W. W., Prendergast F. G., Cormier M. J. (1992). Primary structure of the *Aequorea victoria* green fluorescent protein. *Gene*; 111: 229-233
- Qu J., MacAulay C., Lam S. (1994). Optical properties of normal and carcinomatous bronchial tissue. *Applied Optics*; 33: 7397-7405
- Regula J., MacRobert A. J., Gorchein A., Buonaccorsi G. A., Thorpe T. M., Spencer G. M., Hatfield A. R., Bown S. G. (1995). Photosensitization and photodynamic therapy of oesophageal, duodenal, and colorectal tumors using 5 aminolevulinic acid induced protoporphyrin IX – a pilot study. *Gut*; 36: 67-75
- Rømer M. U., Christiansen J., Brunner N., Spang-Thomsen M. (1995). Dissemination in athymic nude mice of lacZ transfected small cell lung cancer cells identified by X-gal staining. *APMIS*; 103: 582-587
- Ryan A., Banks J., Roberts S. (2001). Methods for lung cancer biopsy. *Lancet*; 358: 1909-1910
- Samet J. M. (1989). Radon and lung cancer. *J. Natl. Cancer Inst.*; 81: 745-757
- Samet J. M. (1991). Health benefits of smoking cessation. *Clin. Chest Med.*; 12: 669-679
- Santini M. T., Rainaldi G. (1999). Three-dimensional spheroid model in tumor biology. *Pathobiology*; 67: 148-157
- Schleich A. B., Frick M., Mayer A. (1976). Patterns of invasive growth in vitro. Human deciduas graviditatis confronted with established human cell lines and primary human explants. *J. Natl. Cancer Inst.*; 56: 221-237
- Seidman H., Selikoff I., Gelb S. (1986). Mortality experience of amosite asbestos factory workers: Dose response relationships 5-40 years after onset of short term work exposure. *Am. J. Ind. Med.*, 10: 479-514
- Shepherd F. A., Ginsberg R. J., Haddad R., Feld R., Sagman U., Evans W. K., DeBoer G., Maki E. (1993). Importance of clinical staging in limited small-cell lung cancer: a valuable system to separate prognostic subgroups. The University of Toronto Lung Oncology Group. *J. Clin. Oncol.*; 8: 1592-1597

REFERENCE LIST

- Shields P. G. (1993). Inherited factors and environmental exposures in cancer risk. *J. Occup. Med.*; 35: 34-41
- Shimomura O., Johnson F. H. (1975). Chemical nature of bioluminescence systems in coelenterates. *Proc. Natl. Acad. Sci. USA*; 72: 1546-1549
- Sørensen J. B., Badsberg J. H., Olsen J. (1989). Prognostic factors in inoperable adenocarcinoma of the lung: A multivariate regression analysis of 259 patients. *Cancer Res.*; 49: 5748-5754
- Statistisches Bundesamt (1996). *Statistisches Jahrbuch für die Bundesrepublik Deutschland*. Statistisches Bundesamt, Wiesbaden.
- Steinmetz K. A., Potter J. D., Folsom A. R. (1993). Vegetables, fruit, and lung cancer in the Iowa Women's Health Study. *Cancer Res.*; 53: 536-543
- Stepp H., Baumgartner R., Betz C. (1997). New developments in fluorescence detection of ALA-induced protoporphyrin IX for cancer detection. *Soc. Photo-Opt. Instrum. Eng.*; 3197: 68-74
- Sutro C. J., Burman M. S. (1933). Examination of pathologic tissue by filtered ultraviolet radiation. *Arch. Pathol.*; 16: 346-349
- Thatcher N. (1998). The role of haematopoietic growth factors. CRC Dept. of Medical Oncology, Christie Hospital, Manchester, U.K.
- Tonato M. (2000). Postoperative treatment in resected NSCLC. 4th Pan-European Cancer Symposium. Cannes, France; March 17
- Tope W. D., Ross E. V., Kollias N., Martin A., Gillies R., Anderson R. (1998). Protoporphyrin IX fluorescence induced in basal cell carcinoma by oral δ -aminolaevulinic acid. *Photochem. Photobiol.*; 67: 249-255
- Uehlinger P., Zellweger M., Wagnieres G., Juillerat-Jeanneret L., van den Bergh H., Lange N. (2000). 5-Aminolevulinic acid and its derivatives: physical chemical properties and protoporphyrin IX formation in cultured cells. *J. Photochem. Photobiol. B.*; 54: 72-80
- Ulbricht B., Spiess E., Schwartz-Albiez R, Ewert W. (1995). Quantification of intracellular cathepsin activities in human lung tumor cell lines by flow cytometry. *Biol. Chem. (Hoppe Seyler)*; 376: 407-414
- Van der Veen N., van Leengoed H., Star W. (1994). In vivo fluorescence kinetics and photodynamic therapy using 5-aminolevulinic acid-induced porphyrin: increased damage after multiple irradiations. *Br. J. Cancer*; 70: 867-872
- Vander A., Sherman J., Luciano D. (1980). *Human Physiology: The Mechanisms of the Body Function*. Third edition, McGraw-Hill Book Company
- Wagner H. Jr., Ruckdeschel J. C. (1995). Screening, early detection, and early intervention strategies for lung cancer. *Cancer Control*; 2: 493-502

Webber J., Kessel D., Fromm D. (1997). Side effects and photosensitization of human tissues after aminolevulinic acid. *J. Surg. Res.*; 68 : 31-37

WHO (1982). The World Health Organization Histological Typing of Lung Tumors. *Am. J. Clin. Pathol.*; 77: 123-136

Woolner L. B., Fontana R. S., Cortese D. A., Sanderson D. R., Bernatz P. E., Payne W. S., Pairolero P. C., Piehler J. M., Taylor W. F. (1984). Roentgenographically occult lung cancer: pathologic findings and frequency of multicentricity during a ten year period. *Mayo Clin. Proc.*; 59: 453-466

Ziegler R. G. (1989). A review of epidemiologic evidence that carotenoids reduce the risk of cancer. *J. Nutr.*; 119: 116-122

9 CURRICULUM VITAE

Name Mirna Castro
Date of birth 11 November, 1964
Place of birth Guayaquil, Ecuador
Nationality Ecuadorian
Home address Leonrodstr. 91
80636 München
Germany
Email mirna.castro@med.uni-muenchen.de; mirna.castro@gmx.net

Education

1999 - to date Ludwig-Maximilian-University, Munich, Germany
1984 - 1990 Masters in Science, Physics, and Mathematics (major field of study: Biophysics) at the V. I. Lenin Belorussian State University, Faculty of Physics, Minsk, Belorussia
1986 - 1990 Russian language teaching certificate
1978 - 1983 Bachelor of Modern Humanities, specialty in physics and mathematics. María Angélica Idrobo National Experimental High School (2nd-6th course), Quito, Ecuador
1977 - 1978 High School of América (1st course), Quito, Ecuador

Work experience

Currently Biological assistant at the Dept. of Neurogenetics, Neurological Research Center, Klinikum Großhadern, LMU, Munich, Germany
1996 - 2000 Graduate assistant at the Laser Research Laboratory, Klinikum Großhadern, LMU, Munich, Germany
1992 - 1995 Sales assistant and tourist guide at Angermeyer's Enchanted Expeditions (Travel Agency), Quito, Ecuador
1994 Coordinator of an indigenous exchange program between Ecuador and Canada
1992 - 1993 Volunteer in small medical projects, Quito, Ecuador
1991 Private teacher of physics and mathematics, Quito, Ecuador
1990 Lecturer at the National Politechnical Institut in Quito, Ecuador

Publications

- 2003** Zimprich A., Asmus F., Leitner P., **Castro M.**, Bereznai B., Homann N., Ott E., Rutgers A. W., Wieditz G., Trenkwalder C., Gasser T. (2003). Point mutations in exon 1 of the NR4A2 gene are not a major cause of familial Parkinson's disease. **EUROGENETICS**, 4: 219-220.
- 2002** Gamarra F., Wagner S., Al-Batran S., Maier I., **Castro M.**, Hautmann H., Bergner A., Baumgartner R., Huber R. M. (2002). Kinetics of 5-aminolevulinic acid induced fluorescence in organ cultures of bronchial epithelium and tumor. **RESPIRATION**, 69: 445-450.
- 2002** Asmus F., Zimprich A., Tezenas Du Montcel S., Kabus C., Deuschl G., Kupsch A., Ziemann U., **Castro M.**, Kuhn A., Strom T. M., Vidailhet M., Bhatia K. P., Durr A., Wood N.W., Brice A., Gasser T. (2002). Myoclonus Dystonia Syndrome: epsilon-sarcoglycan mutations and phenotype. **ANNALS OF NEUROLOGY**, 52: 489-492.
- 2001** Zimprich A., Grabowski M., Asmus F., Naumann M., Berg D., Bertram M., Scheidtmann K., Kern P., Winkelmann J., Muller-Myhsok B., Riedel L., Bauer M., Müller T., **Castro M.**, Meitinger T., Strom T. M., Gasser T. (2001). Mutations in the gene encoding epsilon-sarcoglycan cause Myoclonus Dystonia Syndrome. **NATURE GENETICS** 29: 66-69
- 1999** Huber R. M., Gamarra F., Hautmann H., Häußinger K., Wagner S., **Castro M.**, Baumgartner R. (1999). 5-Aminolevulinic acid (5-ALA) for the fluorescence detection of bronchial tumors. **DIAGNOSTIC AND THERAPEUTIC ENDOSCOPY** 5: 113-118
- 1989** **Castro M.**, Zorin B. P. (1989). Investigation of chlorin e6 derivatives interactions with serum proteins. **RUSSIAN JOURNAL OF CANCER**, Minsk

Awards

- 1991** Scholarship to continue studies toward a PhD in Biophysics at the University of Rio de Janeiro, Brazil (unfortunately the university closed the program before I could begin)
- 1988** First place in the competition of the Belorussian University for competency in the Russian language as a foreign language, Minsk, Belorussia
- 1984** A grant to study in the Soviet Union conferred by the Russian Government and the Society of the Ecuadorian ex-becarios, Quito, Ecuador
- 1983 – 1984** A grant to participate in the International Exchange Program “CANADA WORLD YOUTH”. The competition was among several high schools from all over the country. The project was promoted by the Canadian government and included community assistance, language learning, and a cross-cultural exchange program between Ecuador and Canada

1983 Second honorable mention in the oratorical competition called “The Read Book”, Quito, Ecuador

1975 First place (gold medal) in the oratorical competition on “The Importance of the Guayas River”, promoted by the municipality of Quito and the State School of Guayaquil, Quito, Ecuador

Language skills

	Fluency	Place of study
English	fluent in speech and writing	Bénect, Canada
Russian	fluent in speech and writing	Belorussian State University, Minsk, Belorussia
German	fluent in speech and writing	LMU, Munich, Germany
Portuguese	fair in speech and writing	Brasilian Institut, Quito, Ecuador
Japanese	2 years of study	Catholic University, Quito, Ecuador
Spanish	2 semesters native language	LMU, Munich, Germany

10 ACKNOWLEDGEMENTS

I would like to thank all those, whose help, creativity, and enthusiasm have guided this dissertation from its conception to its completion:

Prof. Dr. med. R. M. Huber, my supervisor, for his kind guidance, time, and patience.

I would especially like to acknowledge my gratitude to Dr. rer. nat. Reinhold Baumgartner for his expert feedback and advice, and also for providing me with a permanent workstation and financial support all these years.

I am indebted to Dr. rer. nat. Herbert Stepp for his excellent guidance, critical remarks on the first draft of this work, and helpful tips on improving this thesis.

I gratefully thank Prof. Dr. Wolfgang Zimmermann for the stimulating conversations and his insightful comments after reading this work.

My sincere thanks to Prof. Dr. med. Thomas Gasser and PD Dr. med. Martin Dichgans for providing me with work in the field of Molecular Biology and Genetics during the last phase of my dissertation.

I would also like to thank my friend Dr. Marius Hoener for his valuable help with cell transfection at the Max-Planck Institute (Martinsried).

I would like to thank my close friend Judy Benson for copyediting the manuscript and for the time and care she devoted to it.

I thank Caroline, Katie, Dodo, and Dana so much for their valuable input.

I thank my colleagues of the Laser Research Laboratory and Tumor Immunology for making the time I spent here so memorable and enjoyable.

Last but not least, I wish to thank all the friends who encouraged me to finish this dissertation.